GEORGIA
DEPARTMENT OF NATURAL RESOURCES
ENVIRONMENTAL PROTECTION DIVISION

Final 2018 Ozone Exceedance Report for Atlanta, Georgia

Prepared by:
Planning and Support Program
Air Protection Branch
Environmental Protection Division

July 19, 2019

Executive Summary

Ozone concentrations in Georgia have decreased over the past 25 years. On October 1, 2015, the 8-hour ozone National Ambient Air Quality Standard (NAAQS) was lowered from 75 ppb to 70 ppb. In 2018, three Metropolitan Statistical Areas (MSAs) – Atlanta-Sandy Springs-Marietta, Athens, and Augusta – experienced ozone exceedance days where the measured 8-hour average ozone concentration was above 70 ppb. In comparison, there were two MSAs with ozone exceedances in 2017. For each ozone exceedance day, the Data and Modeling Unit developed an initial exceedance report with preliminary analyses of air quality, meteorological, and emission data to aid in determining the cause of the ozone exceedance. If ozone exceedances occur frequently, the design value (3-year average of annual 4th highest daily maximum 8-hour average ozone concentrations) can exceed the ozone NAAQS, and EPA can classify the area as nonattainment. The recently certified 2018 ozone measurements show that Atlanta is the only area in Georgia currently violating the 2015 ozone NAAQS.

A final, in-depth ozone exceedance report was developed for the Metro Atlanta area to identify causes of the 2018 ozone exceedances. The report includes: trend analysis of ozone concentrations and meteorological conditions in Atlanta during 1990-2018; multiple linear regression (MLR) analysis; Hybrid Single Particle Lagrangian Integrated Trajectory (HYSPLIT) back trajectory analysis to determine the origin of air masses and establish source-receptor relationships on ozone exceedance days; animation of ozone and wind conditions to illustrate ozone formation and transport; and analysis of VOC and NO_X measurements to understand the impacts of precursors on ozone formation. Also, a preliminary investigation of traffic congestion impacts on ozone exceedances was performed. Note that all analysis results in this report are based on Eastern Standard Time (EST).

In summary, the following factors likely contributed to 2018 ozone exceedances in Atlanta:

1) Low relative humidity in the afternoon;
2) High daily maximum air temperature;
3) Low cloud coverage;
4) High ozone on previous days;
5) Low wind speed;
6) NO_X emissions, mainly from local on-road mobile sources;
7) High traffic congestion (especially in the morning hours) during May, August, and September;
8) VOC emissions, mainly from biogenic sources in the summer months; and
9) Local transport of emissions from the Atlanta urban core to monitors outside the urban core.

This final ozone exceedance report can be used to guide future air quality management practices in Georgia to aid in preventing future ozone exceedances.

List of Acronyms

AQS	Air Quality System
CASTNET	Clean Air Status and Trends Network
CO	Carbon Monoxide
ENSO	El Niño–Southern Oscillation
EPA	U.S. Environmental Protection Agency
EPD	Environmental Protection Division
GIF	Graphics Interchange Format
HCHO	Formaldehyde
HJAIA	Hartsfield-Jackson Atlanta International Airport
HYSPLIT	Hybrid Single Particle Lagrangian Integrated Trajectory
IDL	Interactive Data Language
LIDAR	Light Detection and Ranging
LT	Local Time
MAE	Mean Absolute Error
MB	Mean Bias
mb	millibar (=10^{-3} bar)
MDA8O3	Maximum Daily 8-hour Average Ozone Concentrations
MLR	Multiple Linear Regression
MSAs	Metropolitan Statistical Areas
NAAQS	National Ambient Air Quality Standards
NAM	North American Mesoscale
NCEI	National Centers for Environmental Information
NEI	National Emissions Inventory
NMB	Normalized Mean Bias
NME	Normalized Mean Error
NOAA	National Oceanic and Atmospheric Administration
NO_X	Oxides of Nitrogen
OMI	Ozone Monitoring Instrument
PBL	Planetary Boundary Layer
RMSE	Root Mean Square Error
VOC	Volatile Organic Compounds

Table of Contents

Executive Summary i
1. Introduction 1
2. Ozone Exceedance Trends in the Metro Atlanta Area during 1990-2018 8
3. Meteorological Conditions in the Metro Atlanta Area during 1990-2018 13
4. Ozone Regression Analysis 18
5. Ozone and Meteorological Conditions 22
5.1 Hourly Ozone and Meteorology Time Series Analysis 22
5.2 HYSPLIT Back Trajectory Analysis 25
5.3 Animation of Ozone and Wind Conditions 32
5.4 1-Minute Ozone Concentration Time Series on Exceedance Days 43
6. Ozone and NO_X Precursor 47
6.1 Diurnal Patterns of NO_X Observations on Ozone Exceedance Days 49
6.2 Day-of-Week Patterns of NO_X Observations on Ozone Exceedance Days 54
6.3 Monthly Patterns of NO_X Observations on Ozone Exceedance Days 54
6.4 Indicator Analysis 57
6.5 NO_X Trends Based on OMI Satellite Data 59
6.6 NO_X Trends Based on TROPOMI Satellite Data 63
6.7 Ozone and Traffic Conditions 67
7. Ozone and VOCs Precursors 83
7.1 HCHO Trends Based on OMI Satellite Data 83
8. Summary 87
9. References 89

1. Introduction

Ozone pollution can impair lung function and cardiovascular health. Ground-level ozone is formed in the atmosphere by chemical reactions of volatile organic compounds (VOCs) and oxides of nitrogen (NO_X) in the presence of sunlight. Sources of VOCs include fuel combustion, fuel evaporation, paints, solvents, and vegetation. NO_X emissions are primarily from the combustion of fuels. The U.S. Environmental Protection Agency (EPA) lowered the National Ambient Air Quality Standards (NAAQS) for ground-level ozone from 75 ppb (2008 ozone NAAQS) to 70 ppb (2015 ozone NAAQS) to better protect public health and welfare.

Ozone concentrations in Georgia have decreased over the years (Figure 1) in various Metropolitan Statistical Areas (MSAs). The Metro Atlanta area was the only area in Georgia designated nonattainment for the 2008 ozone NAAQS and was redesignated to attainment in June 2017. On April 30, 2018, EPA designated seven counties (Bartow, Clayton, Cobb, DeKalb, Fulton, Gwinnett, and Henry) as nonattainment areas for the 2015 ozone NAAQS.

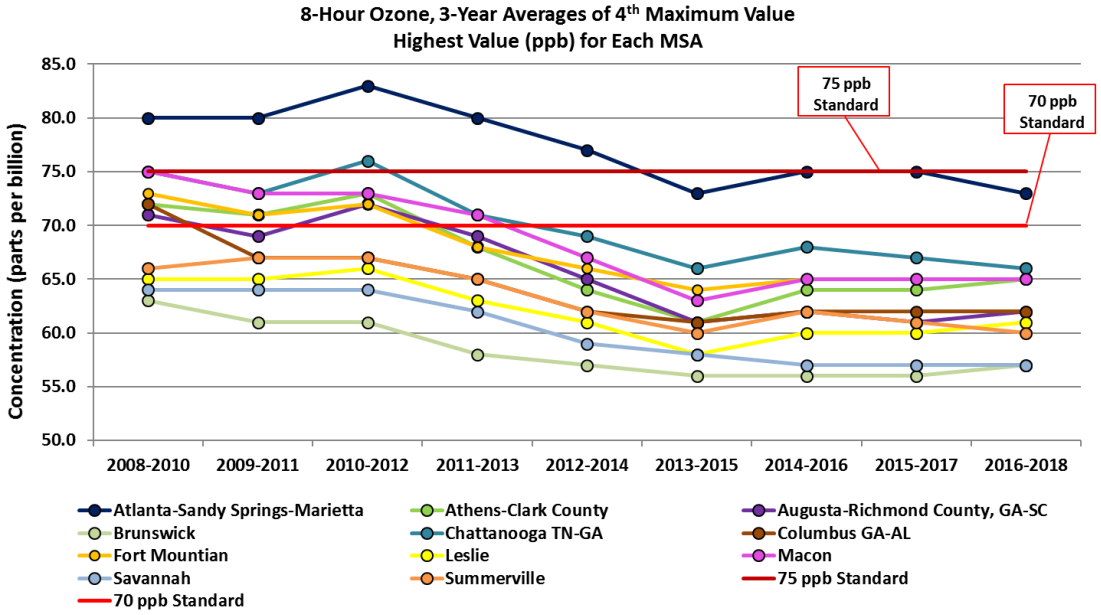

Figure 1. Trend of ozone design values by various MSAs in Georgia.

In 2018, three MSAs (Atlanta-Sandy Springs-Marietta, Athens, and Augusta) experienced ozone exceedances where the measured 8-hour average ozone concentration was above 70 ppb. In comparison, there were two MSAs with ozone exceedances in 2017. For each ozone exceedance day, the Data and Modeling Unit developed an initial exceedance report with a preliminary analysis of air quality, meteorological, and emission data to help understand the cause of the ozone exceedance. If ozone exceedances occur frequently, the design value (3-year average of annual 4th highest daily maximum 8-hour average ozone concentrations) can exceed the ozone NAAQS and EPA can classify the area as nonattainment. Based on 2016-2018 ozone data, Atlanta has two monitors with design values above 70 ppb (Table 1 and Figure 2). Only one monitor – United Ave.[1] – had a 4th highest concentration above 70 ppb in 2018 (Table 2 and Figure 3).

[1] This is the new name for the previously named "Confederate Ave." monitor.

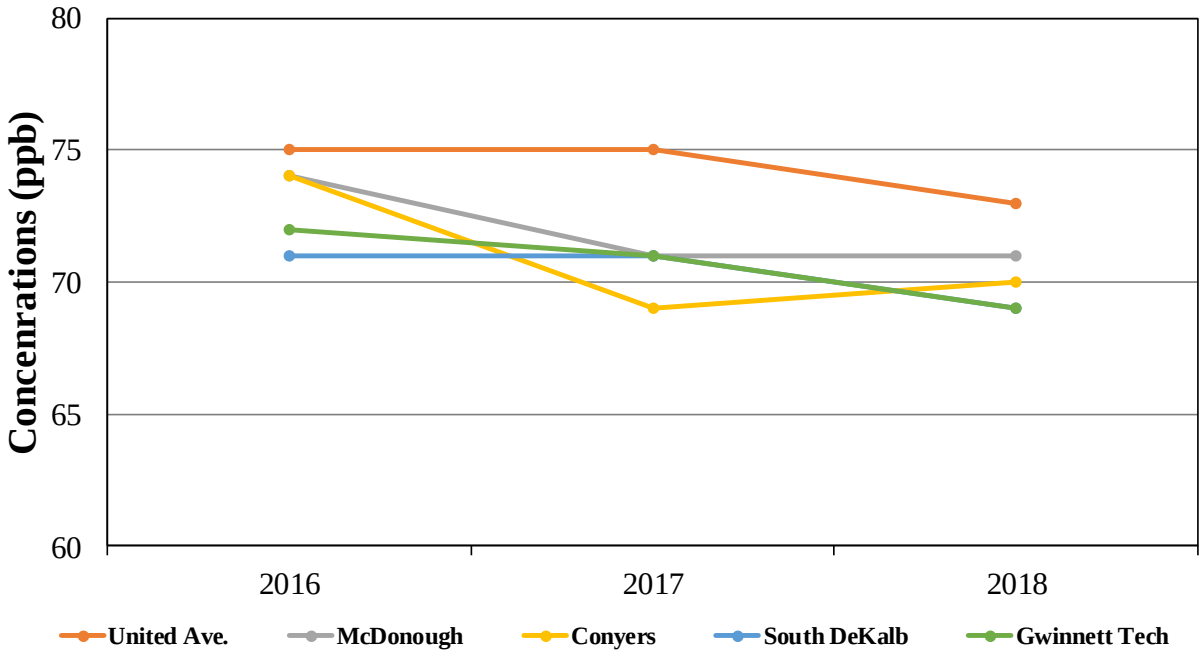

Figure 2. Ozone design values for five high ozone monitors in the Metro Atlanta area during 2014-2018.

Figure 3. Annual 4th highest daily maximum 8-hour average ozone concentrations (ppb) for five high ozone monitors in the Metro Atlanta area during 2014-2018.

Table 1. Annual 4th highest daily maximum 8-hour average ozone concentrations (ppb) and design value for nine ozone monitors in the Metro Atlanta area during 2014-2018.

Site ID	County	Site Name	4th Highest (ppb)					Design Value (ppb)		
			2014	2015	2016	2017	2018	2016	2017	2018
130670003	Cobb	Kennesaw	63	66	70	65	65	66	67	66
130850001	Dawson	Dawsonville	66	63	67	65	65	65	65	65
130890002	DeKalb	South DeKalb	70	71	74	68	67	**71**	**71**	69
130970004	Douglas	Douglasville	65	70	71	66	64	68	69	67
131210055	Fulton	United Ave.	73	77	75	74	72	**75**	**75**	**73**
131350002	Gwinnett	Gwinnett Tech	68	71	78	65	65	**72**	**71**	69
131510002	Henry	McDonough	75	70	78	67	69	**74**	**71**	**71**
132319991	Pike	EPA CASTNET	66	68	71	62	65	68	67	66
132470001	Rockdale	Conyers	79	68	76	65	69	**74**	69	70

The nine ozone monitors in the Metro Atlanta area experienced 10 ozone exceedance days in 2018, compared to 11 ozone exceedance days in 2017. Ozone concentrations by monitors in Atlanta on ozone exceedance days during 2018 are summarized in Table 2. Ozone exceedance days by monitor are displayed in Figure 4 and summarized by month in Table 3. The highest number of 2018 ozone exceedances occurred at the United Ave. monitor located in downtown Atlanta. There were two exceedance days (June 6 and 7, 2018) when ozone exceedances occurred at two Atlanta monitors on the same day. For the other eight exceedance days, the ozone exceedances only occurred at one monitor for each day. Figure 5 contains the daily maximum 8-hour ozone concentrations at monitors in and around the Metro Atlanta area on exceedance days.

Table 2. Ozone concentrations (ppb) for nine ozone monitors in the Metro Atlanta area on exceedances days during 2018. "-" indicates missing data.

Month	Day	Day of Week	United Ave.	McDonough	Dawsonville	South DeKalb	Conyers	Douglasville	EPA CASTNET	Gwinnett Tech	Kennesaw	Number of Exceedance Monitors
May	**1**	Tuesday	60	57	**72**	59	61	51	-	66	55	1
May	**2**	Wednesday	64	59	**73**	62	57	54	-	64	60	1
May	**12**	Saturday	65	69	54	64	**74**	51	59	64	59	1
May	**13**	Sunday	62	**75**	49	61	64	51	66	52	52	1
June	**4**	Monday	65	**71**	51	-	66	58	65	57	59	1
June	**6**	Wednesday	**72**	68	51	67	**71**	58	67	58	55	2
June	**7**	Thursday	**80**	62	54	69	61	68	**75**	64	67	2
July	**9**	Monday	**79**	55	41	67	52	60	51	58	59	1
July	**26**	Thursday	64	**72**	43	57	58	54	-	54	54	1
August	**15**	Wednesday	**74**	61	48	70	56	56	54	64	70	1

Table 3. Summary of 2018 ozone exceedances for five ozone monitors in the Metro Atlanta area.

ID	Site Name	April	May	June	July	August	September	October	Total
131210055	United Ave.			2	1	1			4
131510002	McDonough		1	1	1				3
130850001	Dawsonville		2						2
132470001	Conyers		1	1					2
132319991	EPA CASTNET			1					1
	Total	**0**	**4**	**5**	**2**	**1**	**0**	**0**	**12**

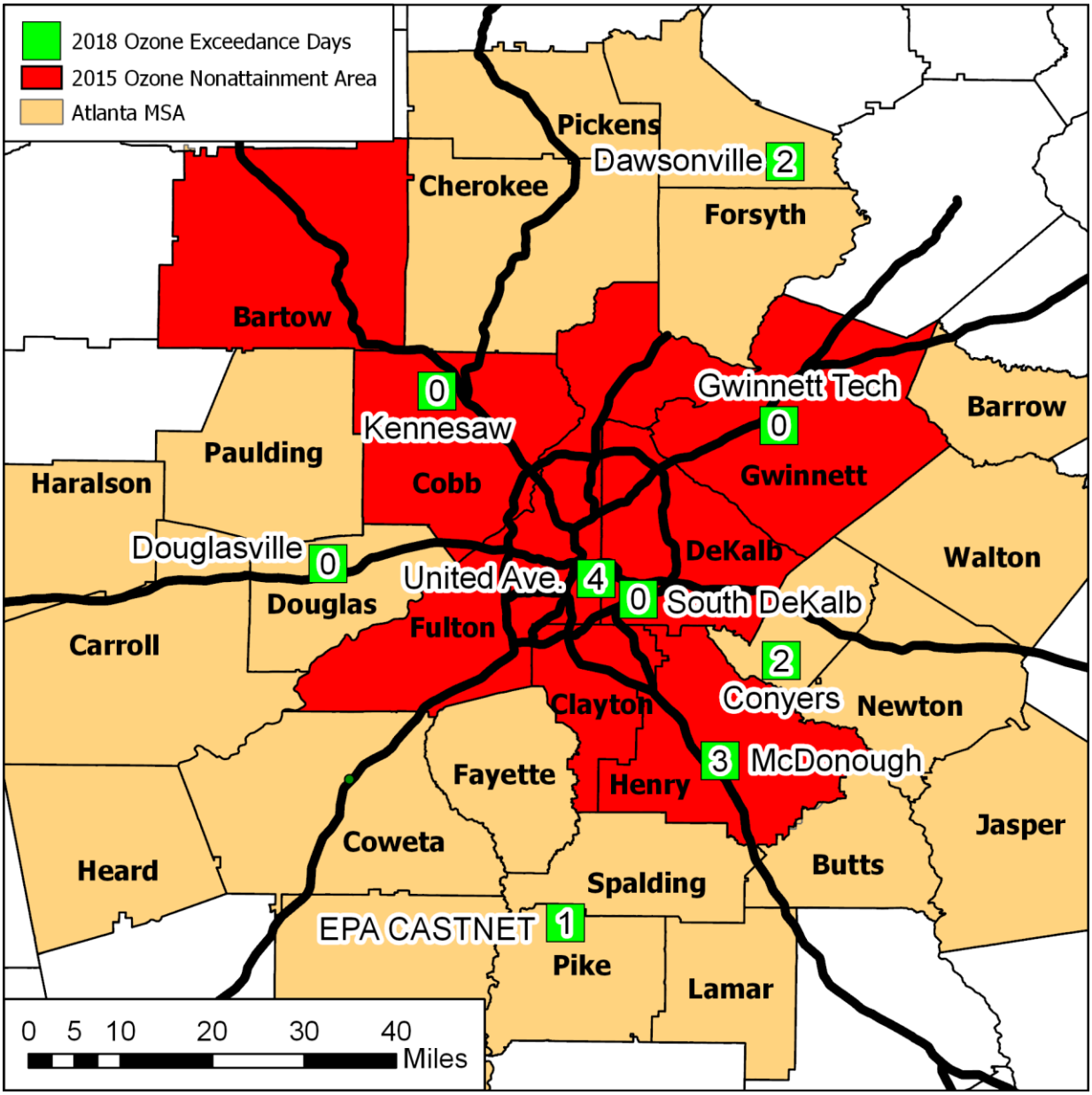

Figure 4. Locations of ozone monitors and the number of 2018 ozone exceedance days in the Metro Atlanta area.

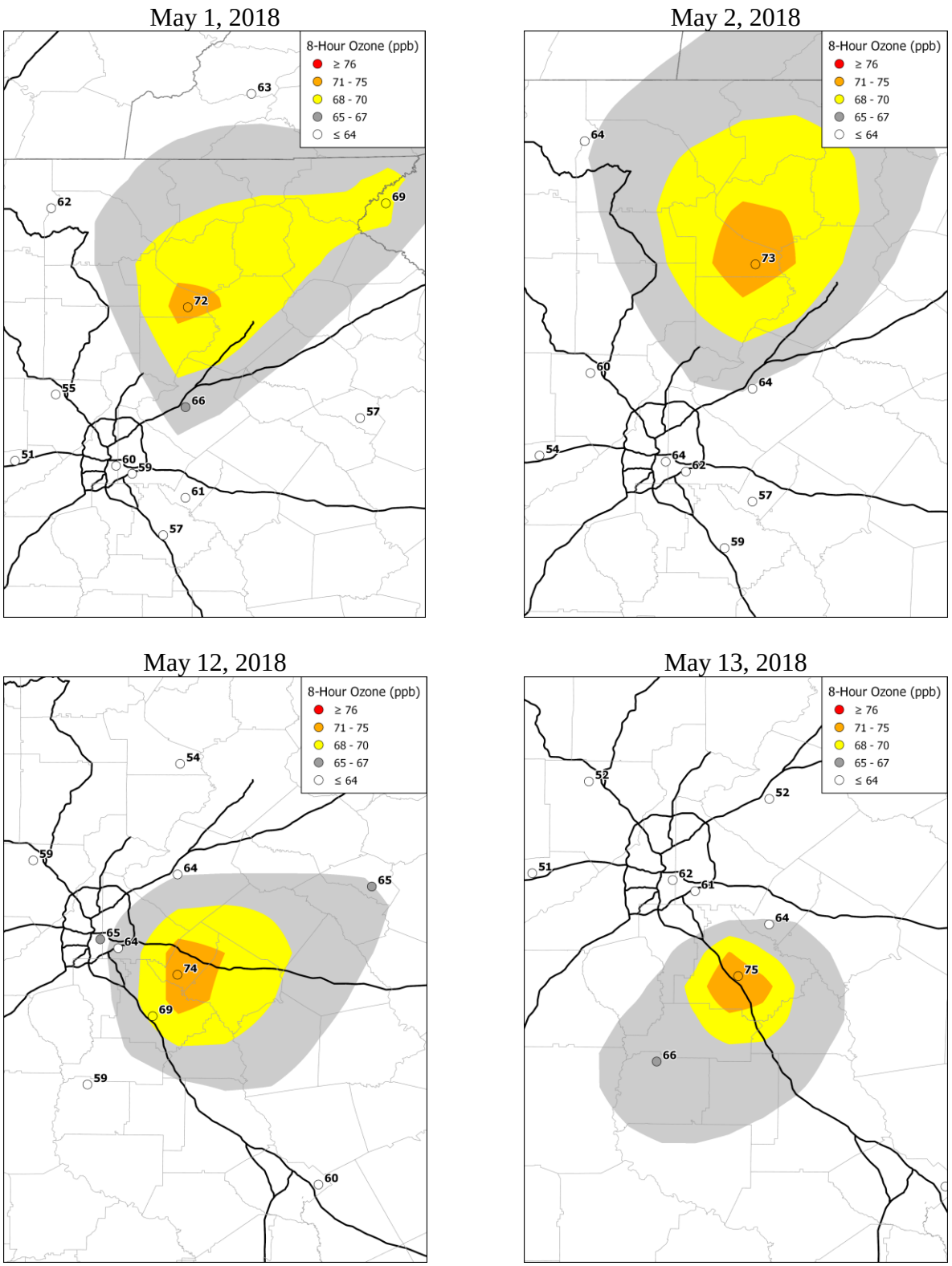

Figure 5. Daily maximum 8-hour ozone concentrations at monitors in and around the Metro Atlanta area on exceedance days.

June 4, 2018

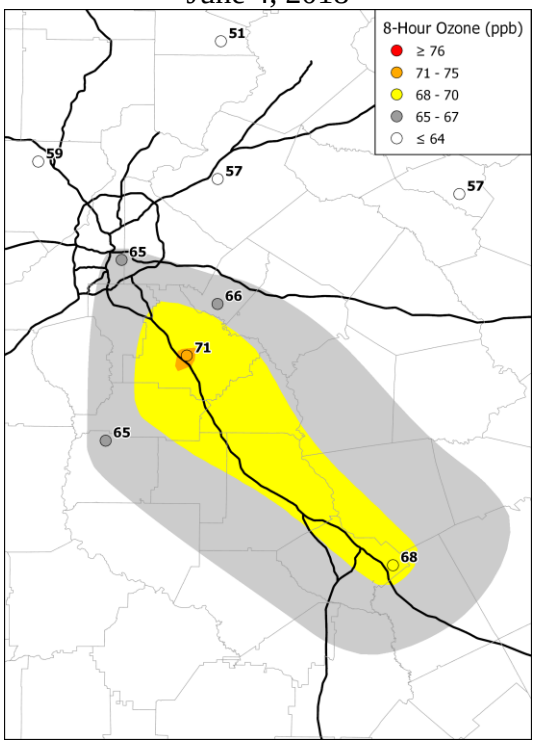

June 6, 2018

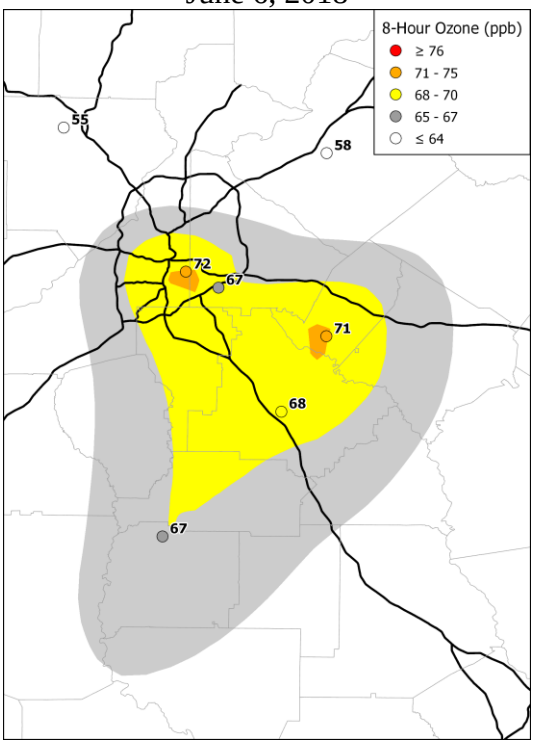

June 7, 2018

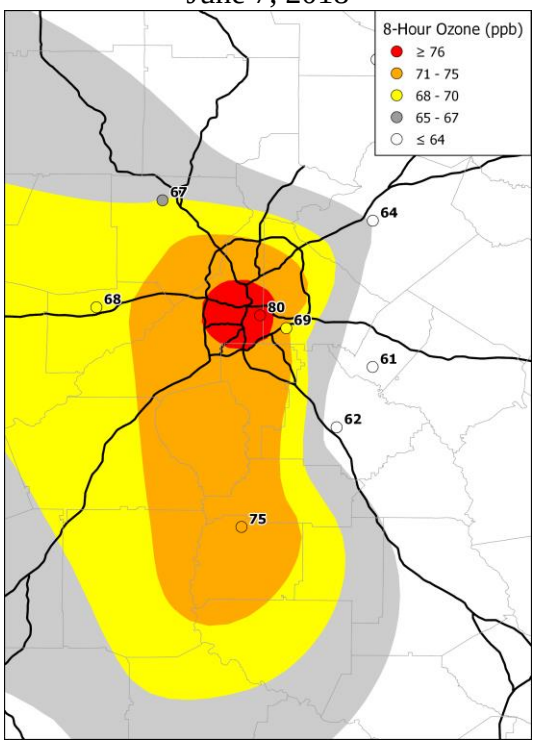

July 9, 2018

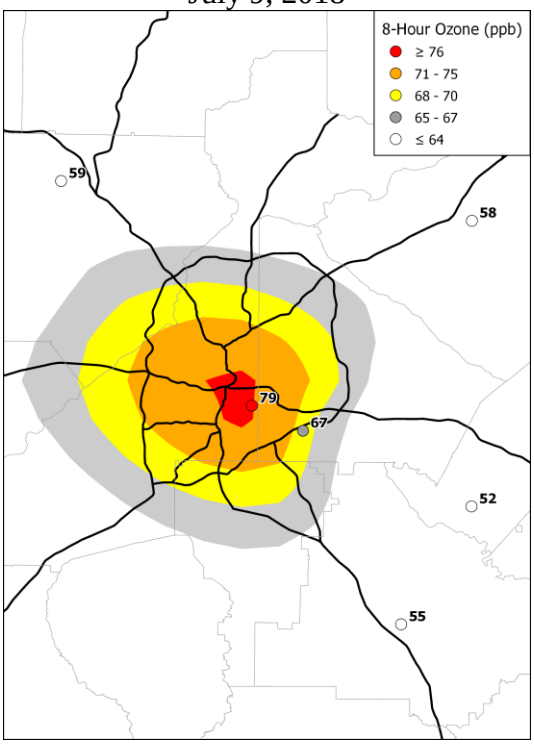

Figure 5 (Continued). Daily maximum 8-hour ozone concentrations at monitors in and around the Metro Atlanta area on exceedance days.

July 26, 2018

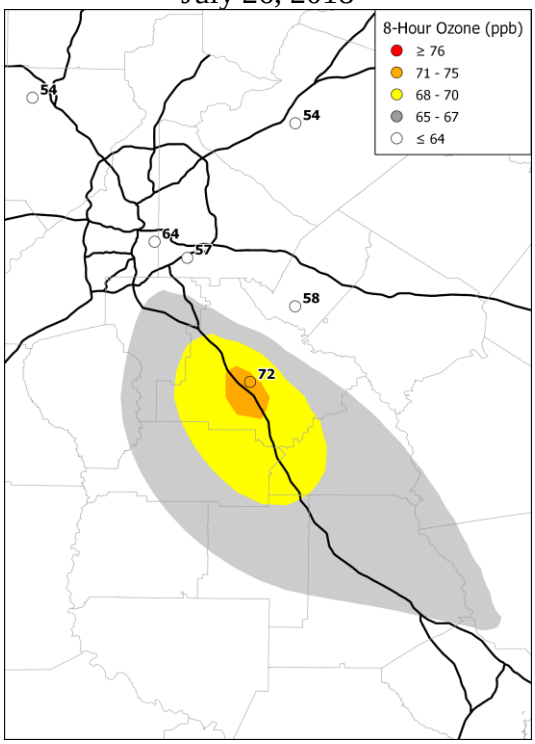

August 15, 2018

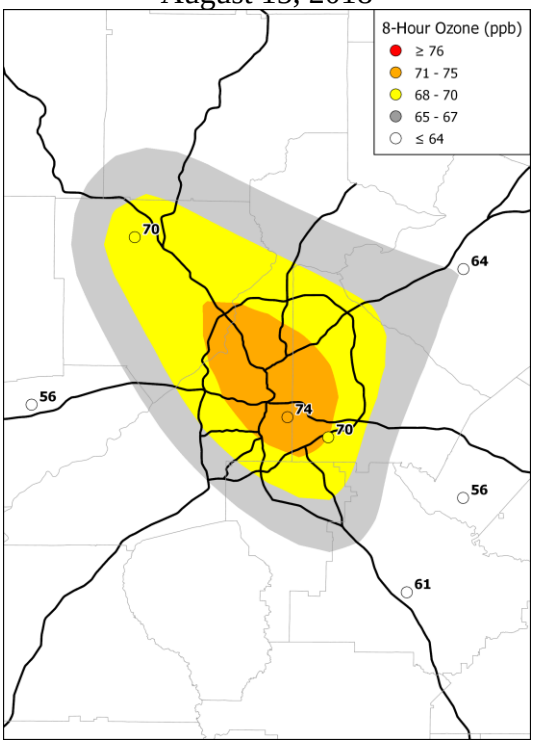

Figure 5 (Continued). Daily maximum 8-hour ozone concentrations at monitors in and around the Metro Atlanta area on exceedance days.

A final in-depth ozone exceedance report was developed for the Metro Atlanta area to identify causes of the 2018 ozone exceedances. The report includes: trend analysis of ozone concentrations and meteorological conditions in Atlanta during 1990-2018; multiple linear regression (MLR) analysis to understand the relationship between ozone and environmental variables; Hybrid Single Particle Lagrangian Integrated Trajectory (HYSPLIT) back trajectory analysis to determine the origin of air masses and establish source-receptor relationships on ozone exceedance days; animation of ozone and wind conditions to illustrate ozone formation and transport; and analysis of NO_X and VOCs measurements to understand the impacts of precursors on ozone formation. Also, a preliminary investigation of traffic congestion impacts on ozone exceedances was performed. This final ozone exceedance report can be used to guide future air quality management practices in Georgia to help prevent future ozone exceedances. Note that all analysis results in this report are based on Eastern Standard Time (EST).

2. Ozone Exceedance Trends in the Metro Atlanta Area during 1990-2018

Ozone exceedance trends in Atlanta during 1990-2018 were analyzed using ozone concentrations measured at nine ozone monitors in the Metro Atlanta area, including eight EPD-operated ozone monitors and one EPA-operated monitor (EPA CASTNET) (Table 4 and Figure 4). Note that the Newnan monitor that was operated in 2017 was discontinued in 2018. The 1990-2018 ozone data were downloaded from EPA's Air Quality System (AQS).

Table 4. Nine ozone monitors and their AIRS IDs in the Metro Atlanta area.

ID	Site Name
130670003	Kennesaw
130890002	South DeKalb
130970004	Douglasville
131210055	United Ave.
131350002	Gwinnett Tech
131510002	McDonough
132470001	Conyers
130850001	Dawsonville
132319991	EPA CASTNET

For the purpose of trend analysis, maximum daily 8-hour average ozone concentrations (MDA8O3) were calculated at the nine ozone monitors in Atlanta. The median and mean (with +/- one standard deviations) MDA8O3 from April to October in 1990-2018 shows the interannual variability with a slight downward trend through the years (Figure 6). The annual mean MDA8O3 in 1999 is the highest at 71.8 ppb and decreases to the lowest in 2013 with 47.6 ppb. This generally coincides with Georgia NO_X (Figure 7) and VOC (Figure 8) emission reductions over the same period of time. The annual mean MDA8O3 of 48.6 ppb in 2018 was the second lowest after 2013.

The MDA8O3 were compared with the 2015 ozone NAAQS (70 ppb) to identify ozone exceedance days. The number of exceedance days during the 1990-2018 ozone seasons shows a similar decreasing pattern. There were less than 20 ozone exceedance days in 2013, 2014, and 2015. The number of exceedance days increased to 29 days in 2016, then dropped to 11 days in 2017 and 10 days in 2018. We see a relatively large number of ozone days above 70 ppb in 1993, 1999, 2006, 2011, and 2016 compared with other years. There seems to be a 5- to 7-year period between these occurrences. This pattern is similar to the 2-year to 7-year period of El Niño–Southern Oscillation (ENSO), but not peaking in the same year. Further work is needed to determine if there is a potential connection between ozone concentrations and climate patterns.

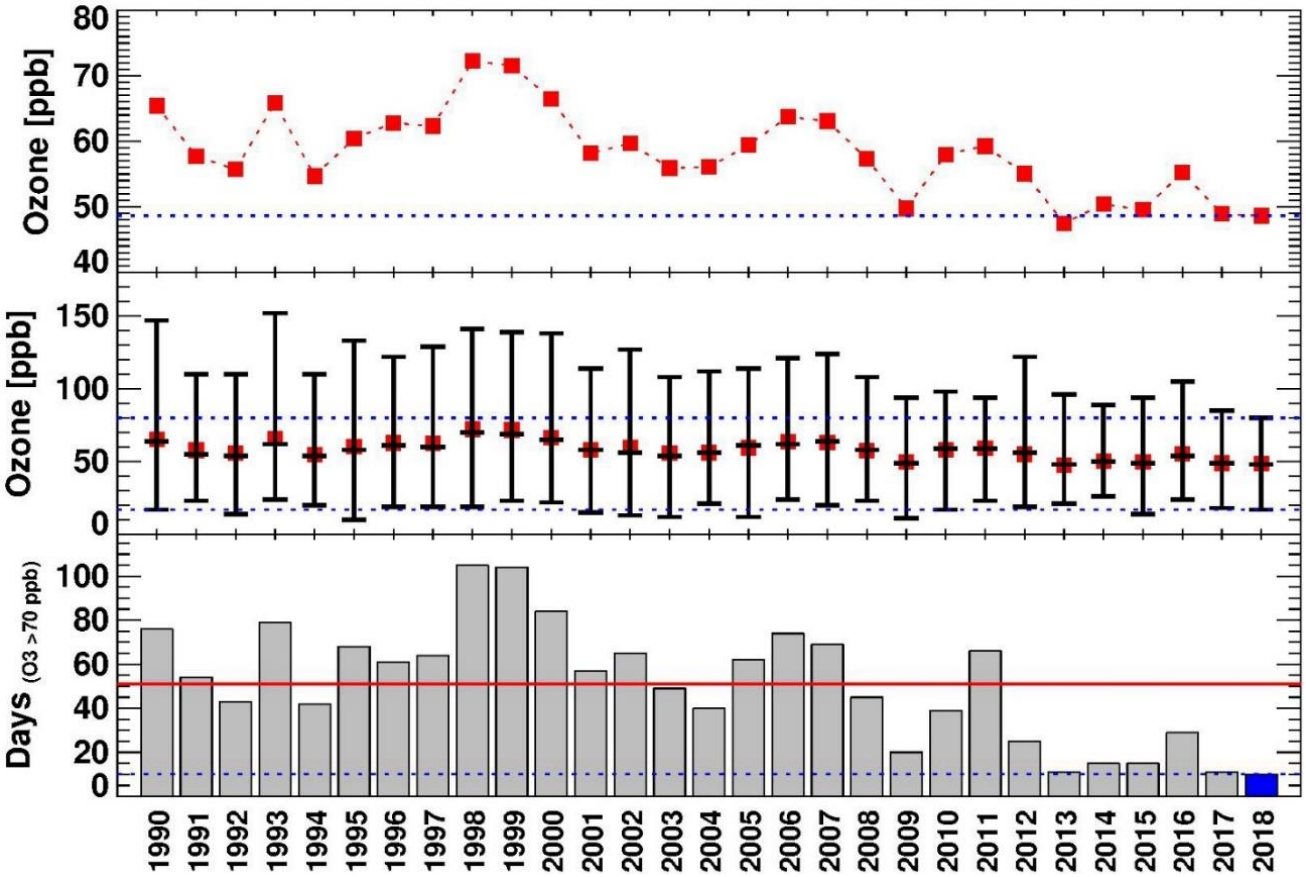

Figure 6. Mean MDA8O3 concentrations (top), mean (red squares), median (middle bars), and minimum and maximum (top and bottom bars) MDA8O3 concentrations (middle), and the number of ozone exceedance days (bottom) from April to October in 1990-2018 in the Metro Atlanta area. 2018 values are highlighted in blue and drawn in blue dotted lines. The red solid line is the average for 1990-2018.

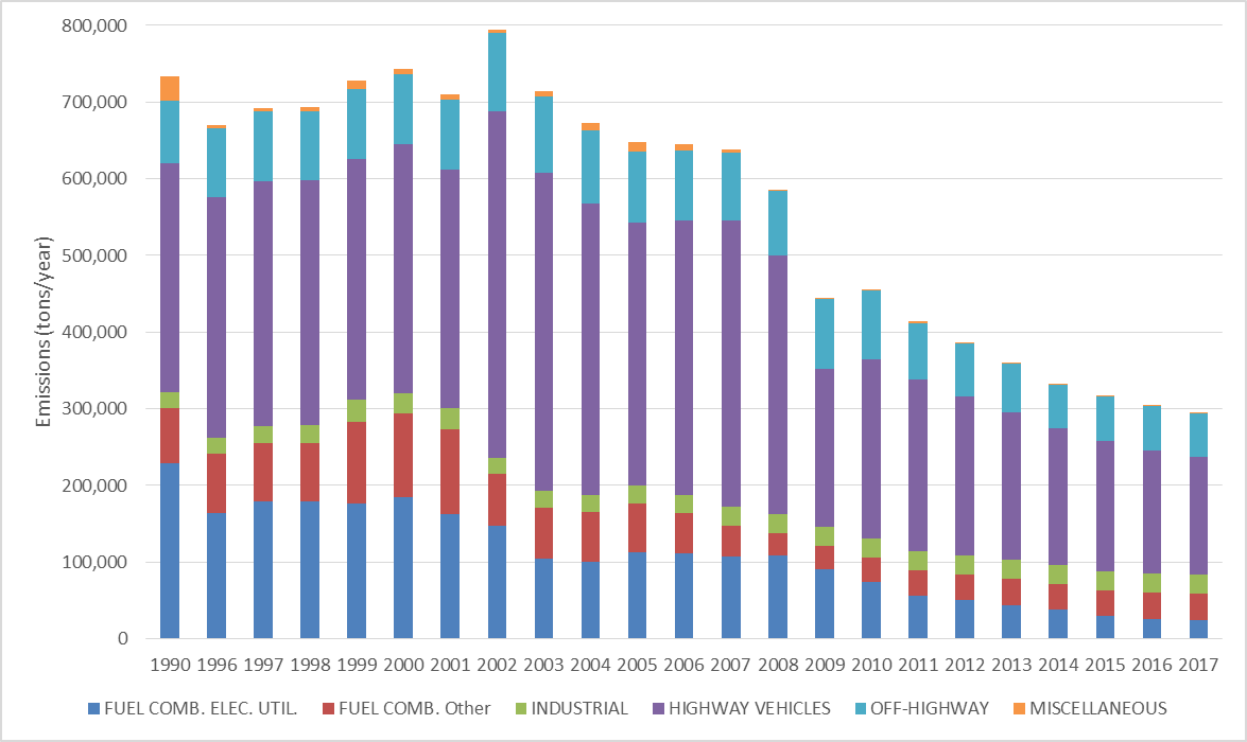

Figure 7. Georgia NO_X emission trends by source sectors during 1990-2017.

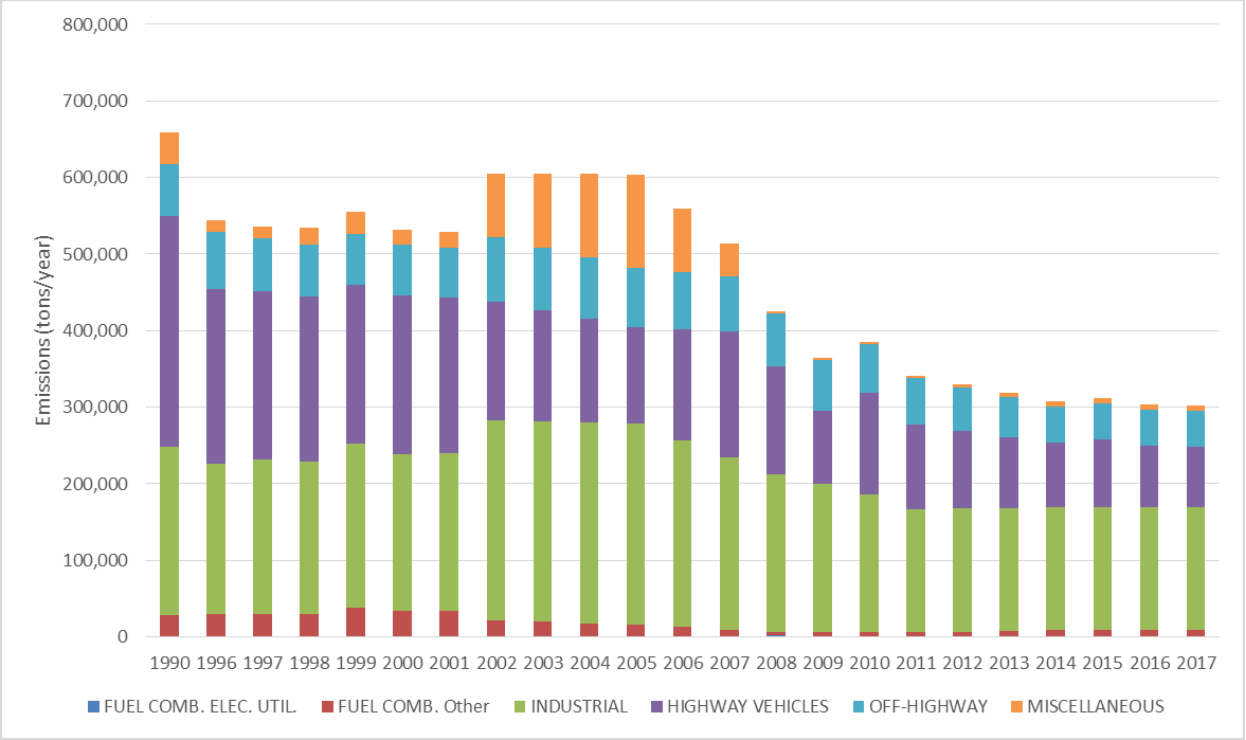

Figure 8. Georgia VOCs emission trends by source sectors during 1990-2017.

The monthly average ozone exceedance days and percentage of exceedance occurring in April to October are summarized by different time periods during 1990-2018 in the Metro Atlanta area (Figure 9). Typically, more than 70% of the ozone exceedances occur during June, July, and August when temperature is higher and sunlight is stronger, and less than 10% of the ozone exceedances occur in April and October when air temperature is relatively low. There were large interannual variations of the monthly patterns. In 2018, the exceedances occur in May, June, July, and August while no exceedances occurred in April, September, or October.

Also, the daily patterns of ozone exceedances were investigated (Figure 10). In recent years, more ozone exceedances occur during weekdays than weekends, but this difference is small before 2010. This is likely due to the large emission reduction for industrial sources which have less daily emissions variation compared with mobile sources. The daily patterns varied significantly in 2018 due to fewer ozone exceedances in that year.

The mean ozone increases on exceedance days were calculated by subtracting ozone concentrations on one day or two days before exceedance days/events from ozone concentrations on exceedance days (Figure 11). During 2018, the average ozone increases from one day before each ozone exceedance day in 2018 returned towards the mean after the largest increase was seen in 2017.

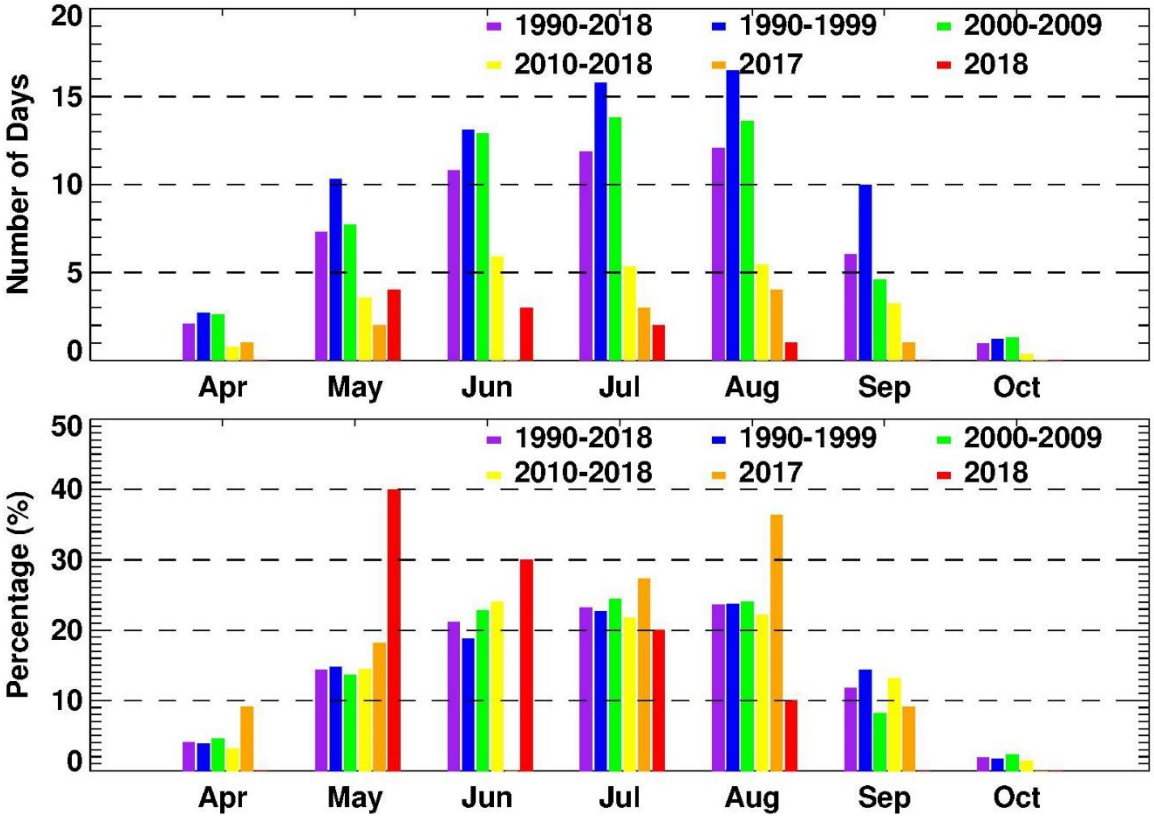

Figure 9. Monthly average number of ozone exceedance days (top) and percentage of exceedances occurring in that month (bottom) in ozone season by different time periods during 1990-2018 in the Metro Atlanta area.

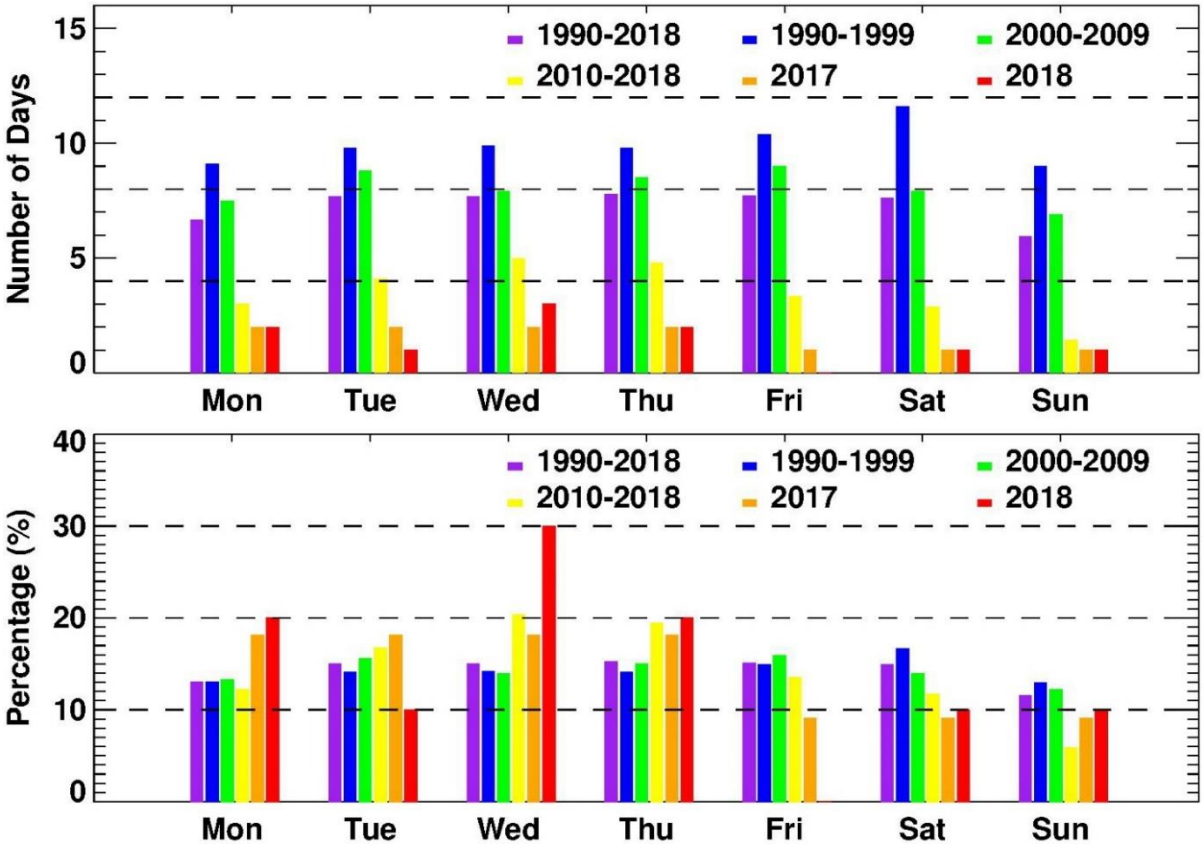

Figure 10. The number (top) and percentage (bottom) of ozone exceedance days by days of week for different periods during 1990-2018 in the Metro Atlanta area.

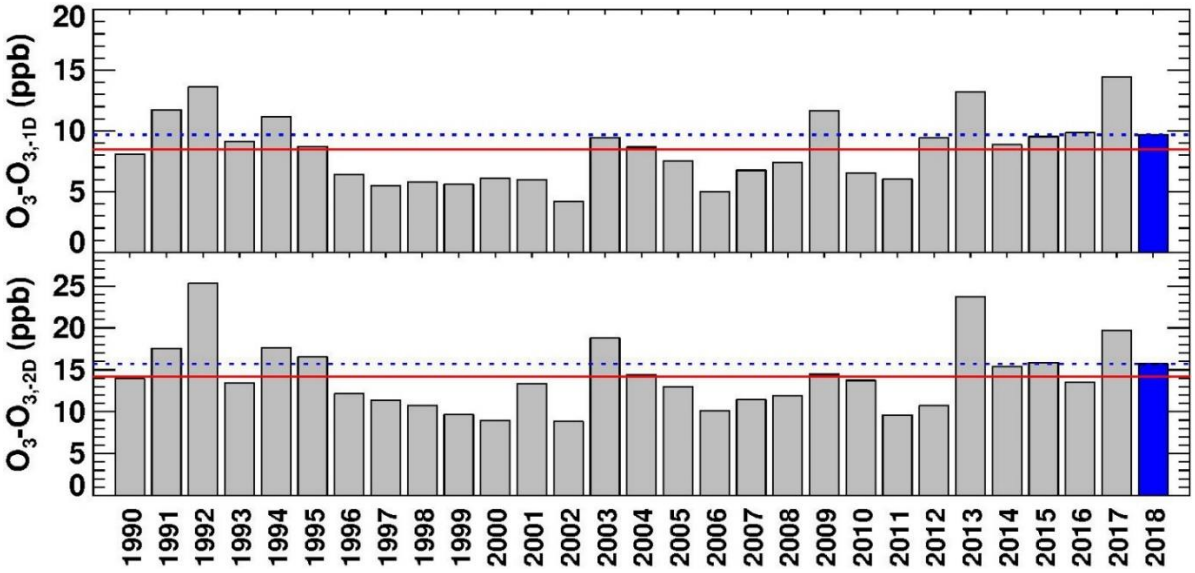

Figure 11. The mean ozone increases (ppb) from one day before (top) and two days before (bottom) the ozone exceedance days during 1990-2018 in the Metro Atlanta area. 2018 value is highlighted in blue and drawn in blue dotted line. The red solid line is the average for 1990-2018.

3. Meteorological Conditions in the Metro Atlanta Area during 1990-2018

Trends of meteorological conditions in Atlanta during 1990-2018 were analyzed using meteorological observations at Hartsfield-Jackson Atlanta International Airport (HJAIA) (Table 5) downloaded from https://mesonet.agron.iastate.edu/request/download.phtml?network=GA_ASOS. The observational intervals varied from one hour to several minutes depending on variables.

Table 5. Observed meteorological variables at HJAIA.

Variables	Definition	Unit
tmpf	Air Temperature, typically @ 2 meters	degree of Fahrenheit
dwpf	Dew Point Temperature, typically @ 2 meters	degree of Fahrenheit
relh	Relative Humidity	%
drct	Wind Direction	degree from north
sknt	Wind Speed	knots
p01i	One-hour precipitation for the period from the observation time to the time of the previous hourly precipitation reset.	inches
alti	Pressure altimeter	inches
mslp	Sea Level Pressure	millibar
vsby	Visibility	miles
gust	Wind Gust	knots
skyc1	Sky Level 1 Cloud Coverage	%
skyc2	Sky Level 2 Cloud Coverage	%
skyc3	Sky Level 3 Cloud Coverage	%
skyc4	Sky Level 4 Cloud Coverage	%

Mean meteorological conditions in ozone season were calculated for each year (Figure 12). Most variables have significant interannual variations, except pressure and wind direction. In 2018, AM and PM cloud coverages (defined as the percentage of sky covered by clouds) were less than the 1990-2018 average cloud coverages but are more than those in 2017. Daily maximum temperature was the third highest and daily minimum temperature was the highest in 2018. Even though dew point temperatures were close to the highest, the relative humidity was only slightly above its average. Temperatures were compared from 1930 to 2018 (Figure 13) and 2018 showed the third highest average temperature since 1930. In summary, the meteorological conditions in 2018 were hot and humid (less favorable for ozone formation compared to the hot and dry conditions in 2016).

The meteorological conditions were investigated further for the 10 ozone exceedance days in 2018. The relative humidity, cloud fractions, wind speeds in the morning and afternoon, and daily maximum and minimum temperatures on the day before and after each exceedance day/event are compared to those on the exceedance day (Figure 14). For the days without observations, the data from two days before or after are used. Continuous exceedances lasting more than one day are considered as one event. In general, the ozone exceedance days feature lower relative humidity, less cloud coverage, lower wind speeds, and higher daily max temperatures compared to non-exceedance days. Other meteorological variables such as dew point temperature, pressure, and wind direction do not show a clear pattern with ozone exceedances. This is consistent with the analysis of meteorological and air quality data during the period from 1990-2018 mentioned above.

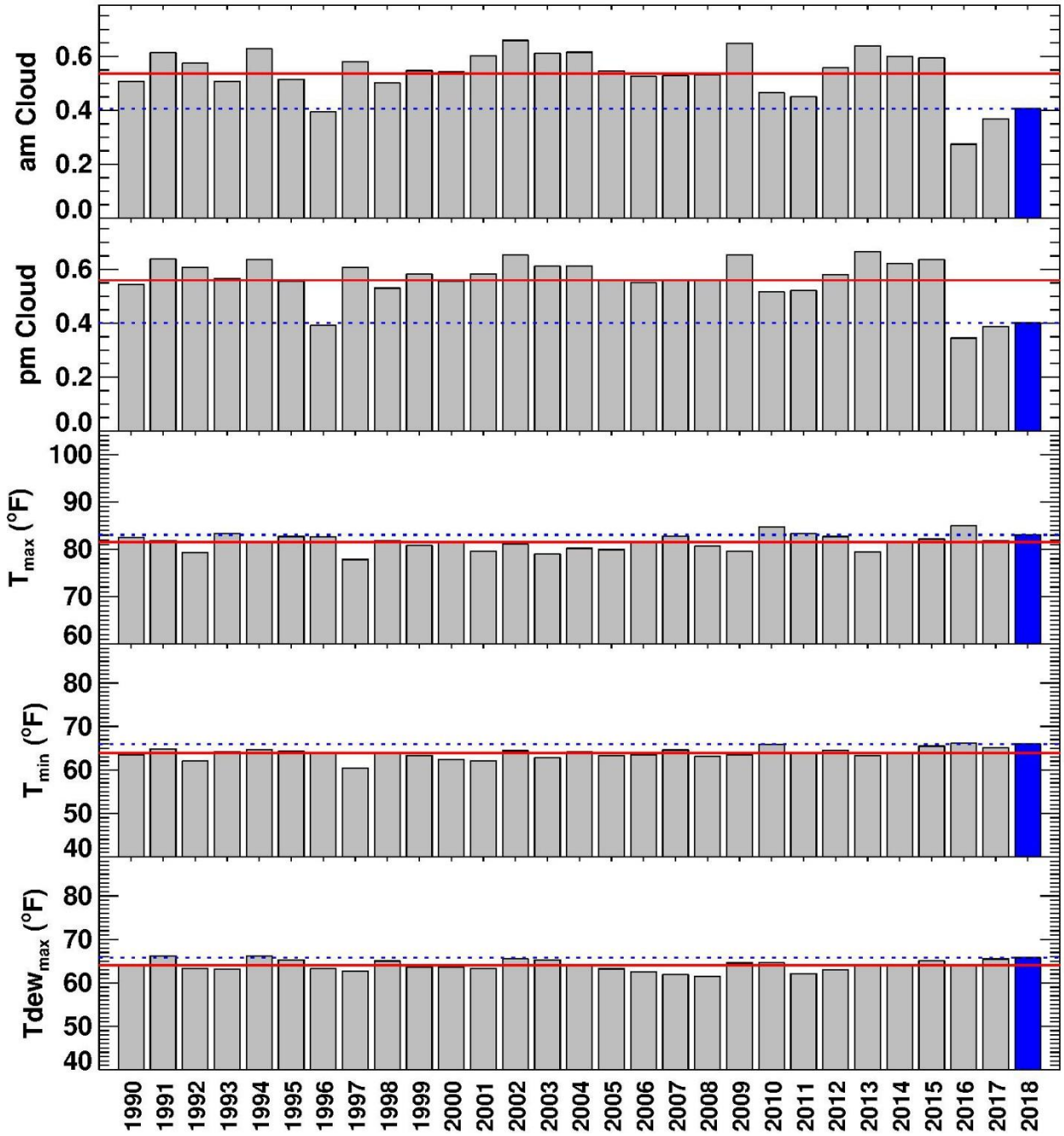

Figure 12. Atlanta ozone season mean meteorological conditions during 1990-2018. 2018 values are highlighted in blue and represented by the blue dotted line. 1990-2018 average values are represented by the red solid line to facilitate comparison.

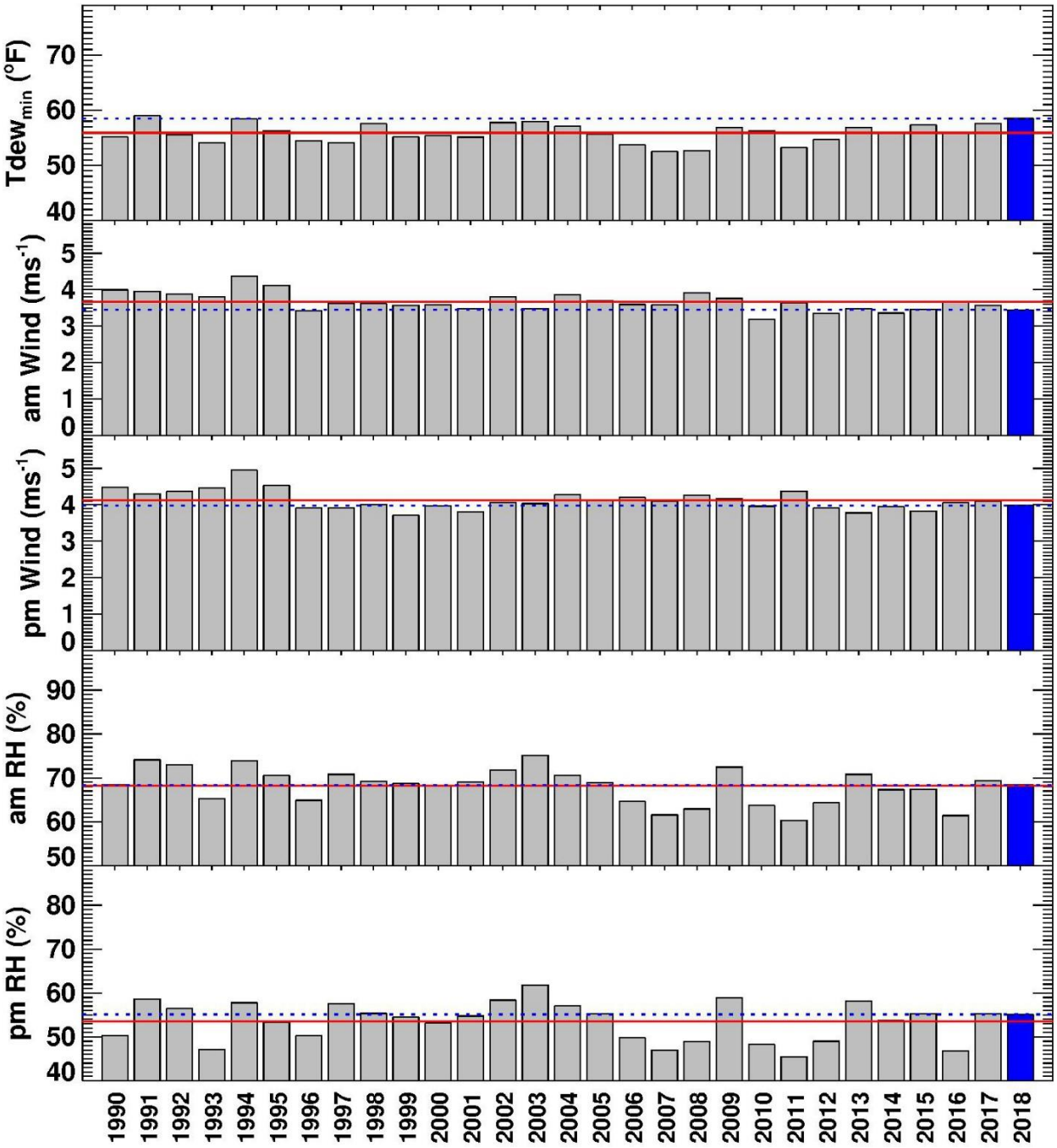

Figure 12 (continued). Atlanta ozone season mean meteorological conditions during 1990-2018. 2018 values are highlighted in blue and represented by the blue dotted line, and 1990-2018 average values are represented by the red solid line to facilitate comparison.

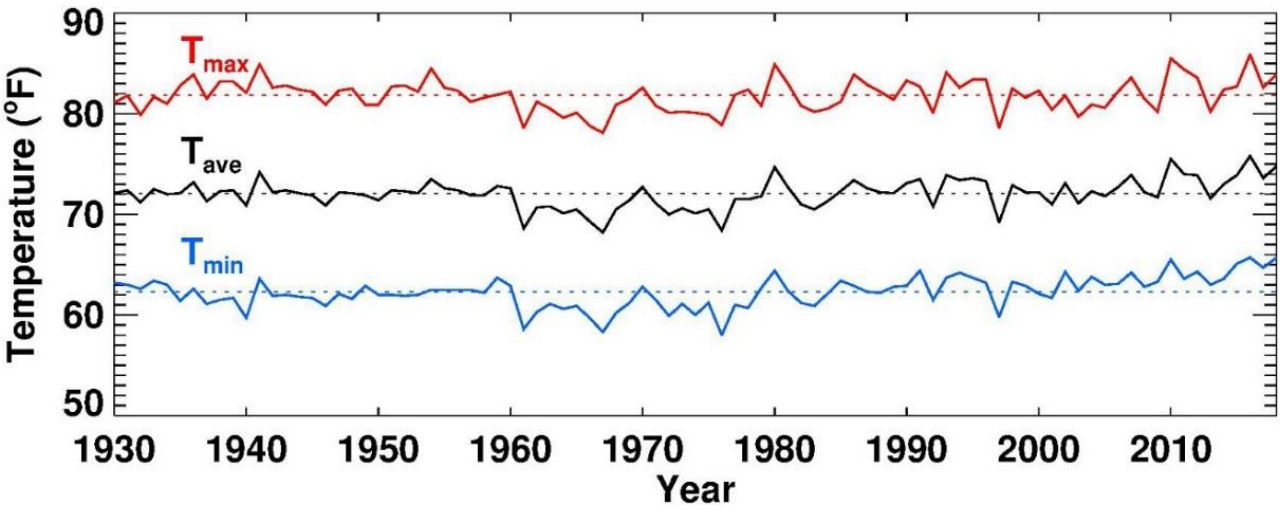

Figure 13. Mean values of maximum temperature (red), average temperature (black), and minimum temperature (blue) during the ozone season (April 1 – October 31) in Atlanta from 1930 to 2018. Data were downloaded from NOAA/NCEI (https://www.ncdc.noaa.gov/).

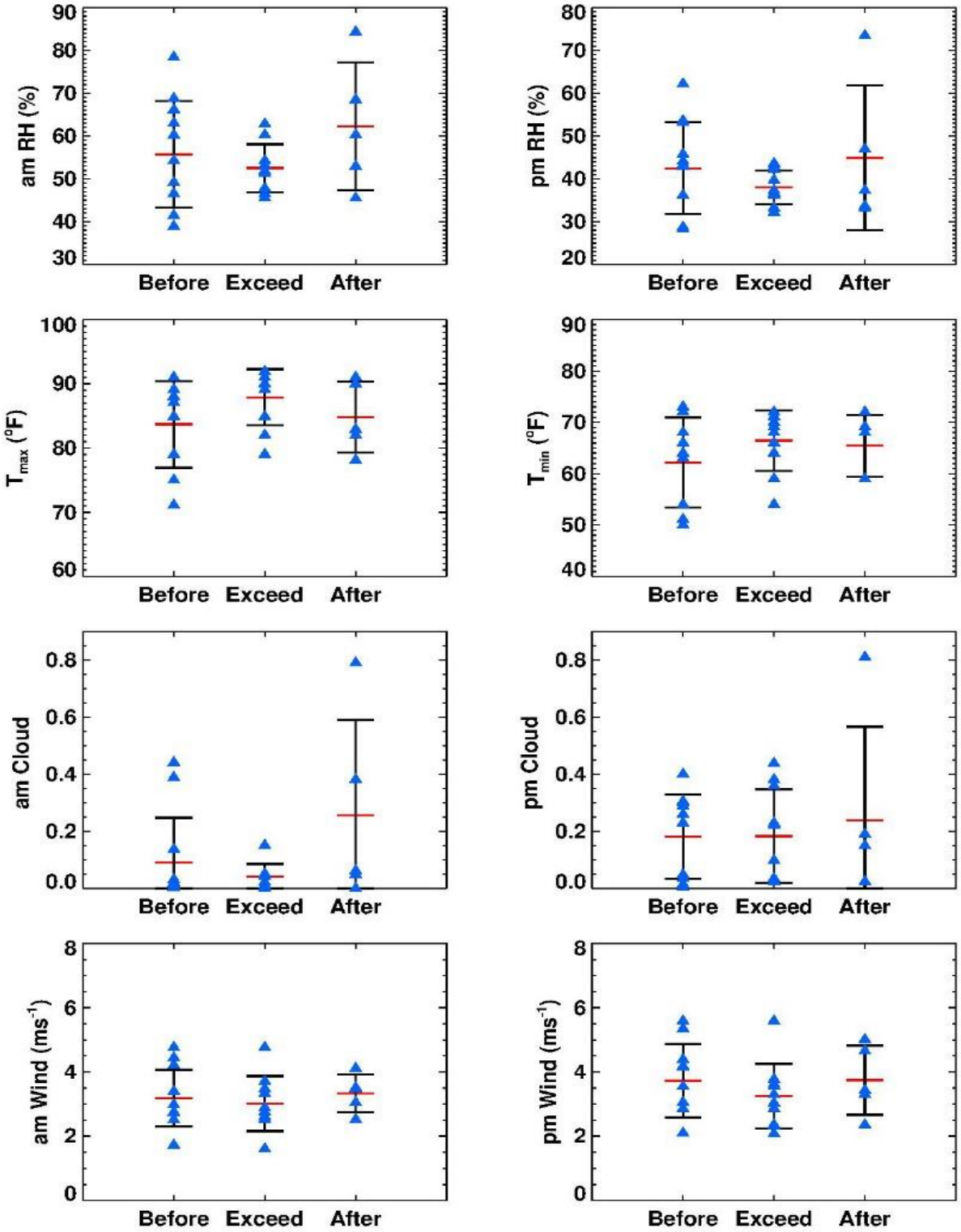

Figure 14. Comparisons of meteorological variables in 2018 on the ozone exceedance days/events and the day before/after the exceedance. The red bar is the mean, and the upper and lower bars (black) represent the standard deviations. All samples are shown (blue triangles).

4. Ozone Regression Analysis

Multiple linear regression (MLR) analysis was previously used to quantify the relationship between Atlanta MDA8O3 and environmental variables in a study (Cardelino, 2011). In this 2011 study, 15 environmental variables (O_3-day1, weekday, and Julian day in addition to 12 meteorological variables) were used (Table 6). O_3-day1 is used to represent chemical production background assuming slow changes, weekday is used to represent emissions variation due to human activities, and Julian day is used to represent the variations of solar radiation throughout the ozone season. In the 2016 final ozone exceedance report, two additional environmental variables (relh1 and relh2) were added in the MLR analysis. In the 2017 report, Julian day (which shows very poor correlation with ozone in the 2016 MLR analysis) is replaced by the daily maximum solar elevation angle (SunAngle) to better represent the intensity of solar radiation (Table 6).

For this analysis, daily data of MDA8O3 and 17 environmental factors are used in the MLR to build a linear relationship of Atlanta MDA8O3 and environmental factors assuming independency among these environmental factors:

$$y = \alpha_0 + \sum_{i=1}^{i=17} \alpha_i x_i$$

where, y stands for MDA8O3, x_i stands for the environmental factor, α_0 is an adjustment factor, and α_i is a weighting factor.

The correlation coefficients of MDA8O3 and the 17 environmental variables during ozone season were calculated for different years during 1990-2018 in Atlanta (Table 7 and Figure 15). The difference of correlation coefficients among different years illustrates how the relationships between Atlanta MDA8O3 and environmental variables changed through the years. The ranking of correlation coefficients is similar for different years. The top 6 most correlated environment variables (i.e., variables with the top 6 highest absolute r) are ozone level one day ago, AM and PM relative humidity, AM and PM cloud coverage, and daily max temperature. The daily maximum 8-hour average ozone one day ago (O_3-Day1) is the most correlated environmental variable except in 2017. Daily max temperature is the 2nd most correlated environmental variable before 2000, and PM relative humidity is the 2nd most correlated environmental variable after 2000. Daily maximum solar elevation angle, the newly introduced variable, ranks right after the 6 most important variables (r=0.337) in 1990-2018. In 2018, daily maximum 8-hour average ozone one day ago was the top correlated variable. The cloud coverage and relative humidity for both AM and PM are the next top 4 variables. The correlation for the daily maximum temperature is moderate in 2018 even though it has the 2nd highest overall correlation with ozone in 1990-2018.

In general, the ozone exceedance days were associated with the following meteorological conditions:

1. High ozone on previous days (persistence)
2. Low relative humidity (dry)
3. High daily temperature (hot)
4. Low cloud coverage (high solar radiation)
5. Relatively low wind speed (calm)

Table 6. Daily variables used for the MLR analysis

Name	Definition	Formula	Unit
Tmax	Daily maximum temperature	max(tmpf)	degree of Fahrenheit
Tmin	Daily minimum temperature	min(tmpf)	degree of Fahrenheit
TDmax	Daily maximum dew point temperature	max(dwpf)	degree of Fahrenheit
TDmin	Daily minimum dew point temperature	min(dwpf)	degree of Fahrenheit
Pres1	Mean surface pressure in the morning (6-12 pm)	mean(mlsp $_{(6\text{-}12)}$)	millibar
Pres2	Mean surface pressure in the afternoon (12-6 pm)	mean(mlsp $_{(12\text{-}18)}$)	millibar
WDir1	Mean wind direction in the morning (6-12 pm)	mean(drct $_{(6\text{-}12)}$)	degree from north
WDir2	Mean wind direction in the afternoon (12-6 pm)	mean(drct $_{(12\text{-}18)}$)	degree from north
WSpd1	Mean wind speed in the morning (6-12 pm)	mean(sknt $_{(6\text{-}12)}$)	m/s
WSpd2	Mean wind speed in the afternoon (12-6 pm)	mean(sknt $_{(12\text{-}18)}$)	m/s
Sky1	Mean cloud coverage in the morning (6-12 pm)	mean(max(skyc1,skyc2,skyc3,skyc4) $_{(6\text{-}12)}$)	%
Sky2	Mean cloud coverage in the afternoon (12-6 pm)	mean(max(skyc1,skyc2,skyc3,skyc4) $_{(12\text{-}18)}$)	%
O3-Day1	Daily Maximum 8-hr average ozone one day ago	-	ppbv
WkDay	Day of week	Weekday(date)	n/a
SunAngle	Daily maximum solar elevation angle	See equations (1) and (2) below	degree
Relh1*	Mean relative humidity in the morning (6-12 pm)	mean(relh $_{(6\text{-}12)}$)	%
Relh2*	Mean relative humidity in the afternoon (12-6 pm)	mean(relh $_{(12\text{-}18)}$)	%

(1) Solar declination, $\delta = 23.45^{o} sin\left[\frac{Julian\ Day+284}{365} \times 360^{o}\right]$

(2) Daily maximum solar elevation angle, $\propto = asin(\cos(latitude)\cos\delta + \sin(latitude)\, sin\delta)$

Table 7. Correlation coefficients of MDA8O3 and environmental variables during ozone season by time periods during 1990-2018 in the Metro Atlanta area.

Name	1990-2018	1990-1999	2000-2009	2010-2018	2017	2018
O3-Day1	**0.715**	**0.702**	**0.723**	**0.66**	0.636	**0.67**
Sky1	-0.468	-0.508	-0.505	-0.501	-0.667	-0.618
Sky2	-0.345	-0.354	-0.393	-0.393	-0.518	-0.481
Tmax	0.534	0.609	0.584	0.474	0.391	0.313
Tmin	0.262	0.34	0.299	0.174	0.021	0.011
Tdmax	0.087	0.177	0.069	-0.03	-0.182	-0.126
Tdmin	0.076	0.174	0.058	-0.051	-0.173	-0.139
SunAngle	0.337	0.345	0.411	0.268	0.073	0.336
Pres1	0.028	-0.045	0.057	0.058	0.192	0.205
Pres2	0.019	-0.081	0.031	0.052	0.174	0.197
WDir1	0.075	0.153	0.049	-0.003	-0.05	0.174
WDir2	0.101	0.192	0.058	0.028	-0.055	0.19
WSpd1	-0.26	-0.33	-0.257	-0.288	-0.333	-0.269
WSpd2	-0.213	-0.255	-0.215	-0.237	-0.31	-0.217
Relh1	-0.475	-0.476	-0.543	-0.569	**-0.682**	-0.6
Relh2	-0.522	-0.501	-0.583	-0.605	-0.665	-0.615
WkDay	-0.018	0	-0.03	-0.036	-0.043	-0.013

Note: Top 6 absolute values are highlighted in red. The highest absolute value is in bold.

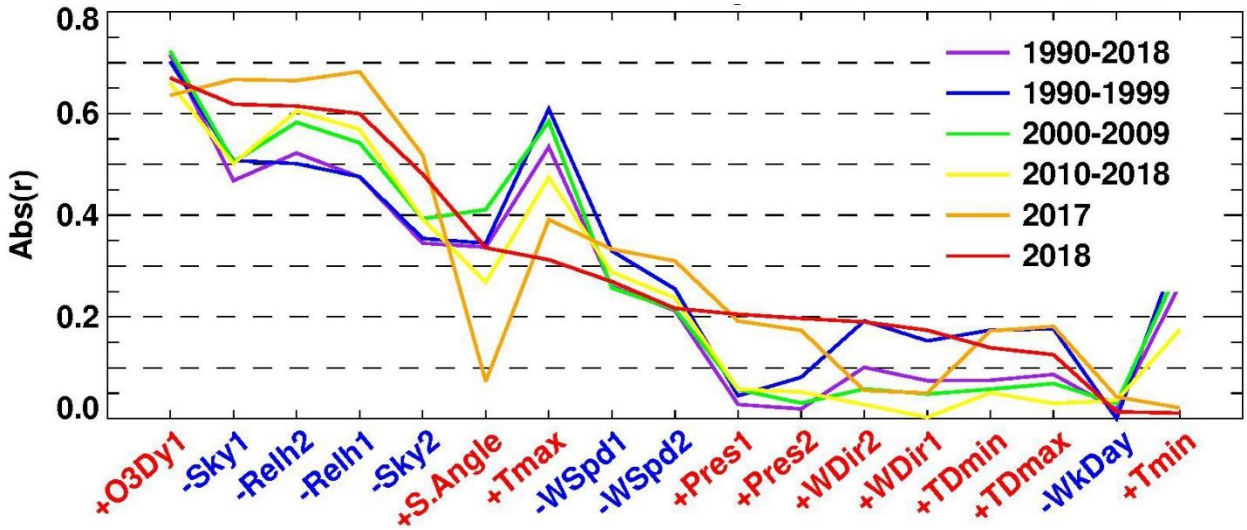

Figure 15. Correlation coefficients of MDA8O3 and environmental variables during ozone season by time periods during 1990-2018 in Atlanta. Variables with positive correlation with MDA8O3 are labeled in red, and variables with negative correlation are labeled in blue.

The above meteorological conditions favor the chemical production of ozone in the lower troposphere. Low relative humidity may reduce the ozone loss through the reaction with water vapor (Seinfeld and Pandis, 1998). Ozone formation increases with high temperatures and low cloud coverage due to higher solar radiation, leading to more active ozone production. High ozone on previous days indicates that the ozone buildup was a multiple-day process. Calm conditions correspond to poor dispersion and less regional transport, indicating that the local ozone production is important for ozone exceedances in Atlanta.

The MLR ozone model was first updated using 2011-2018 observation data, and then used to predict 2018 ozone conditions. Performance of the updated MLR ozone models were evaluated by comparing the predictions with 2018 ozone observations (Table 8). The updated MLR ozone model can explain about 70% of the ozone variance (or R^2). The mean bias (MB) and normalized mean bias (NMB) are only reduced slightly by using recent data (i.e., MB and NMB for 2013-2017 are less than those for 2012-2017 and 2011-2017). The Mean Absolute Error (MAE), Normalized Mean Error (NME), and Root Mean Square Error (RMSE) are also similar among the updated MLR ozone models. The MLR model based on the 2012-2018 data is recommended to be used for future ozone forecast. The coefficients of the MLR ozone model with 2012-2018 dataset are listed in Table 9.

Table 8. Performance of updated MLR ozone model using various datasets during 2011-2018.

Data range	R	R^2	MB[a]	MAE[a]	NMB[a]	NME[a]	RMSE[a]
2011-2018	0.839	0.704	0.933	5.778	1.9%	11.9%	7.192
2012-2018	0.841	0.707	0.66	5.692	1.4%	11.7%	7.097
2013-2018	0.841	0.708	0.527	5.697	1.1%	11.7%	7.076
2011-2017	0.83	0.689	1.191	5.936	2.4%	12.2%	7.414
2012-2017	0.832	0.693	0.865	5.828	1.8%	12.0%	7.293
2013-2017	0.831	0.691	0.703	5.844	1.4%	12.0%	7.293

[a]MB is Mean Bias, MAE is Mean Absolute Error, NMB is Normalized Mean Bias, NME is Normalized Mean Error, RMSE is Root Mean Square Error.

Table 9. The coefficients of the MLR ozone model using dataset during 2012-2018.

Variable	Coefficient	Variable	Coefficient	Variable	Coefficient
O3-Day1	0.35325	Tdmin	-0.07256	WSpd1	-0.17712
Sky1	-2.49579	SunAngle	-0.11154	WSpd2	-0.72501
Sky2	0.03748	Pres1	-0.46102	Relh1	-0.06457
Tmax	0.28067	Pres2	0.11258	Relh2	-0.38795
Tmin	-0.26677	WDir1	-0.00656	WkDay	-0.54249
Tdmax	0.15788	WDir2	-0.00383	Constant	368.76019

5. Ozone and Meteorological Conditions

Impacts of meteorological conditions on ozone formation and transport were investigated with ozone and meteorological condition time series plots, Hybrid Single Particle Lagrangian Integrated Trajectory (HYSPLIT, http://www.arl.noaa.gov/HYSPLIT_info.php) back trajectory modeling, animation of ozone and wind conditions, and analysis of 1-minute ozone time series data.

5.1 Hourly Ozone and Meteorology Time Series Analysis

Time series of hourly ozone at all exceeding monitors during each exceedance period and corresponding meteorological variables (temperature, relative humidity, and solar radiation) at the South DeKalb monitor were developed (Figure 16 - Figure 21). The time series were developed for all exceedance days in the Metro Atlanta area when one or more ozone monitors exceeded the NAAQS. Each time series plot includes the data for one day before each exceedance. Ozone exceedances are associated with high temperature and low relative humidity, as well as high solar radiation as identified in the previous sections.

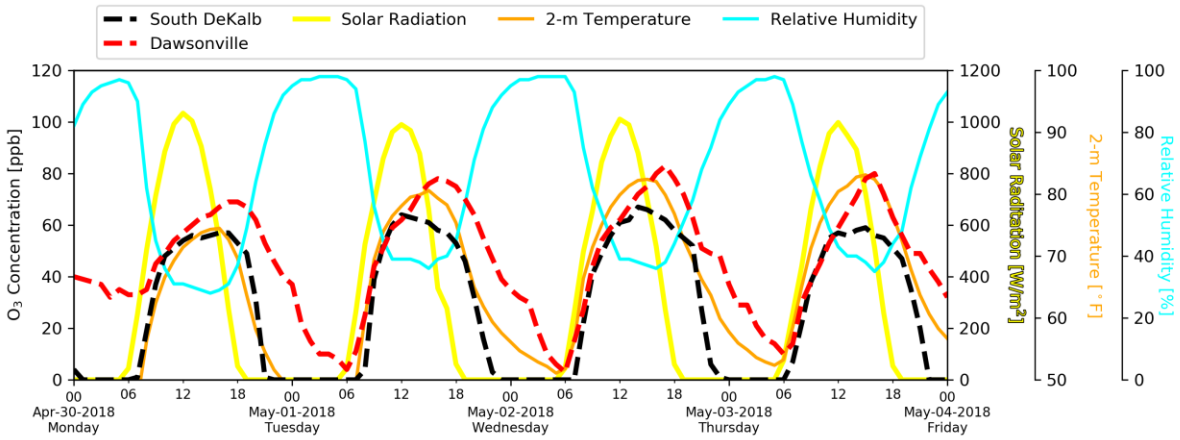

Figure 16. Time series of 1-hour ozone concentrations (left y-axis), solar radiation (the first right y-axis), 2-m temperature (the second right y-axis), and relative humidity (the rightmost y-axis) for April 30-May 3, 2018.

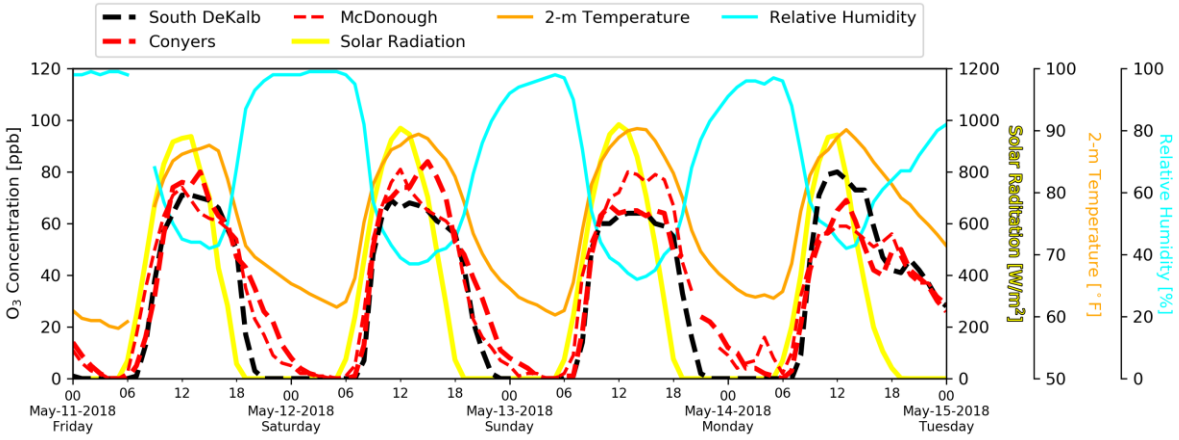

Figure 17. Time series of 1-hour ozone concentrations (left y-axis), solar radiation (the first right y-axis), 2-m temperature (the second right y-axis), and relative humidity (the rightmost y-axis) for May 11-14, 2018.

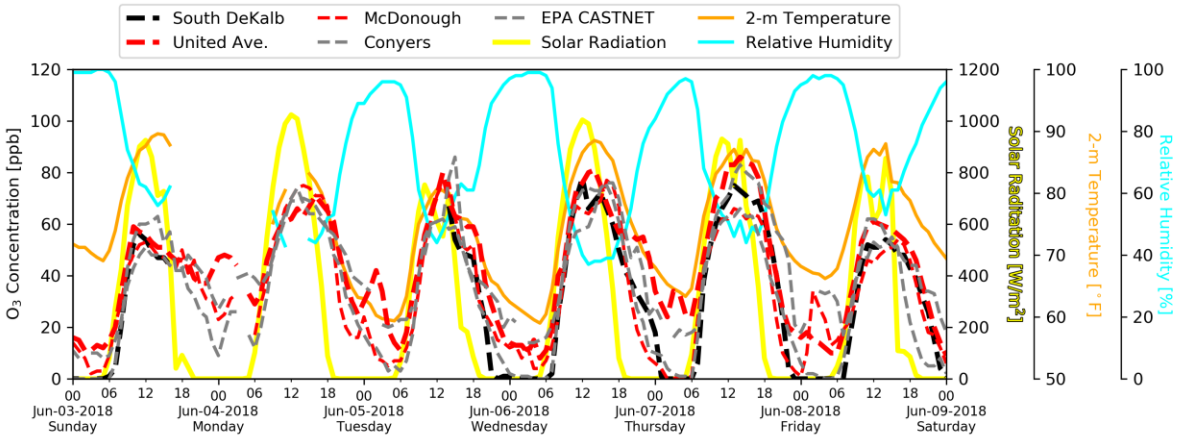

Figure 18. Time series of 1-hour ozone concentrations (left y-axis), solar radiation (the first right y-axis), 2-m temperature (the second right y-axis), and relative humidity (the rightmost y-axis) for June 3-8, 2018.

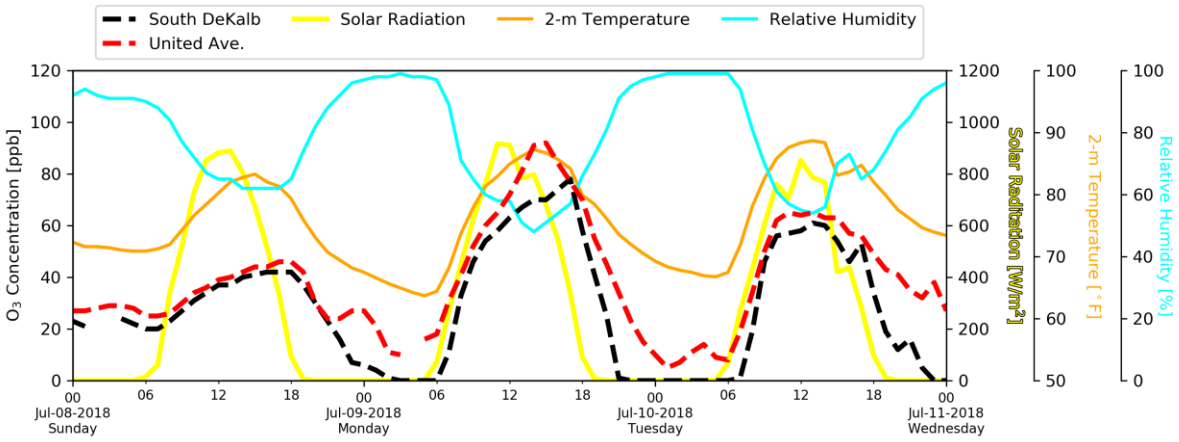

Figure 19. Time series of 1-hour ozone concentrations (left y-axis), solar radiation (the first right y-axis), 2-m temperature (the second right y-axis), and relative humidity (the rightmost y-axis) for July 8-10, 2018.

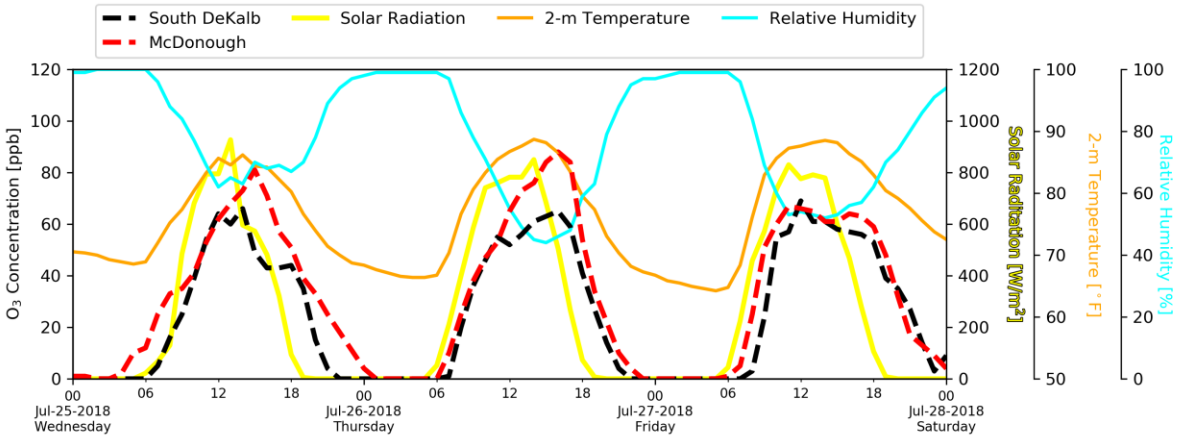

Figure 20. Time series of 1-hour ozone concentrations (left y-axis), solar radiation (the first right y-axis), 2-m temperature (the second right y-axis), and relative humidity (the rightmost y-axis) for July 25-27, 2018.

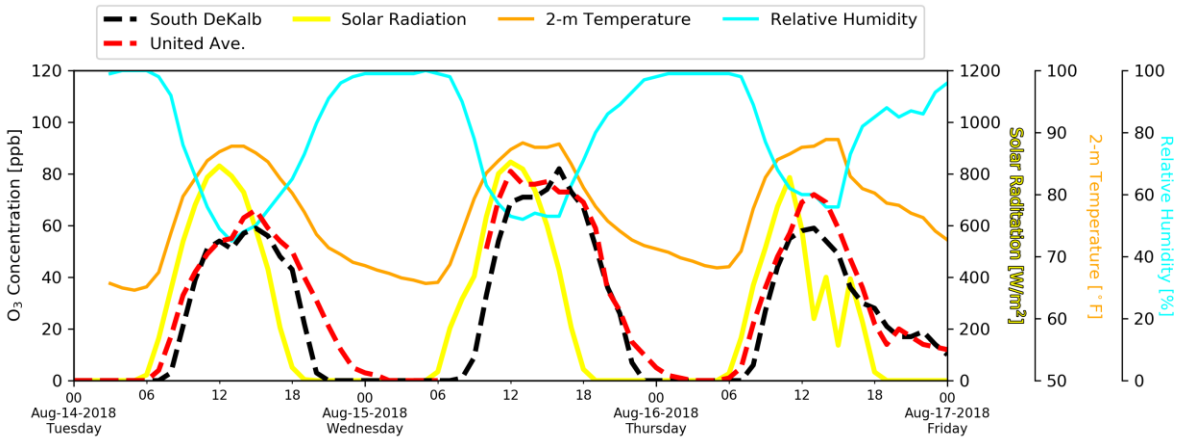

Figure 21. Time series of 1-hour ozone concentrations (left y-axis), solar radiation (the first right y-axis), 2-m temperature (the second right y-axis), and relative humidity (the rightmost y-axis) for August 14-16, 2018.

5.2 HYSPLIT Back Trajectory Analysis

The Hybrid Single Particle Lagrangian Integrated Trajectory (HYSPLIT) back trajectory analysis was conducted to determine the origin of air masses and establish source-receptor relationships on ozone exceedance days. The HYSPLIT model is one of the most extensively used atmospheric transport and dispersion models in the atmospheric sciences community. In this analysis, HYSPLIT 24-hour back-trajectories were computed for each ozone exceedance in 2018 at each exceeding ozone monitor in Atlanta using the North American Mesoscale (NAM) archive dataset[2] available at a 12-km resolution from National Oceanic and Atmospheric Administration (NOAA). For each 2018 ozone exceedance at a monitor, three back-trajectories were computed for air parcels ending at heights of 100 meters, 500 meters, and 1,000 meters at the time of the 1-hour peak ozone concentrations.

Figure 22-Figure 26 contain HYSPLIT trajectories for all exceeding monitors in 2018. The long trajectories are associated with higher wind speed and indicate more opportunities for transport impacts, while short or circular trajectories are associated with lower wind speeds and indicate stagnant or recirculation conditions and more opportunities for local impacts.

The trajectories for the height of 100 meters at exceedance monitors show mixed effects of a strong local impact and a long-range transport. The trajectories at the United Ave. monitor on June 7 and July 9, 2018 (Figure 22), the McDonough monitor on July 26, 2018 (Figure 23), the Conyers monitor on June 6, 2018 (Figure 25), and the EPA CASTNET monitor on June 7, 2018 were relatively long and indicate northerly or northeasterly winds were dominant. The trajectories at the United Ave. monitor on June 6 and August 15, 2018 (Figure 22), the McDonough monitor on May 13, 2018 (Figure 23), and the Conyers monitor on May 12, 2018 (Figure 25) were relatively short and indicate northwesterly winds were dominant. The trajectory at the McDonough monitor on June 4, 2018 (Figure 23) was relatively long and

[2] ftp://arlftp.arlhq.noaa.gov/archives/nam12/

indicate northerly winds were dominant. The trajectories at the Dawsonville monitor were relatively short and indicate southeasterly winds. Overall trajectories on exceedance days passed through nonattainment counties in the Metro Atlanta area. In 2018, no urban-scale recirculation was observed for exceedance days at a 100-m height. Based on these trajectory analysis results, exceedances in 2018 appear to be transport of ozone and precursors from the Atlanta urban core as well as local ozone production in the downtown Atlanta area.

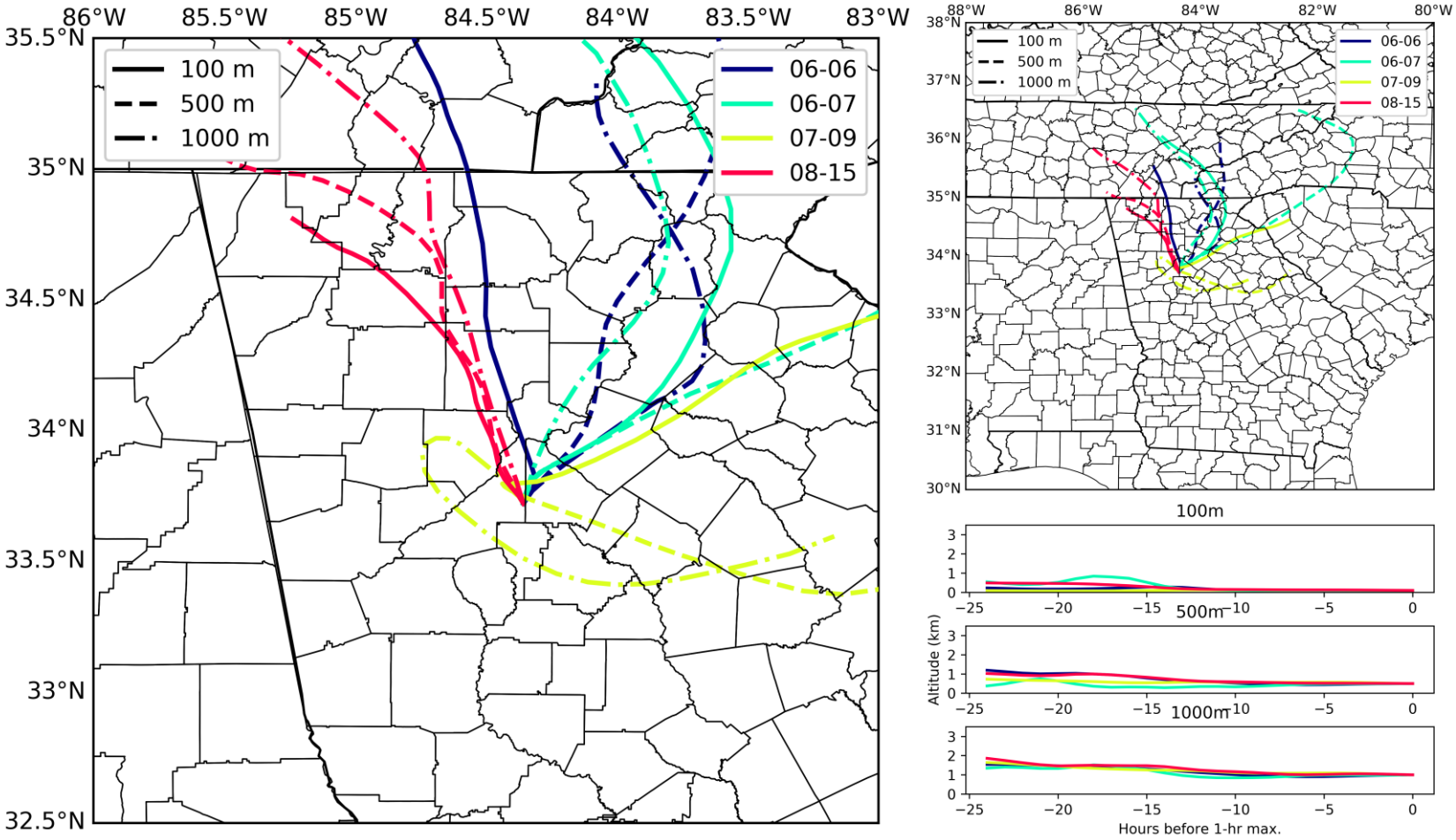

Figure 22. HYSPLIT 24 hour back-trajectories for exceedances at the United Ave. monitor and trajectory path heights.

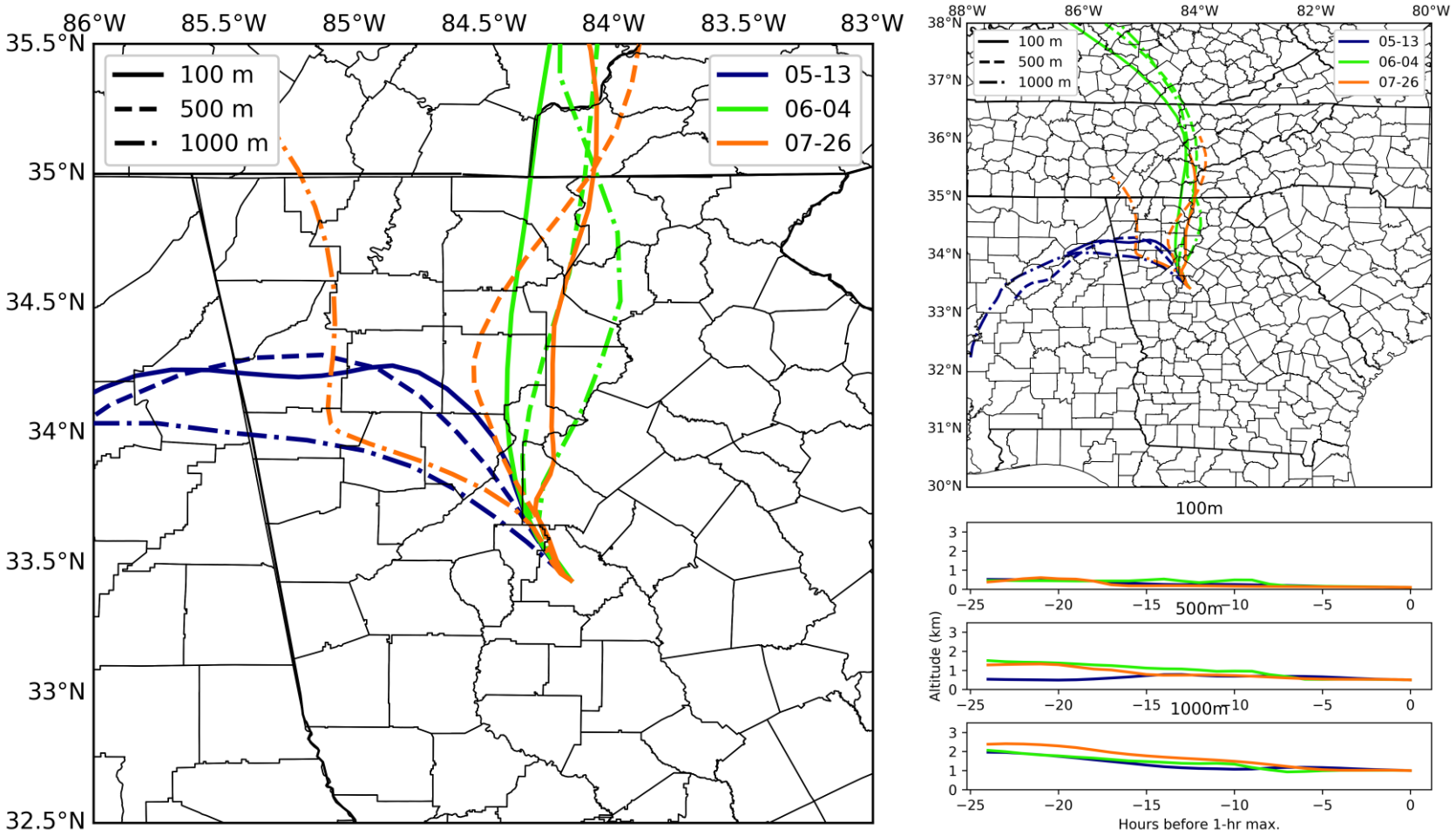

Figure 23. HYSPLIT 24 hour back-trajectories for exceedances at the McDonough monitor and trajectory path heights.

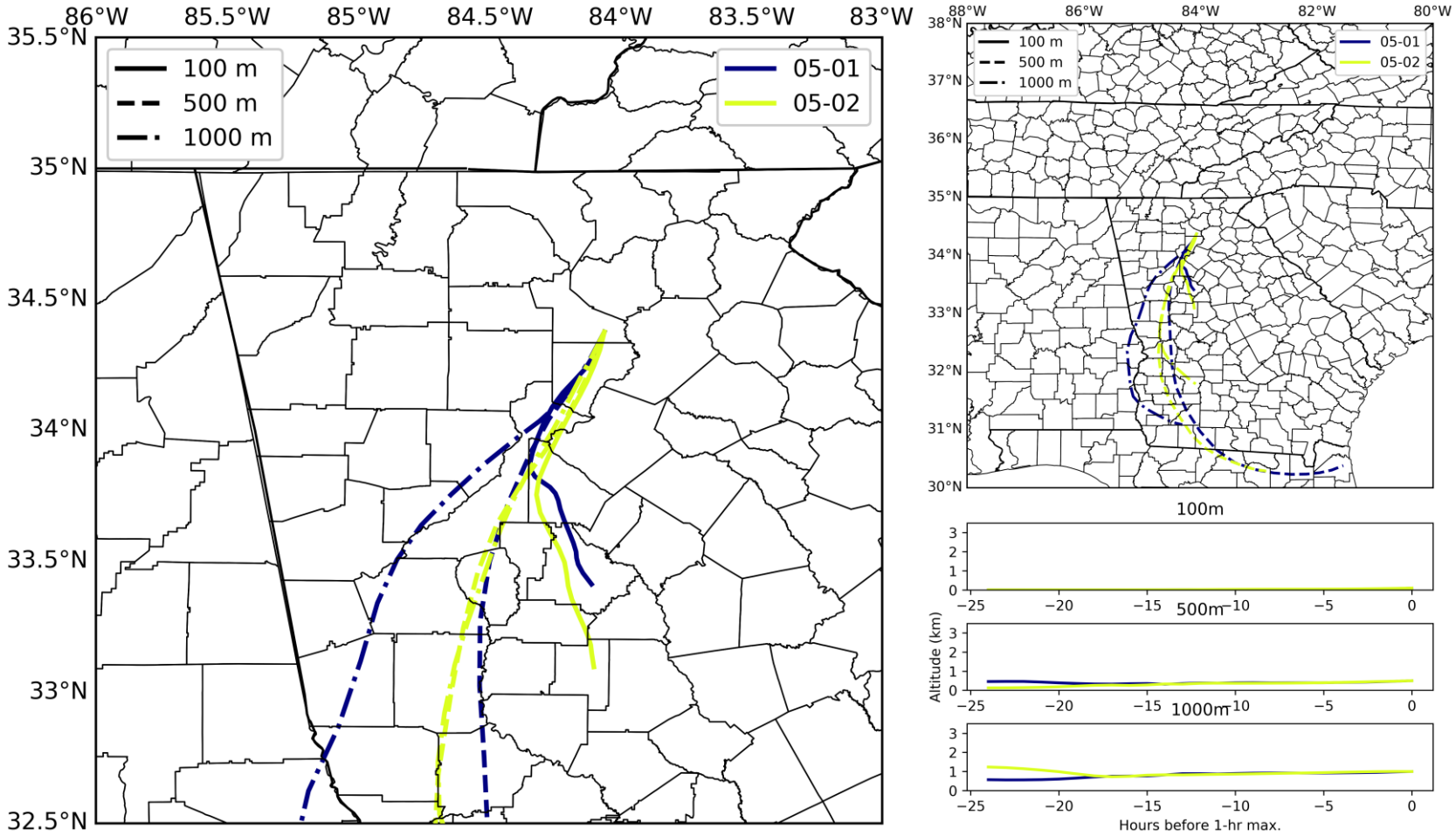

Figure 24. HYSPLIT 24 hour back-trajectories for exceedances at the Dawsonville monitor and trajectory path heights.

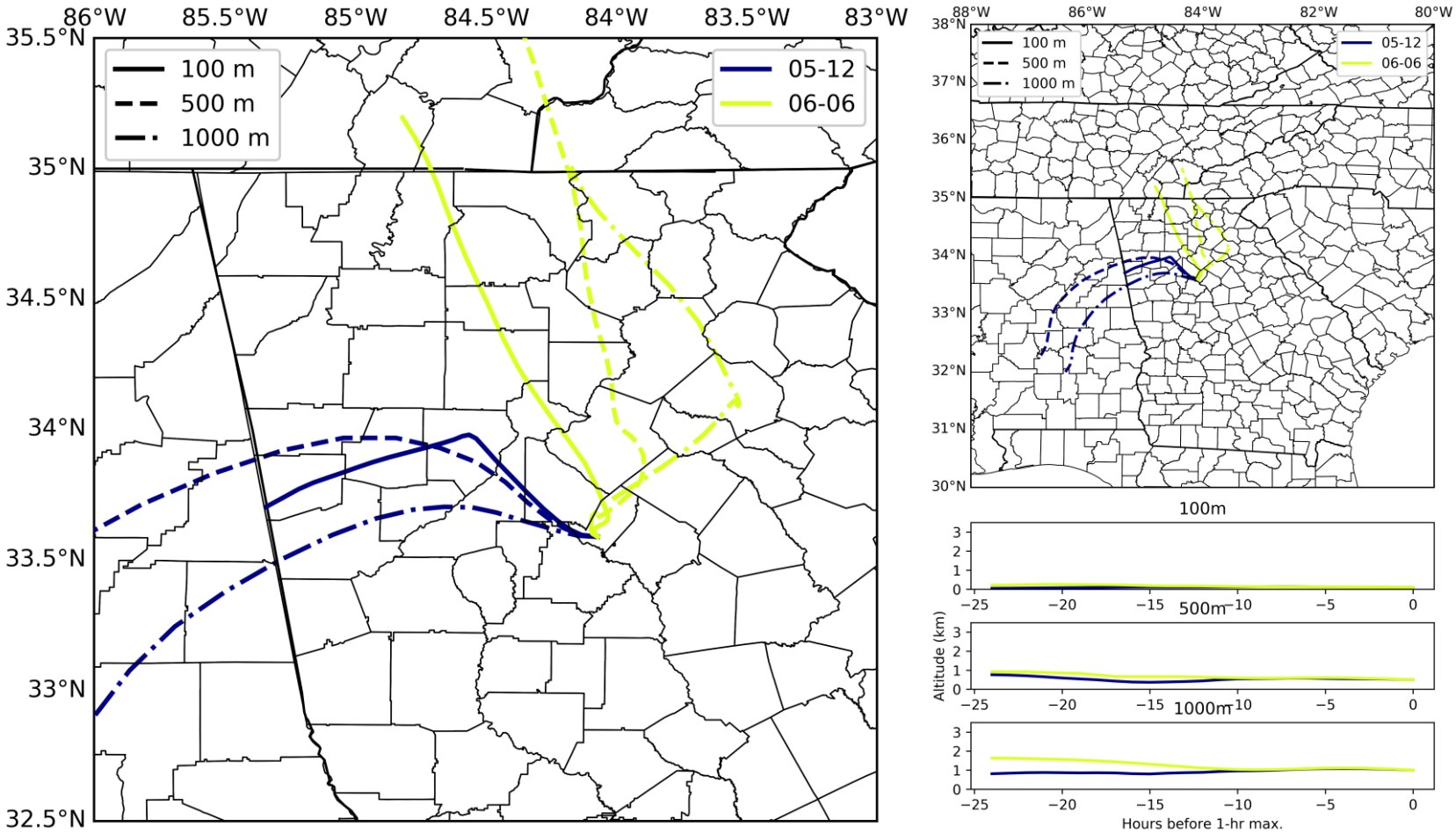

Figure 25. HYSPLIT 24 hour back-trajectories for exceedances at the Conyers monitor and trajectory path heights.

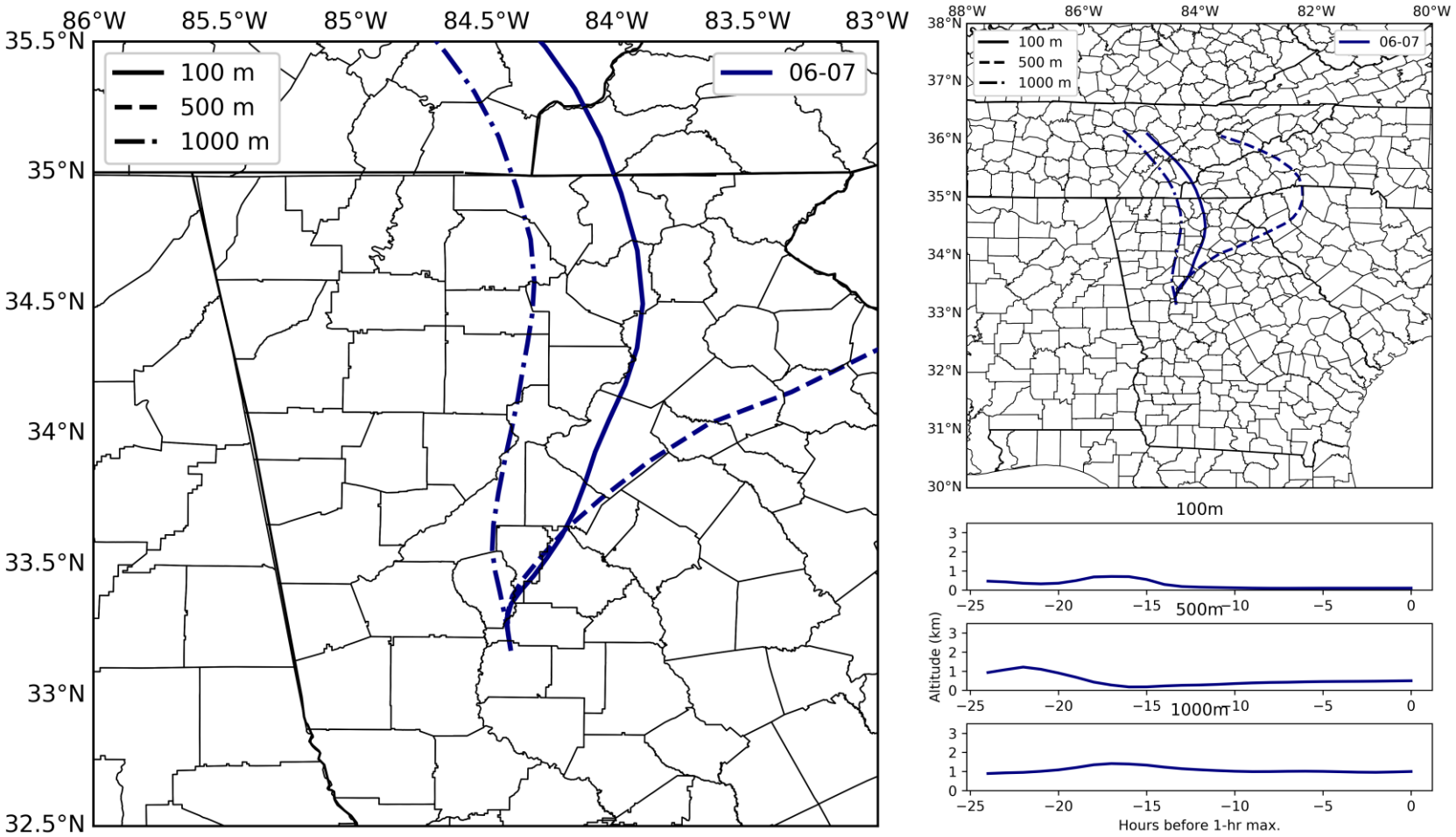

Figure 26. HYSPLIT 24 hour back-trajectories for exceedances at the EPA CASTNET monitor and trajectory path heights.

5.3 Animation of Ozone and Wind Conditions

Animation of 5-minute ozone concentrations and wind conditions were developed for the 10 ozone exceedance days in 2018 over 4-km grids covering the Metro Atlanta area in order to further understand the formation and transport of ozone. The 5-minute ozone concentrations were calculated using 1-minute observations at ozone monitors collected by the Ambient Monitoring Program. The 5-minute surface wind conditions were simulated using the Weather Research and Forecasting (WRF) model (v3.9.1.1). WRF was first run for the 12-km domain over the eastern United States (69×68 grids) and then run for the 4-km nested domain over Georgia (148×145 grids) (Figure 27) with the NAM analysis meteorological data downloaded from NOAA FTP server (ftp://nomads.ncdc.noaa.gov/NAM/analysis_only/). The WRF configuration for physics and dynamics was the same as EPA's 2016 WRF modeling setup. Thirty-five (35) vertical layers extending up to 50 mb were used. The simulation episode was 36 hours for each exceedance day with 6 spin-up hours. The 5-minute ozone data at monitors were further processed to 4-km WRF grids using Kriging 2D interpolation method with IDL[3] and plotted together with 5-minute WRF simulated wind data to generate 288 figures (24 hours/day x 12 figures/hour) in postscript format for each exceedance day. These postscript format figures were then processed to a GIF animation using Linux scripts.

For each exceedance day, sixteen hourly ozone and wind condition plots (7:00 AM to 10:00 PM) were shown below (Figure 28-Figure 37). For ozone exceedances that occurred outside of the Atlanta urban core, the general pattern is that wind blew from the urban core to the exceedance monitor (e.g., Figure 28). For ozone exceedances inside the Atlanta urban core, wind speeds were generally low (e.g. Figure 35). The animations dynamically demonstrate the Atlanta urban core as the origin of most high ozone events.

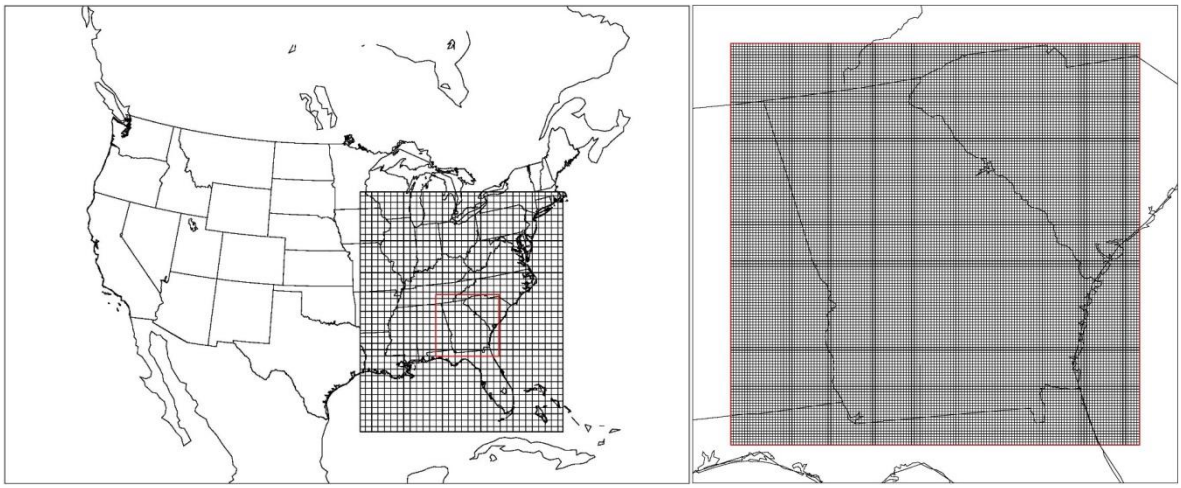

Figure 27. WRF 12-km domain over the eastern United States (left) and 4-km nested domain over Georgia (right).

[3] https://www.harrisgeospatial.com/SoftwareTechnology/IDL.aspx

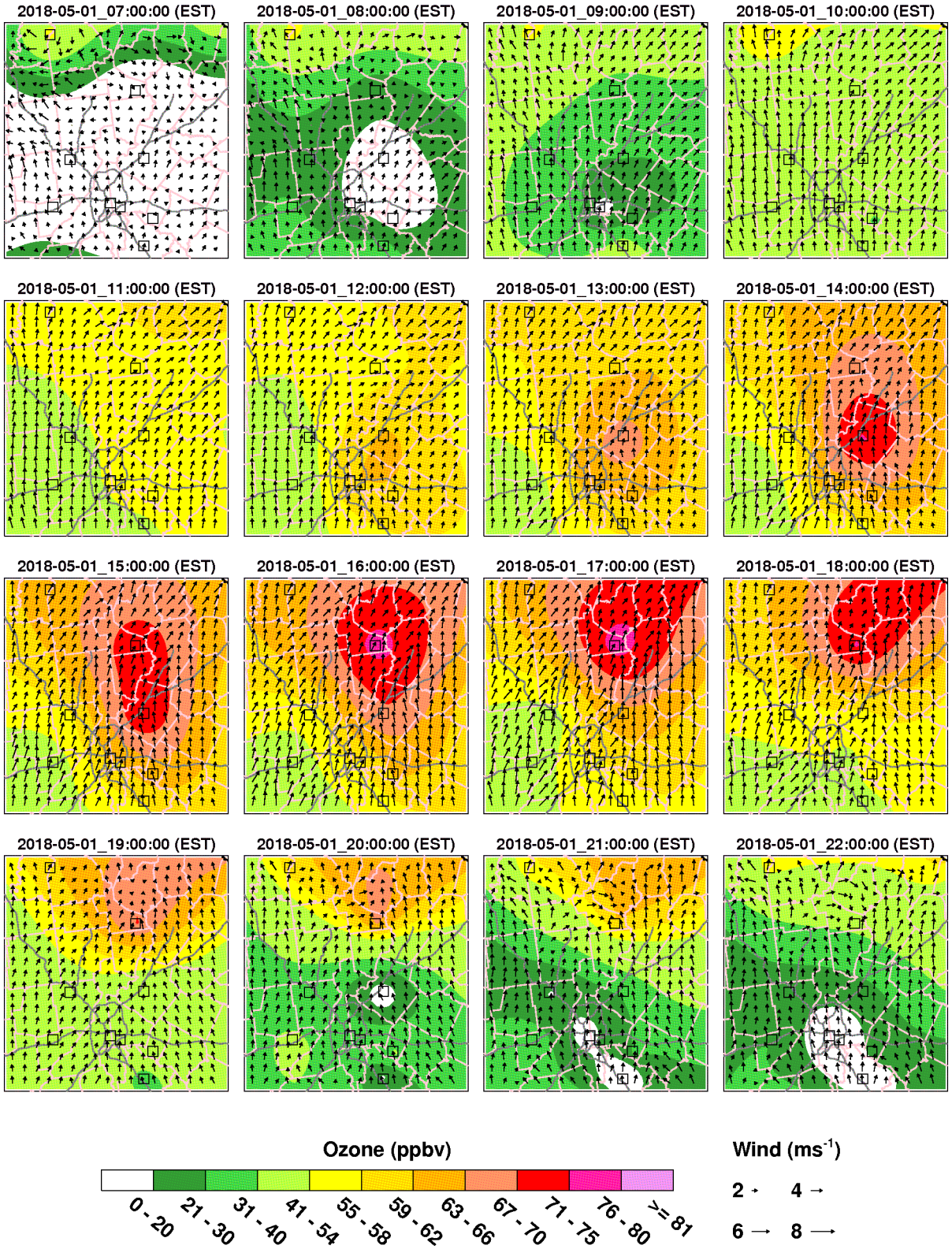

Figure 28. WRF simulated wind barbs and ozone observations (ppb) over the Metro Atlanta area from 7 AM to 10 PM on May 1, 2018. Ozone monitors are in black squares. The ozone exceedance occurred at the Dawsonville monitor.

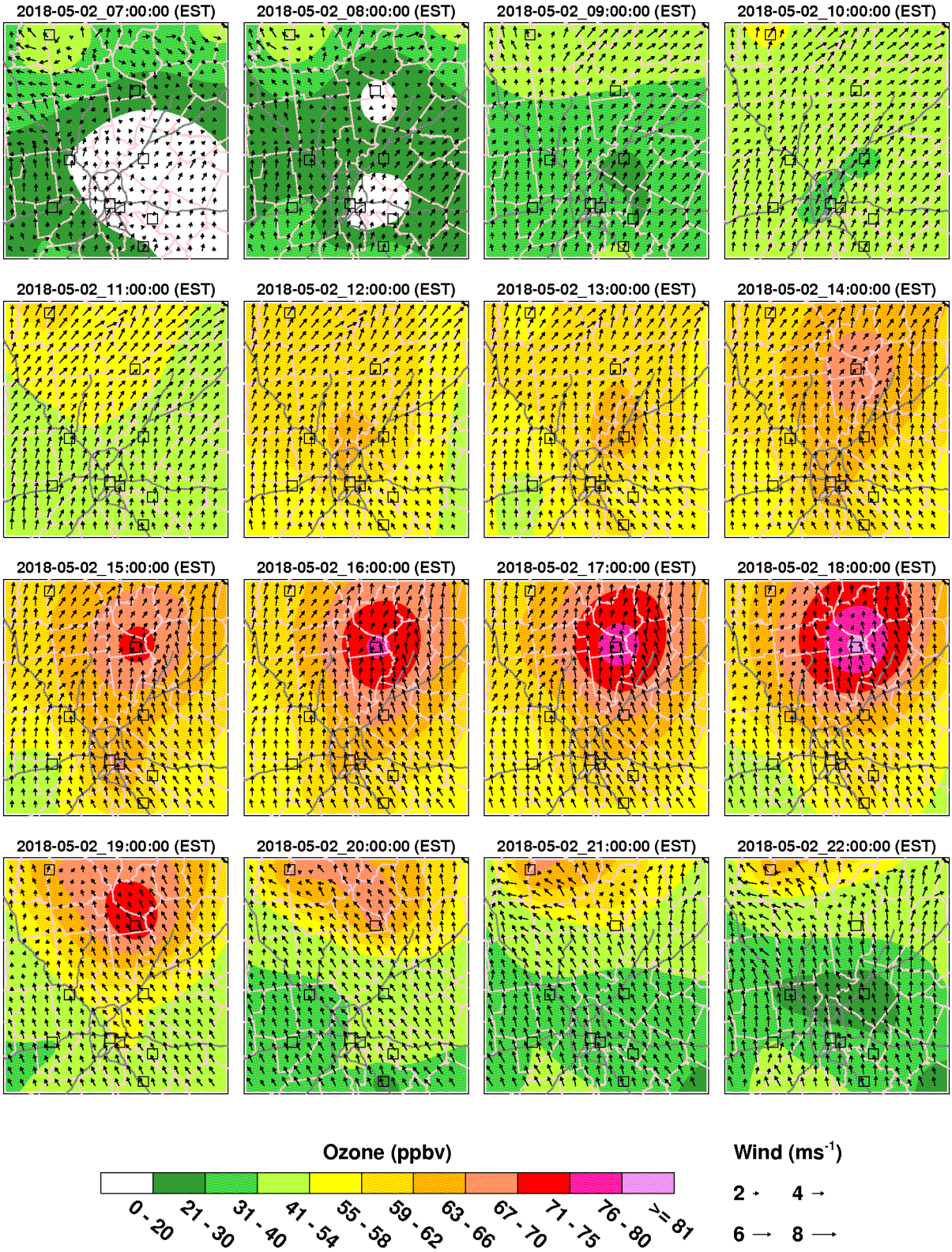

Figure 29. WRF simulated wind barbs and ozone observations (ppb) over the Metro Atlanta area from 7 AM to 10 PM on May 2, 2018. Ozone monitors are in black squares. The ozone exceedances occurred at the Dawsonville monitor.

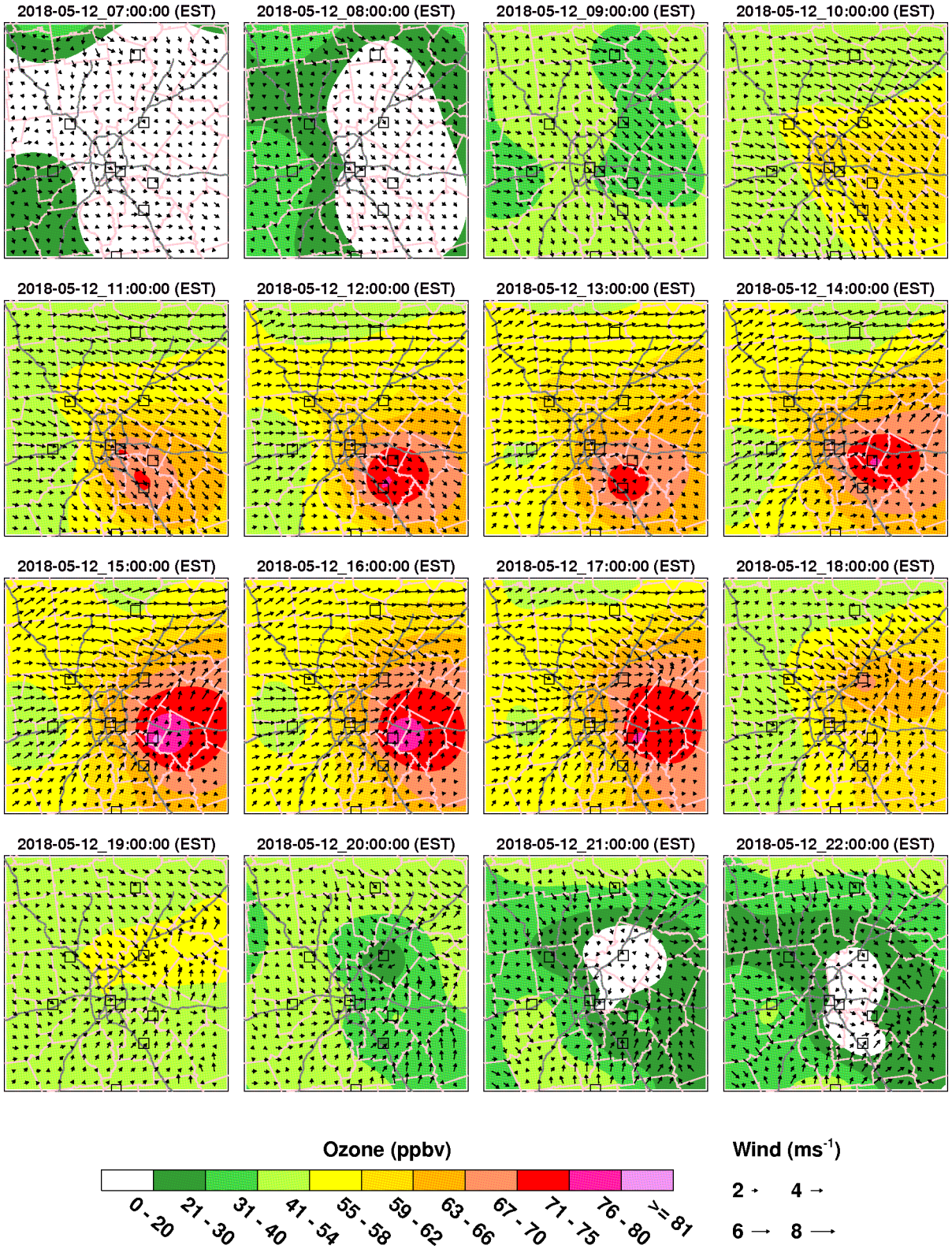

Figure 30. WRF simulated wind barbs and ozone observations (ppb) over the Metro Atlanta area from 7 AM to 10 PM on May 12, 2018. Ozone monitors are in black squares. The ozone exceedance occurred at the Conyers monitor.

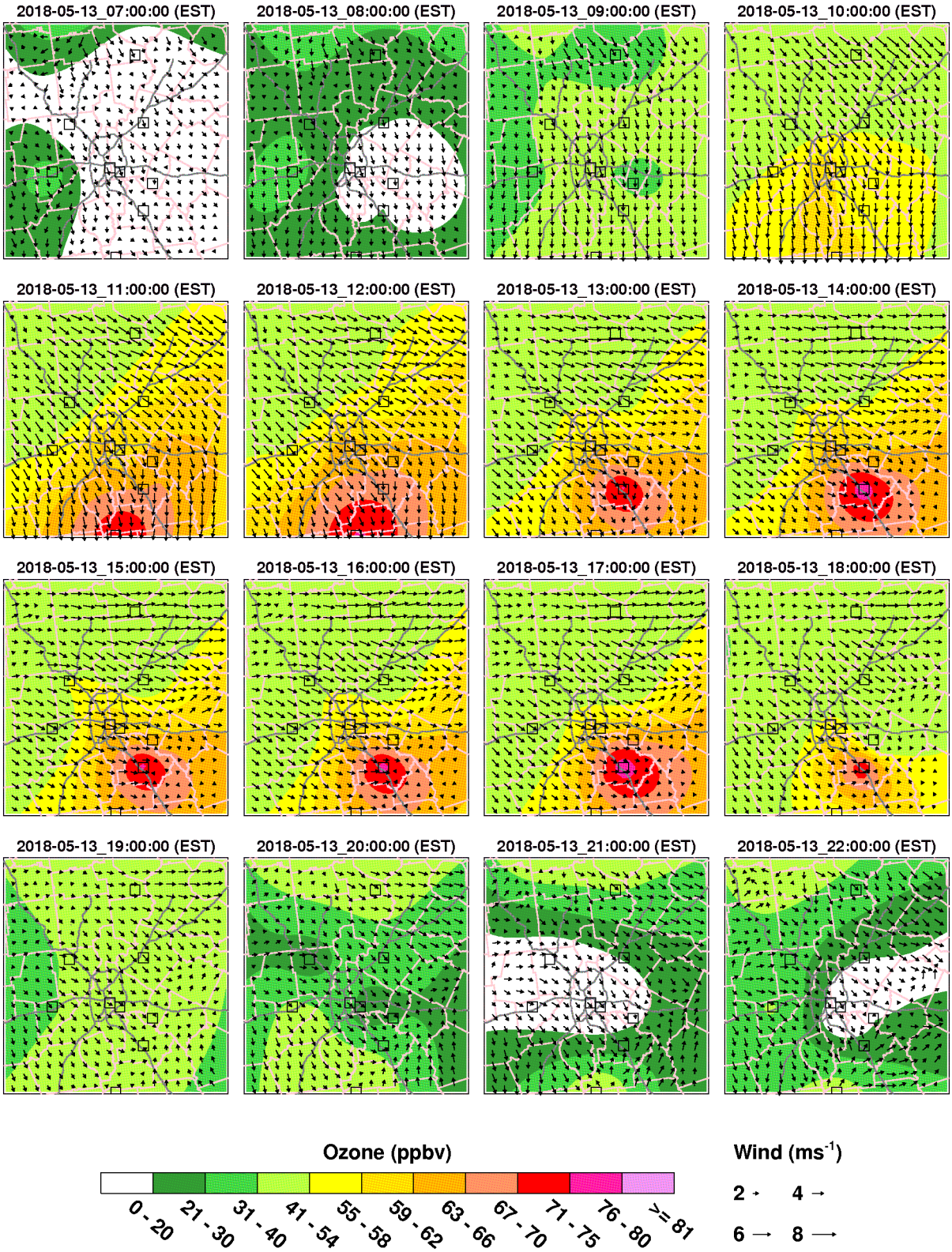

Figure 31. WRF simulated wind barbs and ozone observations (ppb) over the Metro Atlanta area from 7 AM to 10 PM on May 13, 2018. Ozone monitors are in black squares. The ozone exceedance occurred at the McDonough monitor.

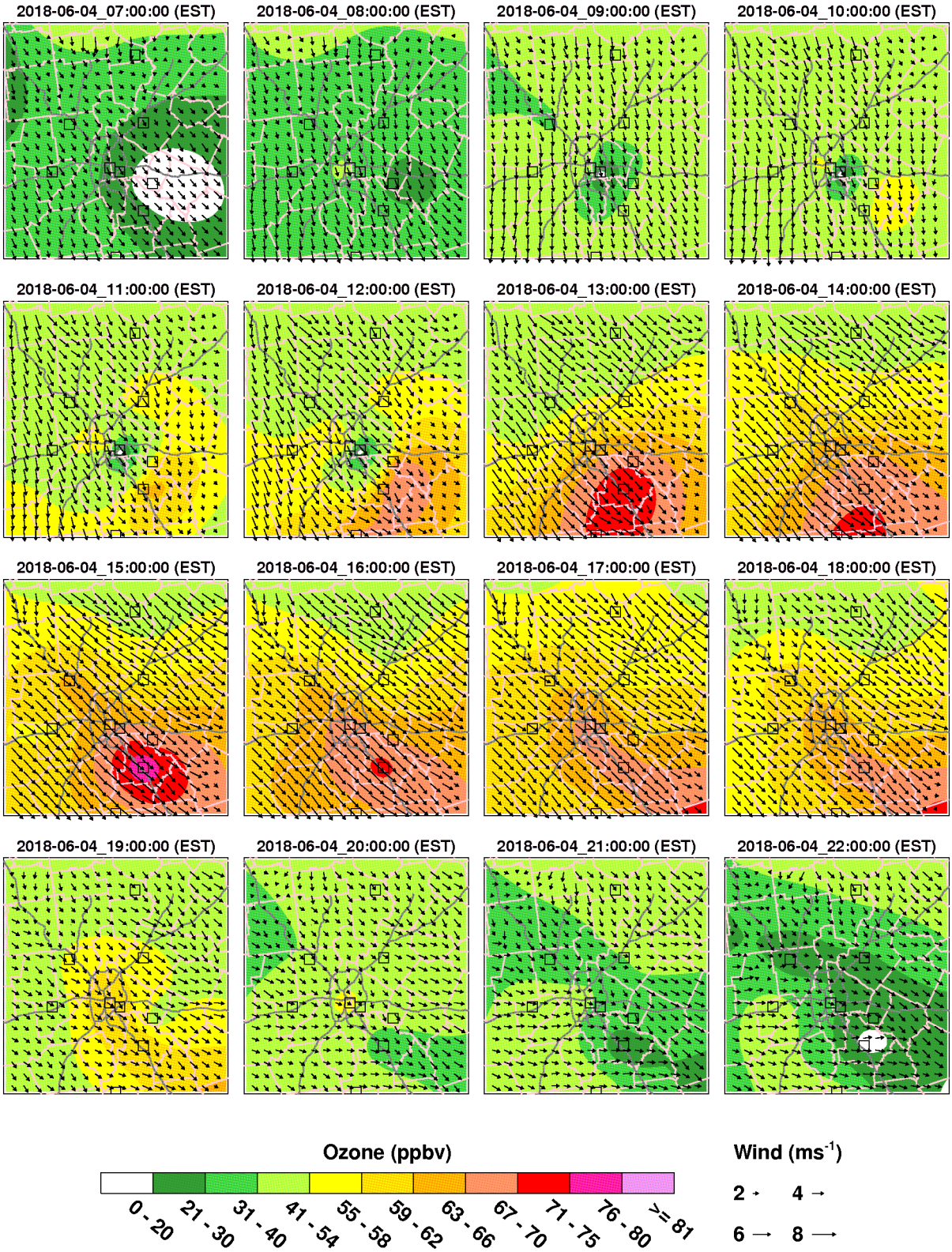

Figure 32. WRF simulated wind barbs and ozone observations (ppb) over the Metro Atlanta area from 7 AM to 10 PM on June 4, 2018. Ozone monitors are in black squares. The ozone exceedances occurred at the McDonough monitor.

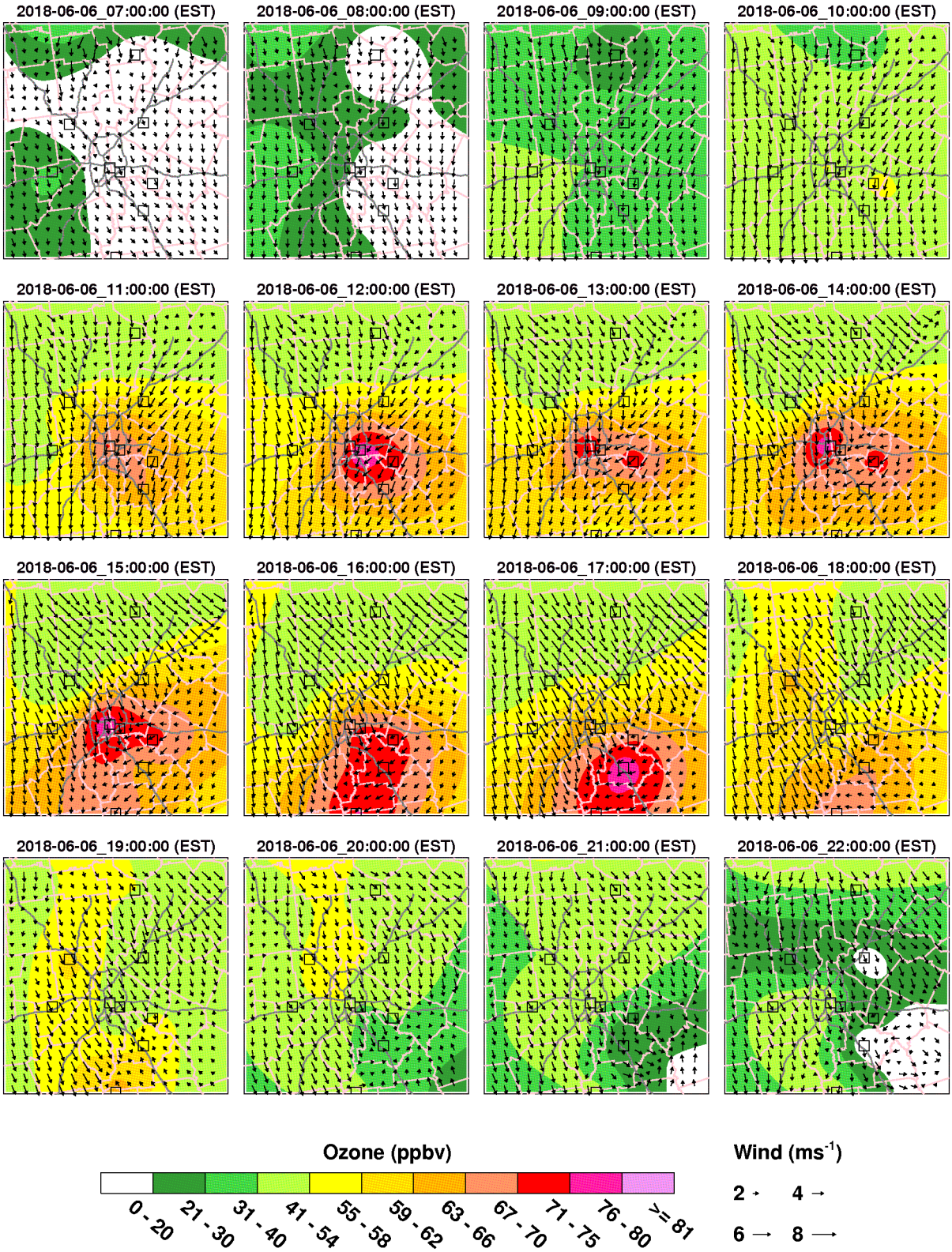

Figure 33. WRF simulated wind barbs and ozone observations (ppb) over the Metro Atlanta area from 7 AM to 10 PM on June 6, 2018. Ozone monitors are in black squares. The ozone exceedance occurred at the United Ave. and Conyers monitors.

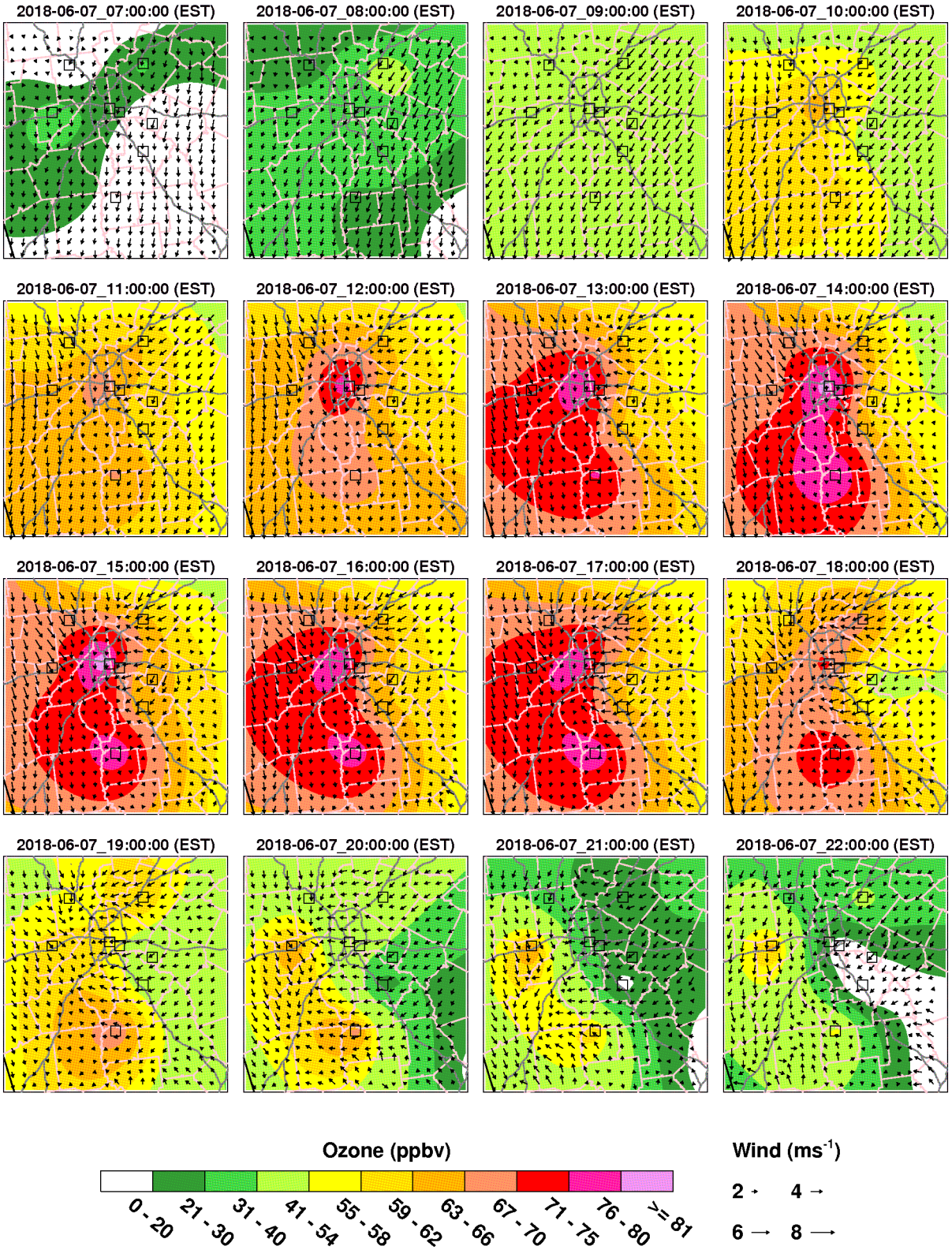

Figure 34. WRF simulated wind barbs and ozone observations (ppb) over the Metro Atlanta area from 7 AM to 10 PM m on June 7, 2018. Ozone monitors are in black squares. The ozone exceedance occurred at the United Ave. and EPA CASTNET monitors.

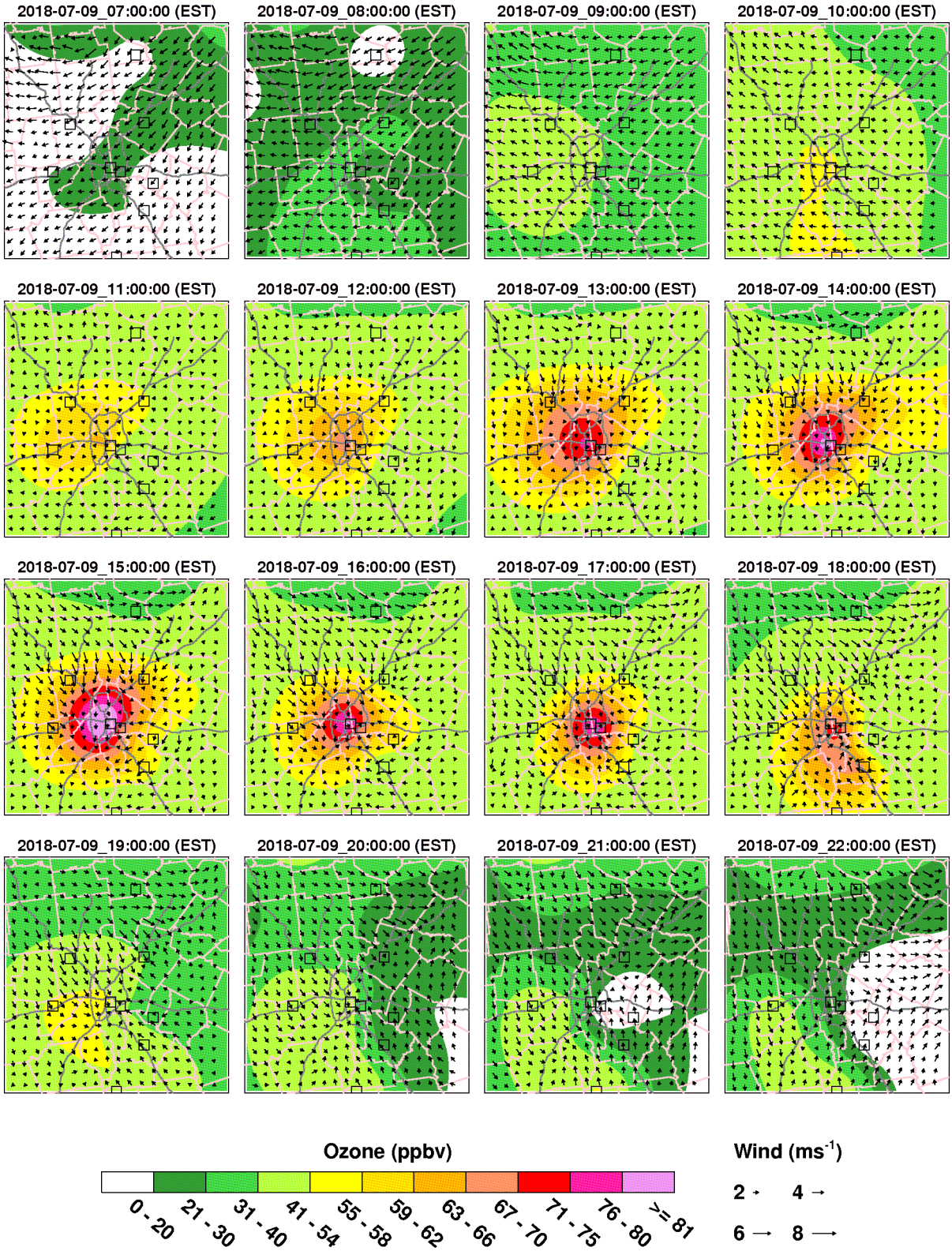

Figure 35. WRF simulated wind barbs and ozone observations (ppb) over the Metro Atlanta area from 7 AM to 10 PM on July 9, 2018. Ozone monitors are in black squares. The ozone exceedances occurred at the United Ave. monitor.

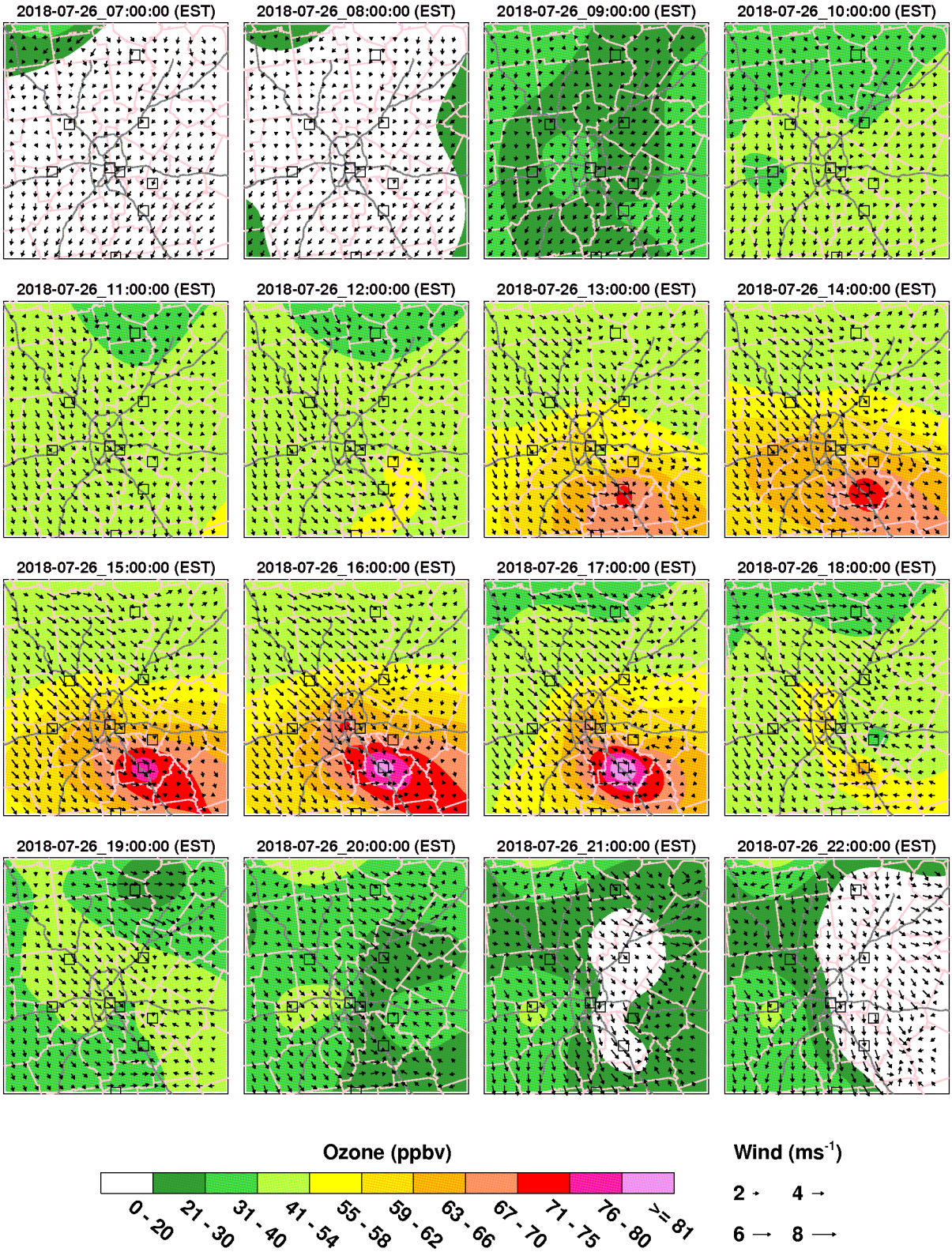

Figure 36. WRF simulated wind barbs and ozone observations (ppb) over the Metro Atlanta area from 7 AM to 10 PM on July 26, 2018. Ozone monitors are in black squares. The ozone exceedance occurred at the McDonough monitor.

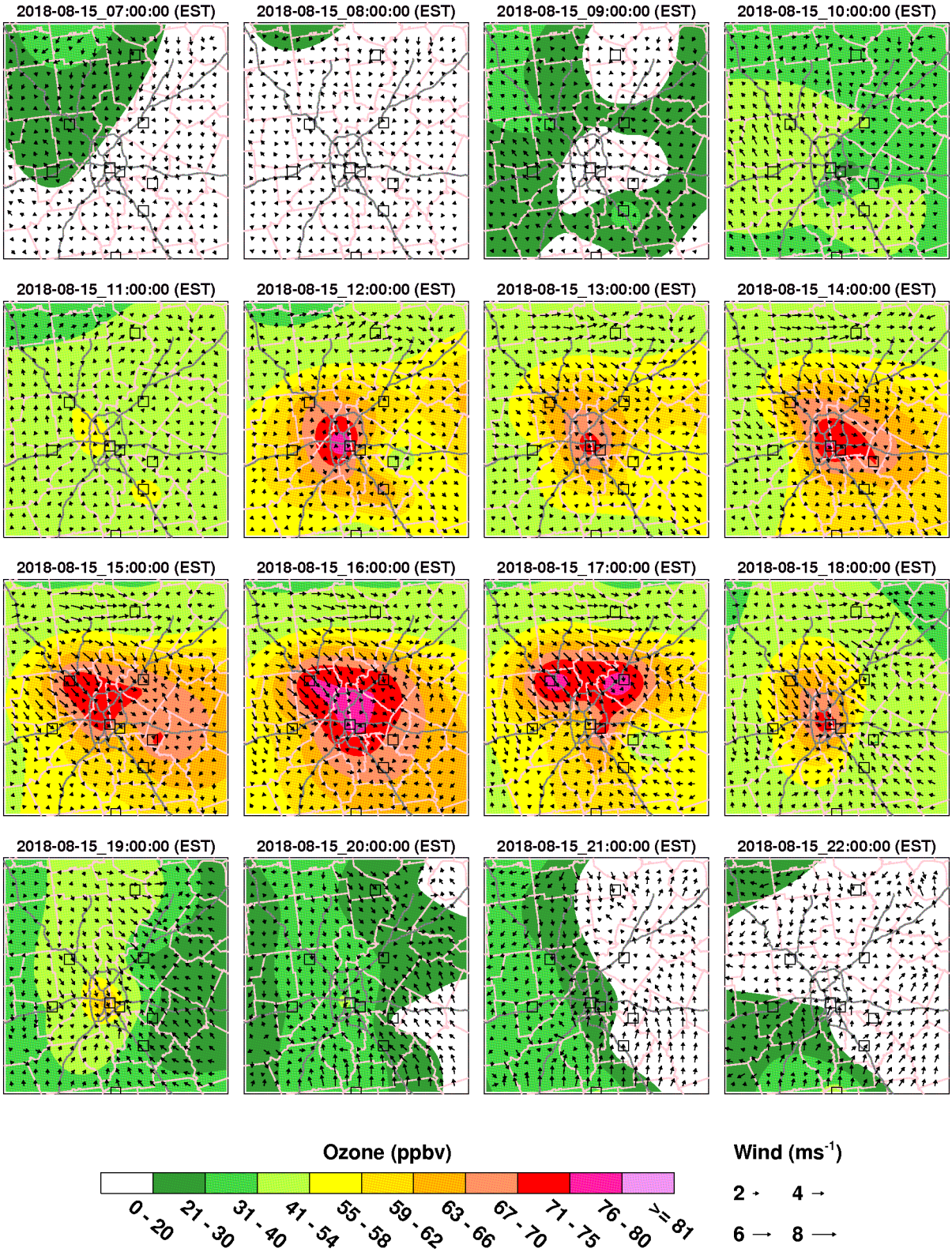

Figure 37. WRF simulated wind barbs and ozone observations (ppb) over the Metro Atlanta area from 7 AM to 10 PM on August 15, 2018. Ozone monitors are in black squares. The ozone exceedance occurred at the United Ave. monitor.

5.4 1-Minute Ozone Concentration Time Series on Exceedance Days

The 1-minute ozone concentrations on exceedance days at exceeding monitors were further examined to study the timing of elevated ozone formation (Figure 38 - Figure 40). For ozone exceedances at Dawsonville (outside the Atlanta urban core), ozone concentrations (Figure 38) reached 70 ppb around 2:00 PM on May 1 and 2, 2018. For ozone exceedances at monitors inside the Atlanta urban core, ozone concentrations usually reached 70 ppb before noon. The earliest was 11 AM and occurred at the Conyers monitor on May 12, 2018 and the United Ave. monitor on June 6 and 7, 2018. The late occurrence time of the elevated ozone at the monitors outside the Atlanta urban core implies that either ozone formed in the Atlanta urban core is transported to the exceedance monitor or ozone precursor emissions from the Atlanta urban core are transported to the exceedance monitors where ozone is formed. This is consistent with the findings from the "Animation of Ozone and Wind Conditions" section.

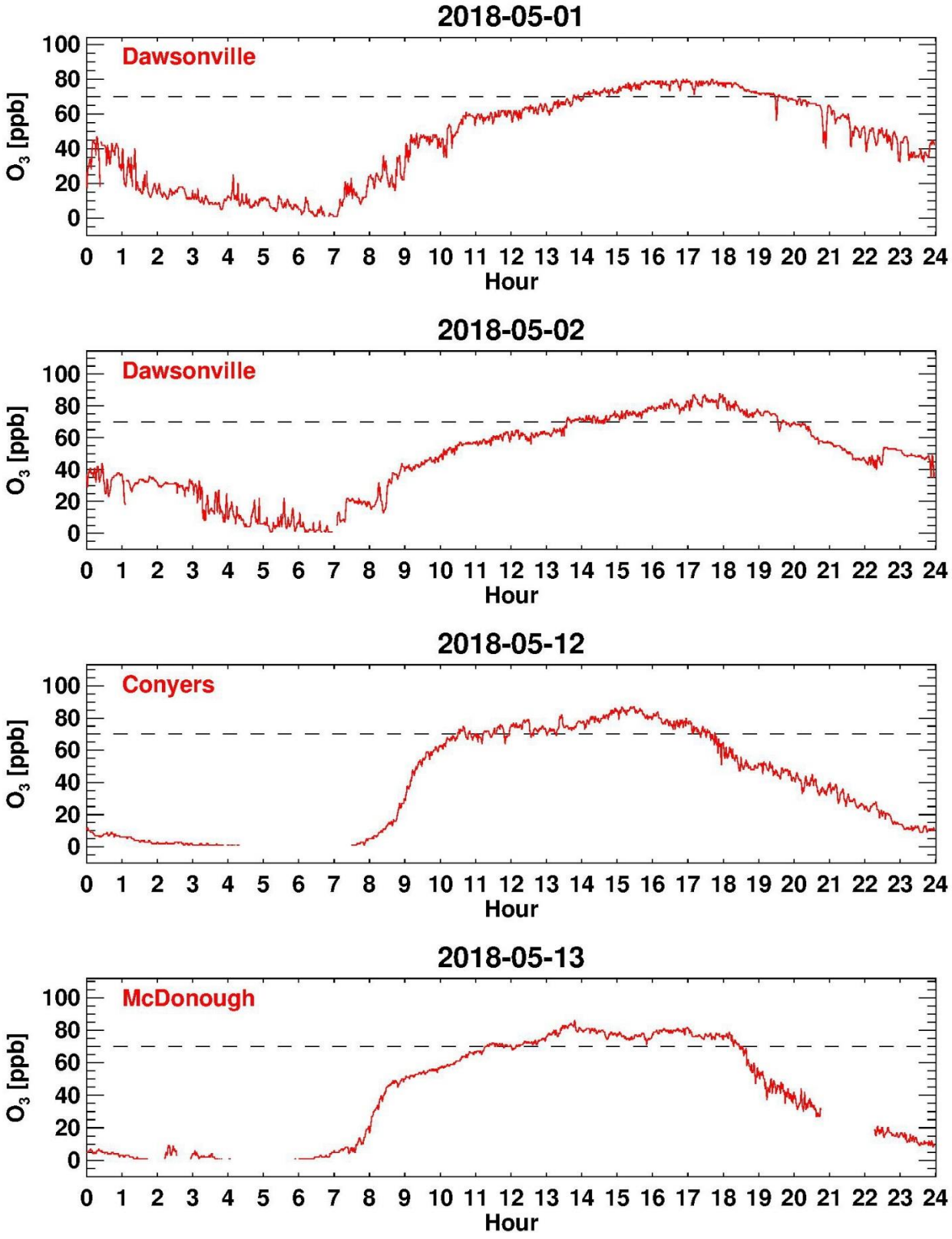

Figure 38. 1-minute ozone concentrations on exceedance days.

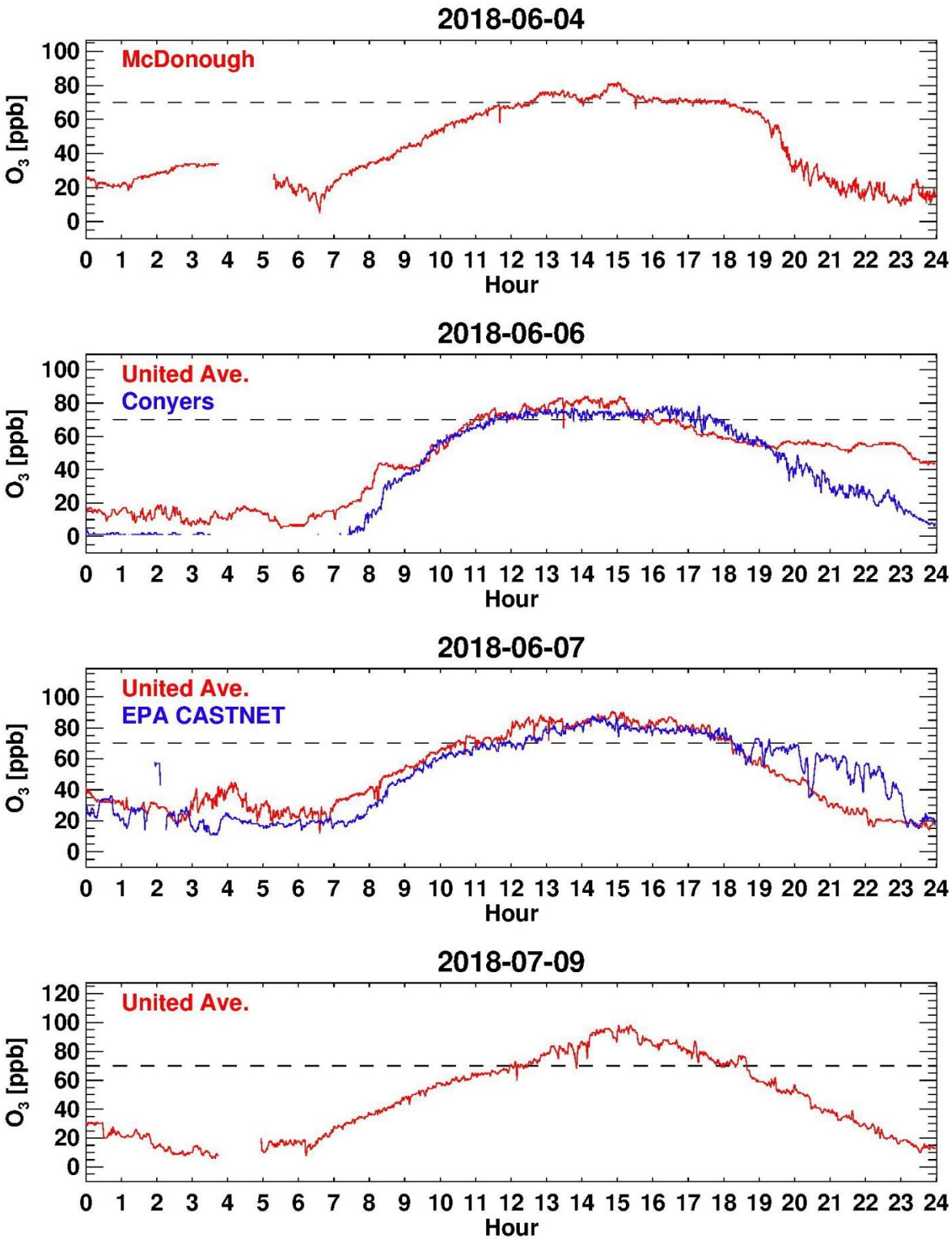

Figure 39. 1-minute ozone concentrations on exceedance days.

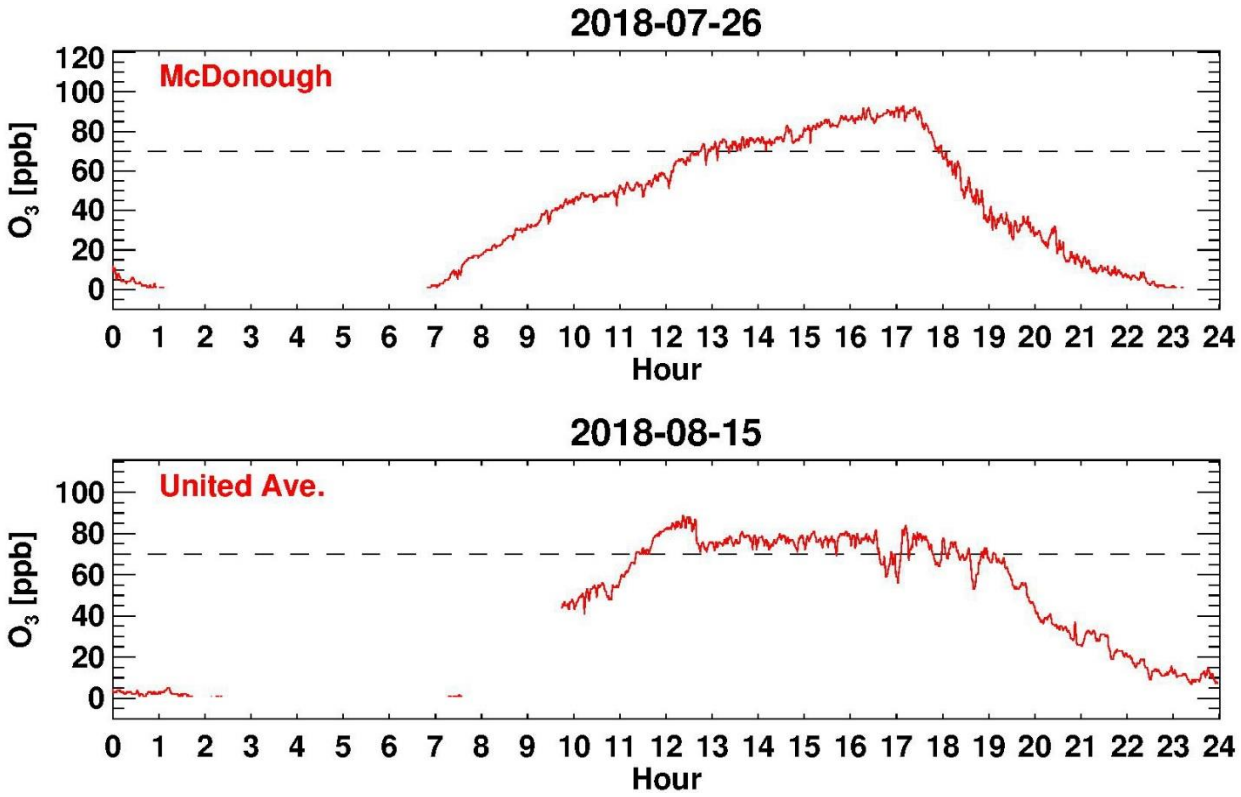

Figure 40. 1-minute ozone concentrations on exceedance days.

6. Ozone and NO_X Precursor

Ozone is not emitted directly into the air but formed by the reaction of VOCs and NO_X in the presence of heat and sunlight. The relationship of ozone and NO_X is very nonlinear since NO_X can not only help ozone formation, but also deplete ozone through NO_X titration. NO_X can be emitted from passenger cars, trucks, and various non-road vehicles (e.g., construction equipment, boats, etc.) as well as stationary combustion sources such as power plants, industrial boilers, cement kilns, and turbines. In the Metro Atlanta area during 2014, 58% of NO_X emissions were from on-road mobile sources and 20% from non-road mobile sources (Figure 41).

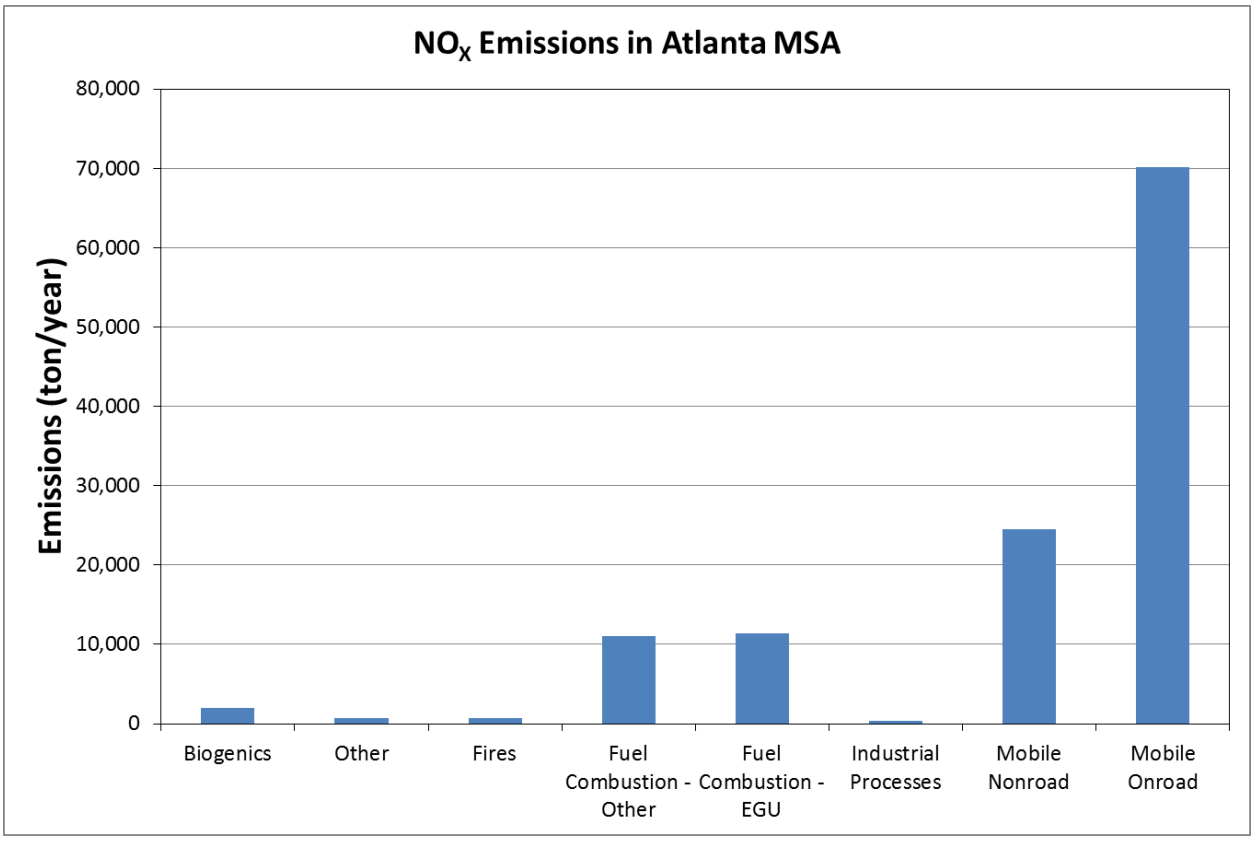

Figure 41. 2014 NO_X emissions (tons/year) by source sectors in the Metro Atlanta area.

In this study, the impacts of local NO_X on ozone exceedances are investigated by analyzing NO_X observations at the South DeKalb monitor and two roadside monitors (NR-285 and NR-GA Tech) located adjacent to major interstates (Figure 42) during ozone seasons (April - October). The two roadside monitors are investigated to identify impacts from on-road mobile NO_X emissions. Scatter plots of MDA8O3 and NO_X measurements at 8 AM and 4 PM (Figure 43) imply that high ozone concentrations generally occur when NO_X concentrations are within a specific window. When NO_X concentrations are low in the morning, ozone concentrations in the afternoon are also low since not enough radicals are propagated. However, when NO_X concentrations are too high (>150 ppb at 8:00 AM or >11 ppb at 4:00 PM), the excess NO_X removes ozone via NO_X titration. Figure 43 shows that high ozone concentrations in the Metro Atlanta area are highly correlated with low relative humidity (dry condition).

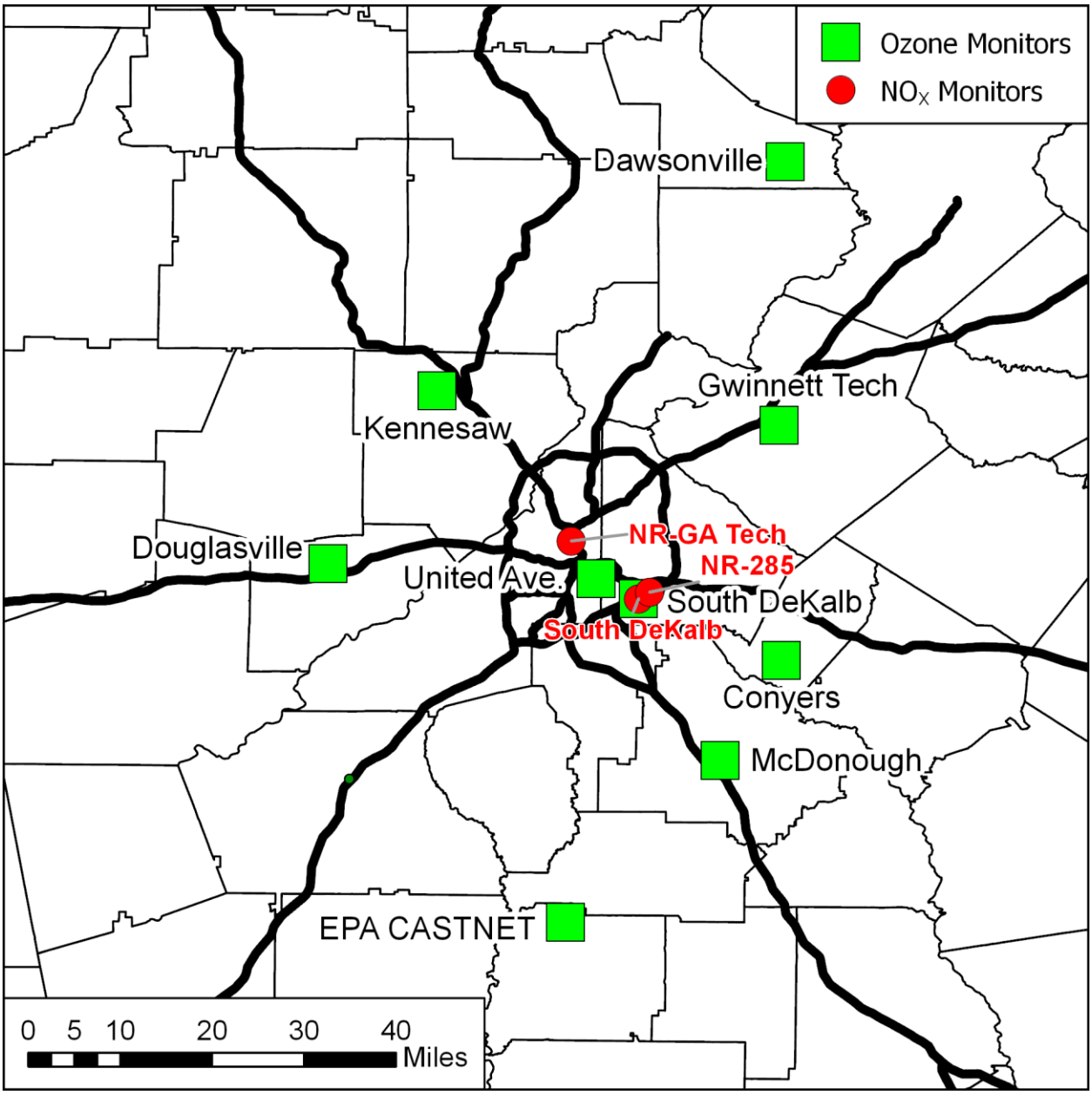

Figure 42. Locations of ozone and NO_X monitors in the Metro Atlanta area.

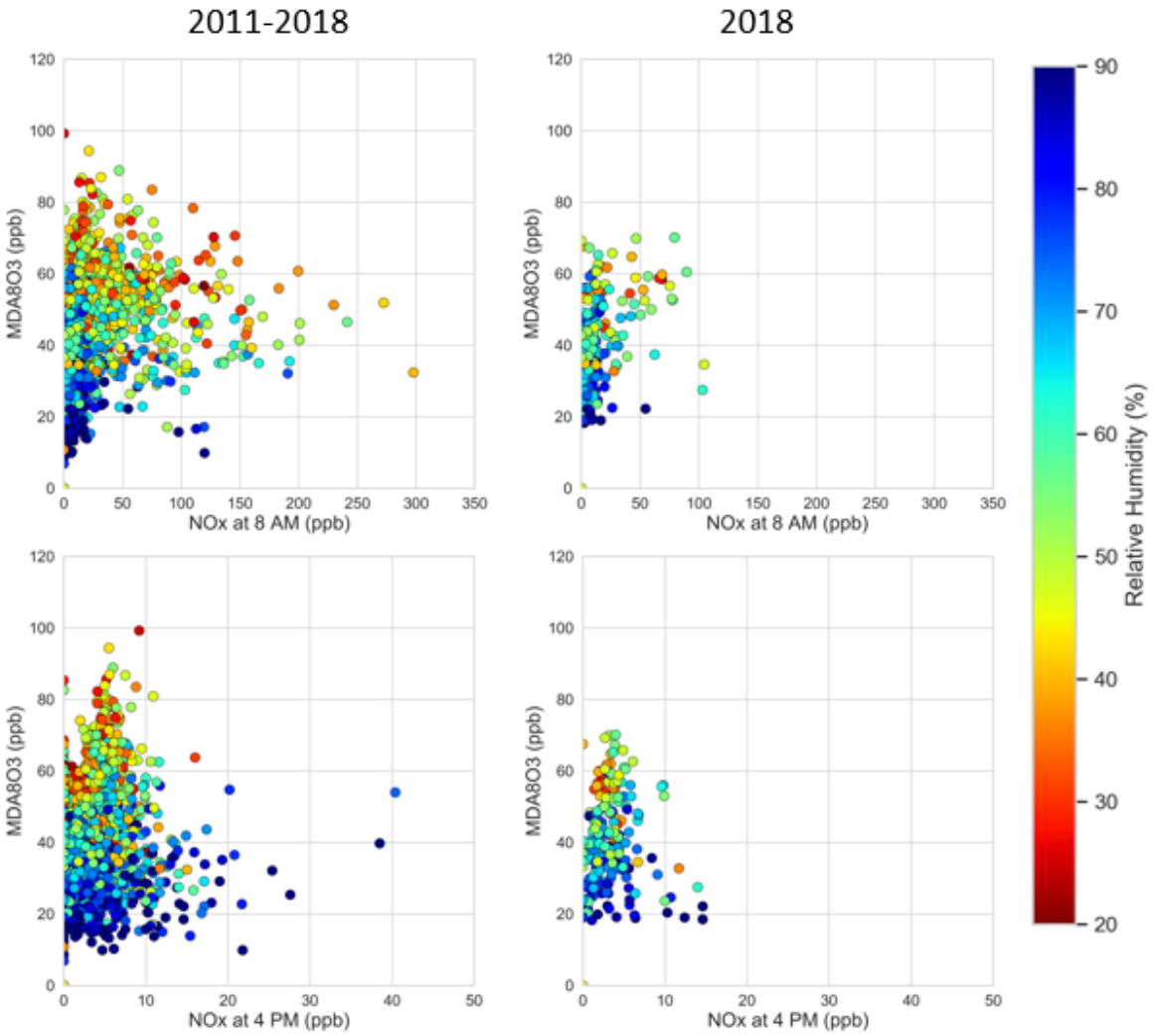

Figure 43. Scatter plots of MDA8O3 and NO_X at 8 AM (top row) and 4 PM (bottom row) at the South DeKalb monitor. The color of dots reflects afternoon (noon-6 PM) relative humidity levels.

6.1 Diurnal Patterns of NO_X Observations on Ozone Exceedance Days

The boxplots showing the statistics (mean, 10th, 25th, 75th, and 90th percentiles) of NO_X observations by hour of day were developed during the 2018 ozone season at the three NO_X monitors (Figure 44-Figure 47). These boxplots are overlaid with NO_X observations on ozone exceedance days at the United Ave. (Figure 44), Conyers (Figure 45), McDonough (Figure 46), and Dawsonville (Figure 47) monitors. NO_X observations at the two roadside monitors are higher than those at the South DeKalb monitor, indicating large impacts from mobile sources. There is a clear diurnal variation in NO_X observation, peaking in the morning when NO_X emissions are high due to commuter traffic and NO_X emissions are trapped at low altitudes as the planetary boundary layer (PBL) is still quite low. NO_X observations then rapidly decrease when the PBL expands and photochemistry becomes stronger during the day. Then they increase again at night when the PBL collapses. On ozone exceedance days, morning time NO_X observations

tend to be higher than the average NO_X observations, especially from 6 AM to 8 AM when traffic volumes are highest, although the pattern is not clear for NO_X observations during evening/nighttime compared with morning time. However, morning time NO_X concentrations on May 13, 2018 at NR-285 and NR-GA Tech are lower than average values when exceedances occurred at the McDonough monitor. Since May 13, 2018 is a Sunday, there were no increased NO_X emissions from morning commuter traffic.

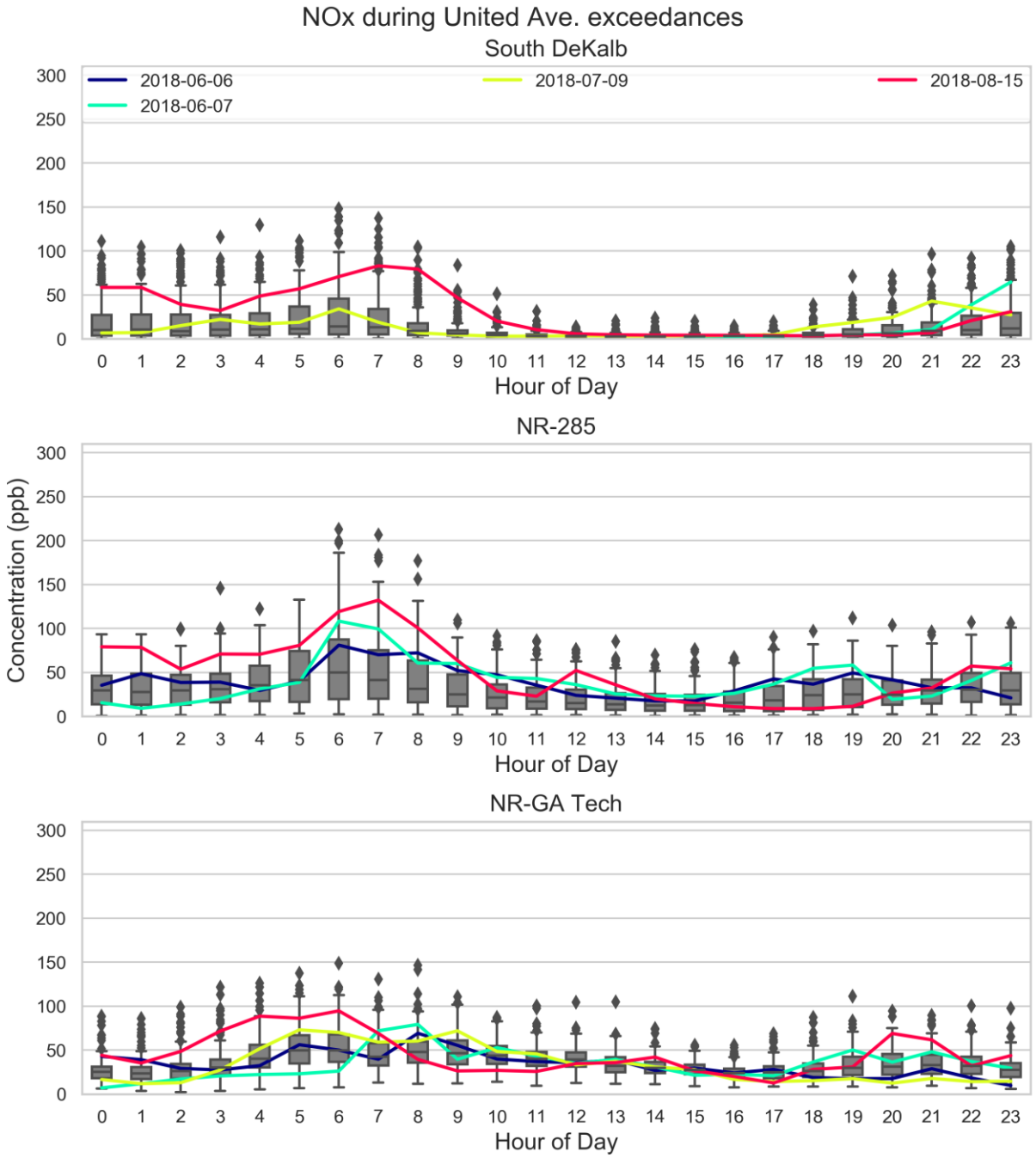

Figure 44. Boxplots by hour of day for NO_X observations during 2018 ozone seasons at three NO_X monitors. Colored lines are NO_X observations on ozone exceedance at the United Ave. monitor.

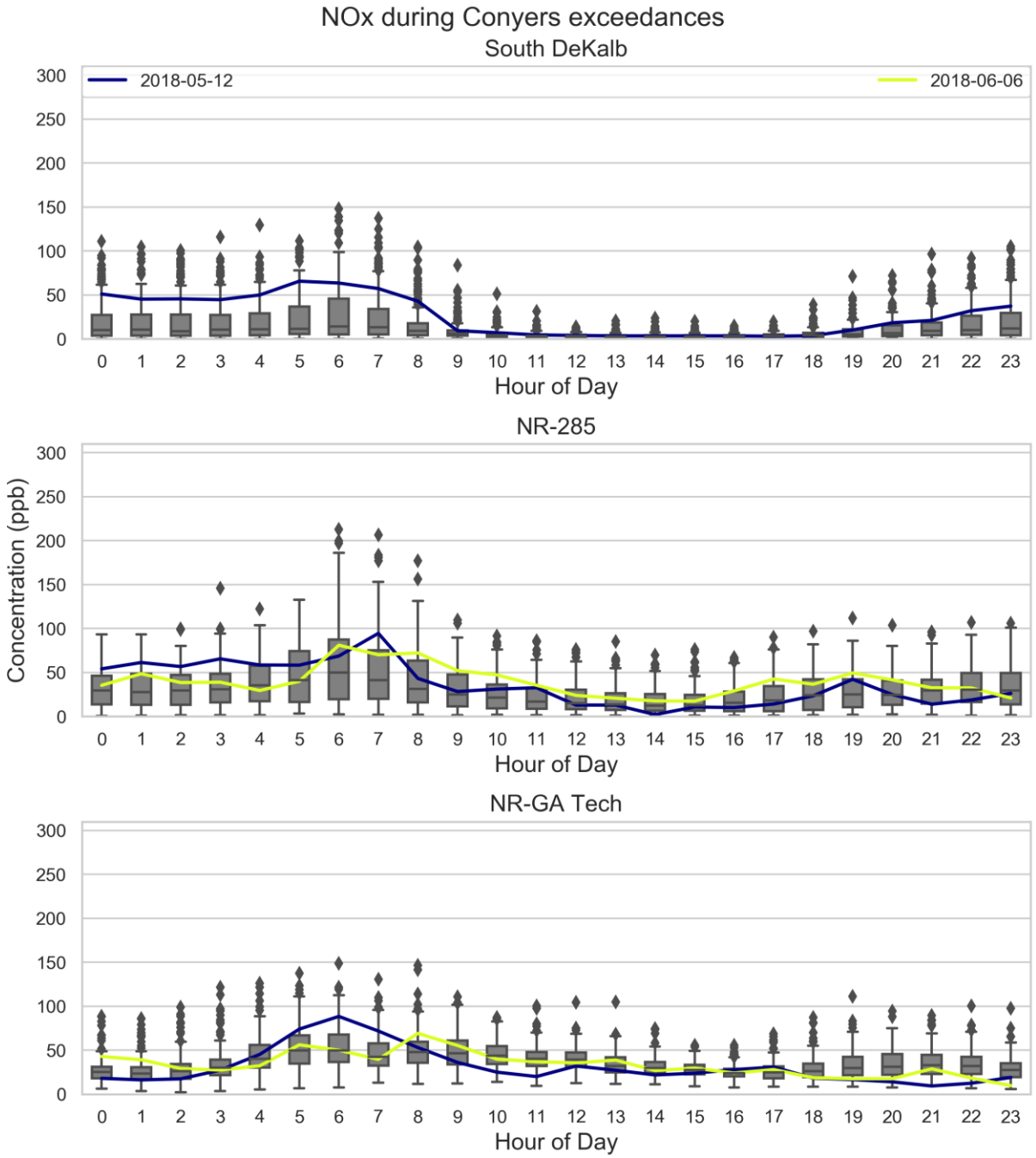

Figure 45. Boxplots by hour of day for NOx observations during 2018 ozone seasons at three NOx monitors. Colored lines are NOx observations on ozone exceedance at the Conyers monitor.

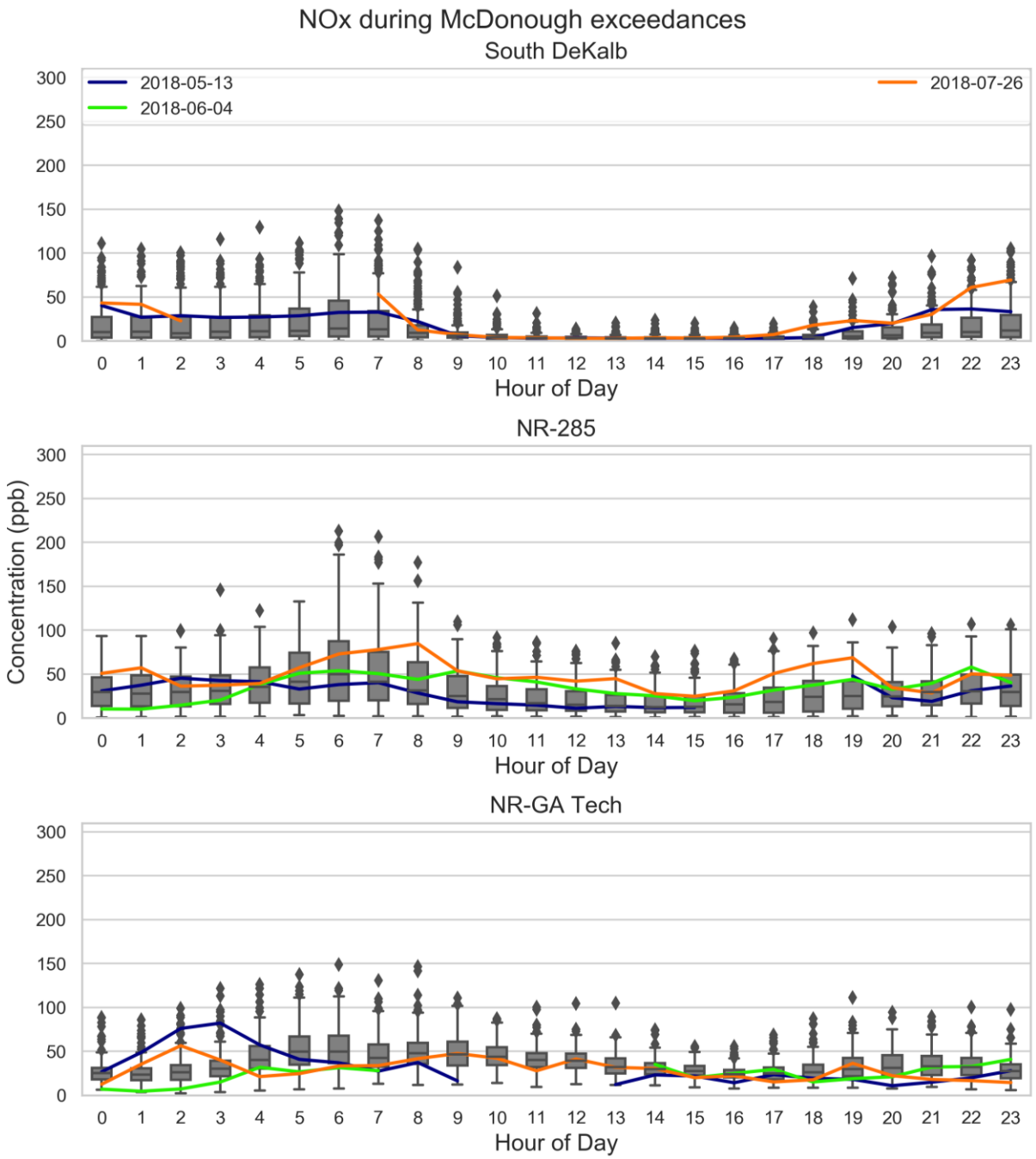

Figure 46. Boxplots by hour of day for NOx observations during 2018 ozone seasons at three NOx monitors. Colored lines are NOx observations on ozone exceedance at the McDonough monitor.

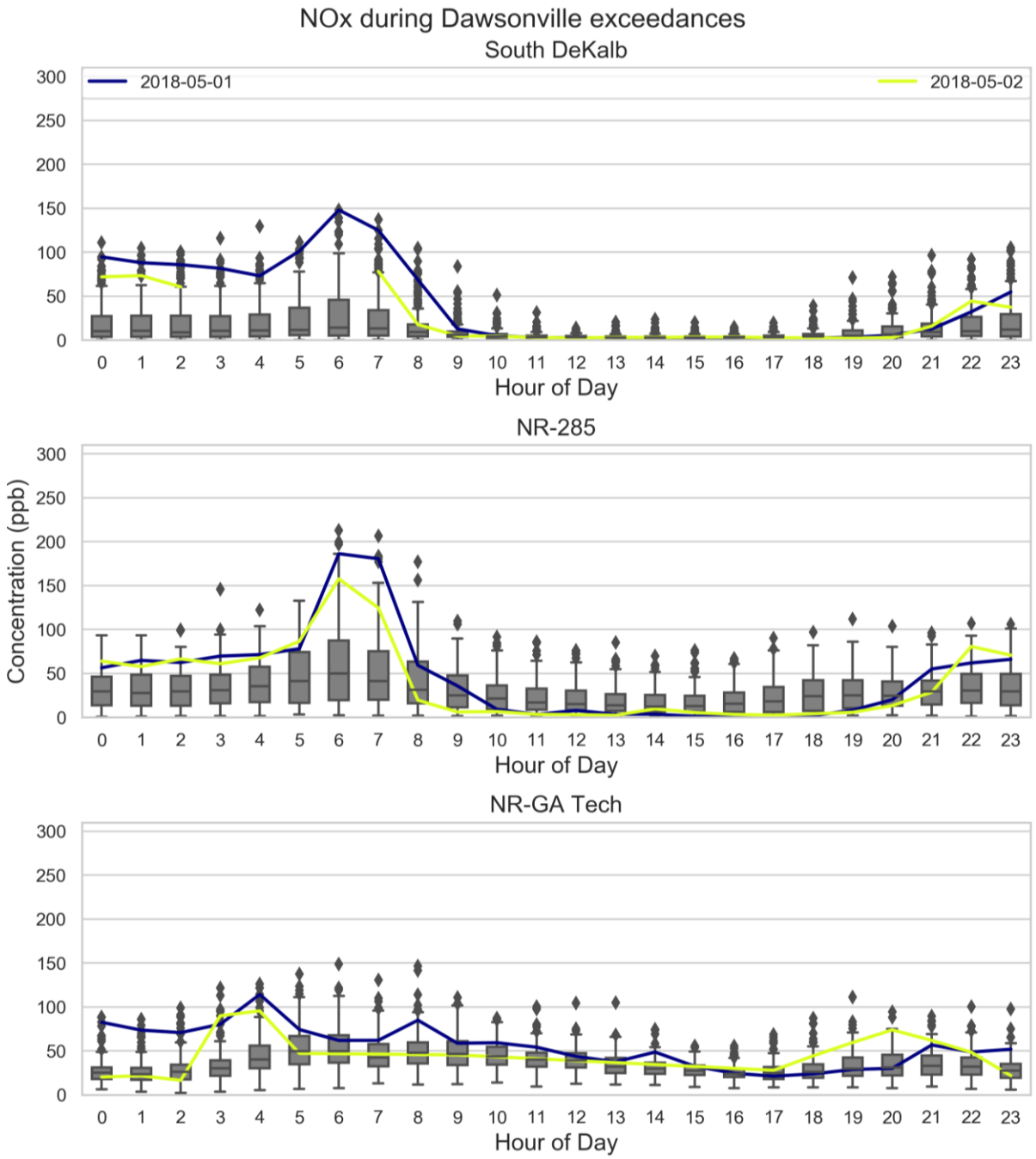

Figure 47. Boxplots by hour of day for NO_X observations during 2018 ozone seasons at three NO_X monitors. Colored lines are NO_X observations on ozone exceedance at the Dawsonville monitor.

6.2 Day-of-Week Patterns of NO_X Observations on Ozone Exceedance Days

Variation of NO_X observations by day of week is analyzed by developing boxplots for NO_X observations at 8 AM at the three NO_X monitors (Figure 48). The NO_X observations at 8 AM are chosen since they are likely correlated with high ozone levels as identified in the diurnal pattern analysis for the NO_X observations. The NO_X observations are higher on weekdays than the weekends, corresponding to similar traffic patterns (i.e., heavier commuter traffic during weekdays than weekend). Sunday morning NO_X observations are typically lower than Saturday morning. Mean Friday morning NO_X observations also tend to be slightly lower than mean Wednesday or Thursday NO_X observations at the NR-285 roadside monitor. The boxplots are overlaid with NO_X observations on ozone exceedance days (red circles). At the South DeKalb and NR-285 monitors, NO_X observations on ozone exceedance days are mostly higher than average conditions. However, NO_X observations on ozone exceedance days at three NO_X monitors are not consistently higher than the average conditions on Mondays, Wednesdays, and Thursdays.

6.3 Monthly Patterns of NO_X Observations on Ozone Exceedance Days

Variation of NO_X observation by month is then analyzed by developing similar boxplots for NO_X observations at 8 AM at the three NO_X monitors (Figure 49). The mean morning time NO_X observations at the two roadside monitors are between 20 and 75 ppb, usually higher than NO_X observations at the South DeKalb monitor. The mean morning time NO_X observations at the South DeKalb monitor tend to be less than 20 ppb throughout the ozone season. NO_X begins to increase through colder months such as October because there is less photochemistry to remove atmospheric NO_X. NO_X observations at the NR-285 and NR-GA Tech monitors also start to increase in September and October. The boxplots are overlaid with NO_X observations on ozone exceedance days (red circles). All exceedances took place in May, June, July, and August. The lack of red circles in June at the South DeKalb monitor is due to missing NO_X data. Usually, morning time NO_X observations on an ozone exceedance day are higher than the mean NO_X observations in a month when the exceedance took place, except for some days in May at the NR-285 and NR-GA Tech monitors.

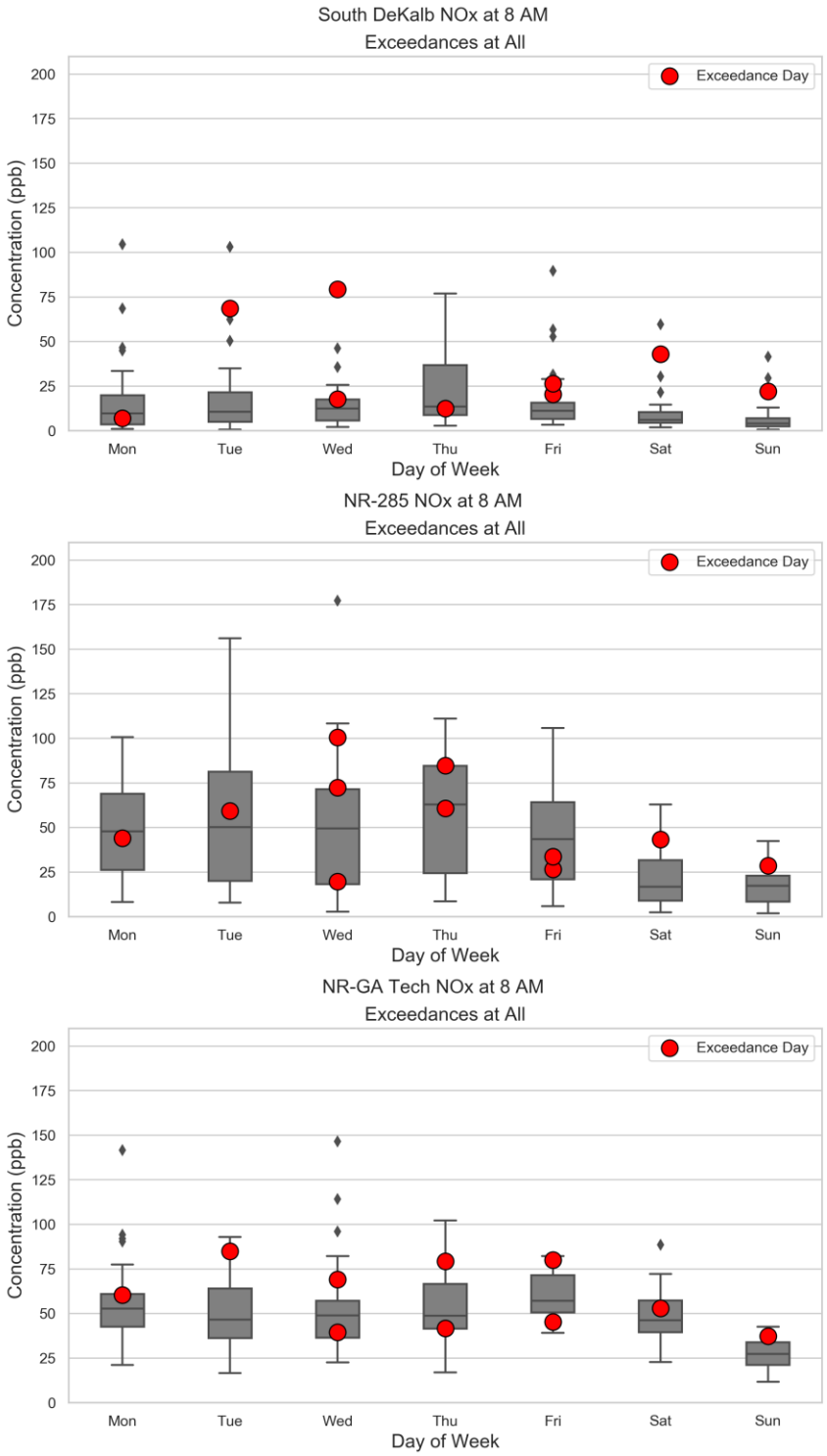

Figure 48. Boxplots by day of week for NO_X observations at 8 AM during the 2018 ozone seasons at three NO_X monitors. Red dots are NO_X observations on ozone exceedance days at each NO_X monitor. NO_X observations at 8 AM on June 4 (Monday), 6 (Wednesday), and 7 (Thursday) are not available at the South DeKalb monitor. NO_X observation at 8 AM on July 9 (Monday) is not available at the NR-285 monitor. NO_X observations at 8 AM on May 2 (Wednesday) and June 4 (Monday) are not available at the NR-GA Tech monitor.

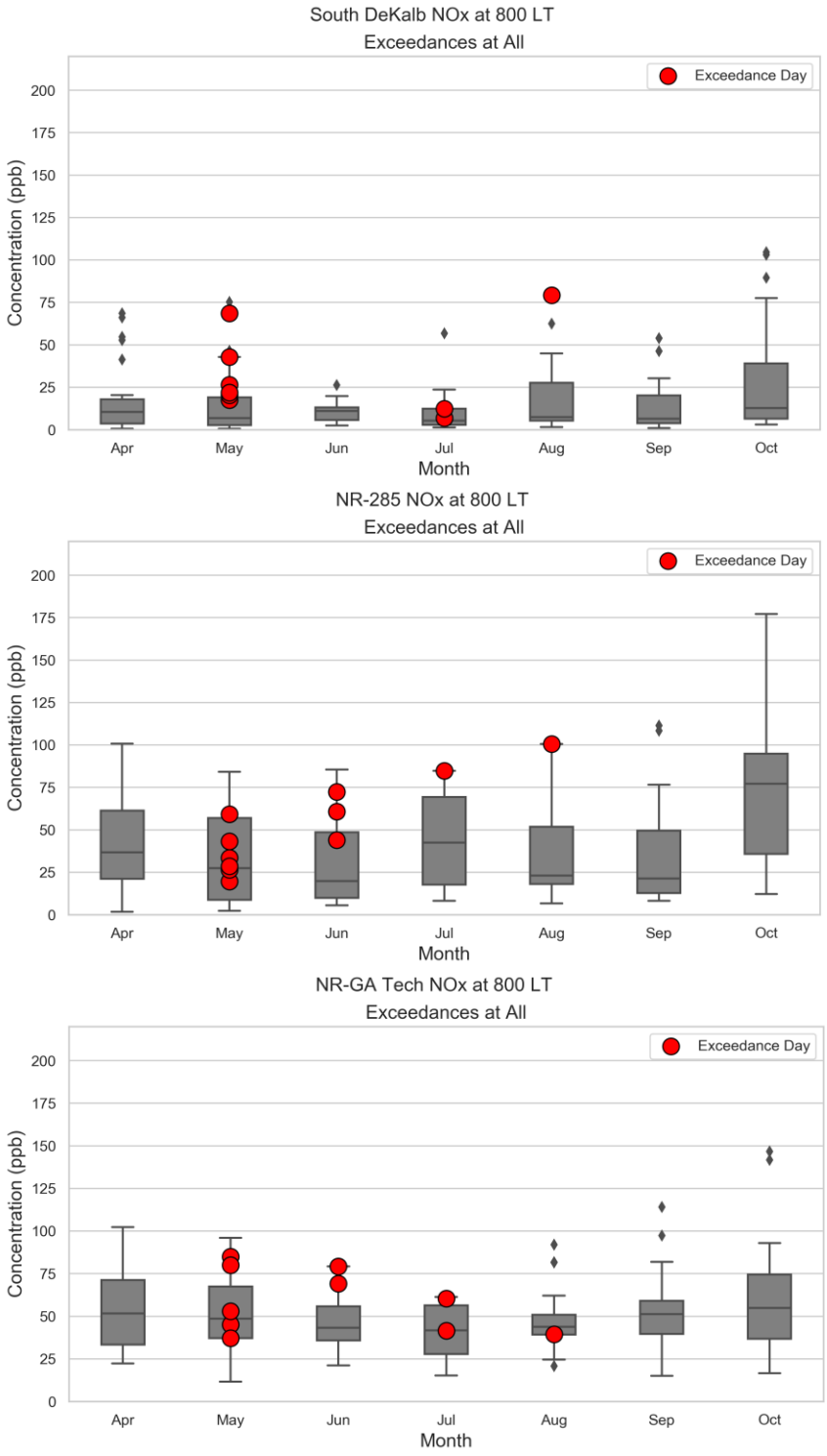

Figure 49. Boxplots by month for NO_X observations at 8 AM during the 2018 ozone seasons at three NO_X monitors. Red dots are NO_X observations on ozone exceedance days at each monitor. NO_X observations at 8 AM on June 4 (Monday), 6 (Wednesday), and 7 (Thursday) are not available at the South DeKalb monitor. NO_X observation at 8 AM on July 9 (Monday) is not available at the NR-285 monitor. NO_X observations at 8 AM on May 2 (Wednesday) and June 4 (Monday) are not available at the NR-GA Tech monitor.

6.4 Indicator Analysis

The ratio of ozone to NO_X is calculated for 2011-2018 data at the South DeKalb monitor in this study as an indicator of local ozone production efficiency (Tonnesen et al., 2000). When the ratio of ozone to NO_X is low, NO can remove ozone through titration. In the 2010 Tonnesen study, ozone is produced most efficiently with the ratio of ozone to NO_X is ~8 during a morning period (9 AM to 10 AM), the ratio is ~15 around noon (12 PM to 1 PM), and the ratio is 16-20 during the afternoon period (4 PM to 5 PM). Because there was no exceedance at the South DeKalb monitor in 2018, days with MDA8O3 over 60 ppb were used as a proxy for exceedance days.

Diurnal profiles of median ozone and NO_X for each ozone season and exceedance days during 2011-2018 (Figure 50 and Figure 51) have shown that NO_X concentration decreases when ozone increases, and vice versa. In general, NO_X concentrations during low-ozone hours are much higher on ozone exceedance days. The ratios of ozone to NO_X calculated here are compared with the ratios suggested in the 2010 Tonnesen study (Figure 52). In the morning period (9 AM to 10 AM), the ozone exceedance days show higher ratios than the average conditions during the ozone season except in 2013. In 2018, the ratio is higher than Tonnesen's ratio for peak ozone production. In the noon period (12:00 PM to 1:00 PM), the ratios of ozone to NO_X for ozone exceedance days are higher than the average conditions during ozone season. In 2018, the ratio is much higher than Tonnesen's ratio for peak ozone production. The same tendency was observed for the ratio of ozone to NO_X for ozone exceedance days in the afternoon period (4 PM to 5 PM). Overall, 2018 showed higher than Tonnesen's ratio for peak ozone production. This may imply that ozone in 2018 is more efficient compared to other years. However, due to the limited number of ozone exceedance days at the South DeKalb monitor in 2018, further investigation is needed.

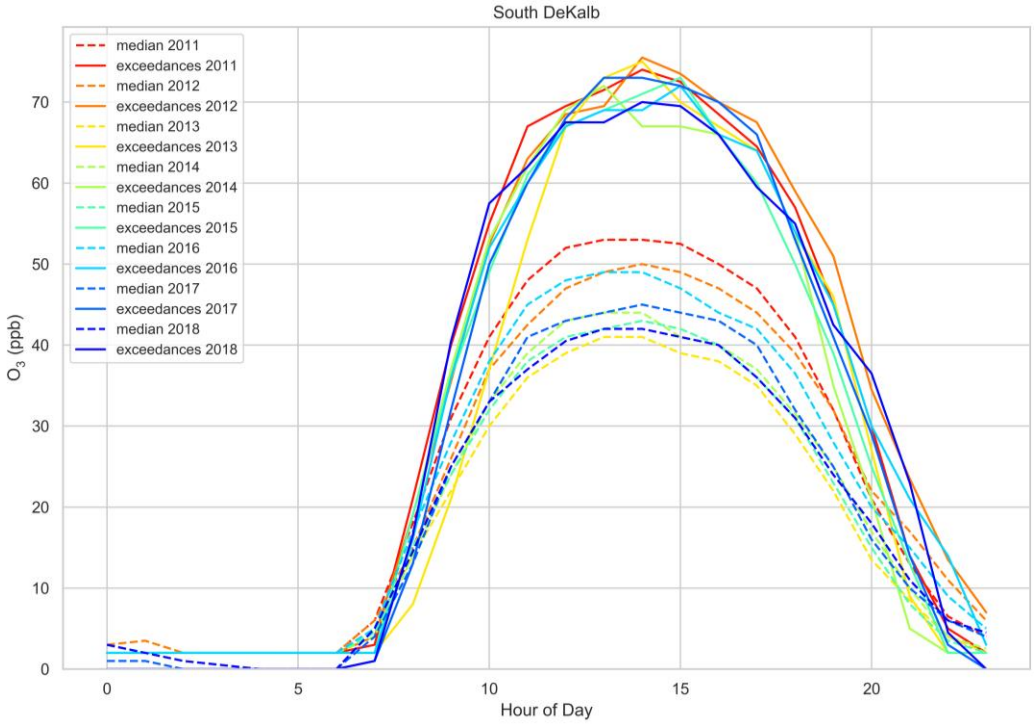

Figure 50. Diurnal profile of median ozone for each ozone season (dashes) and exceedance days (solid lines) during 2011-2018.

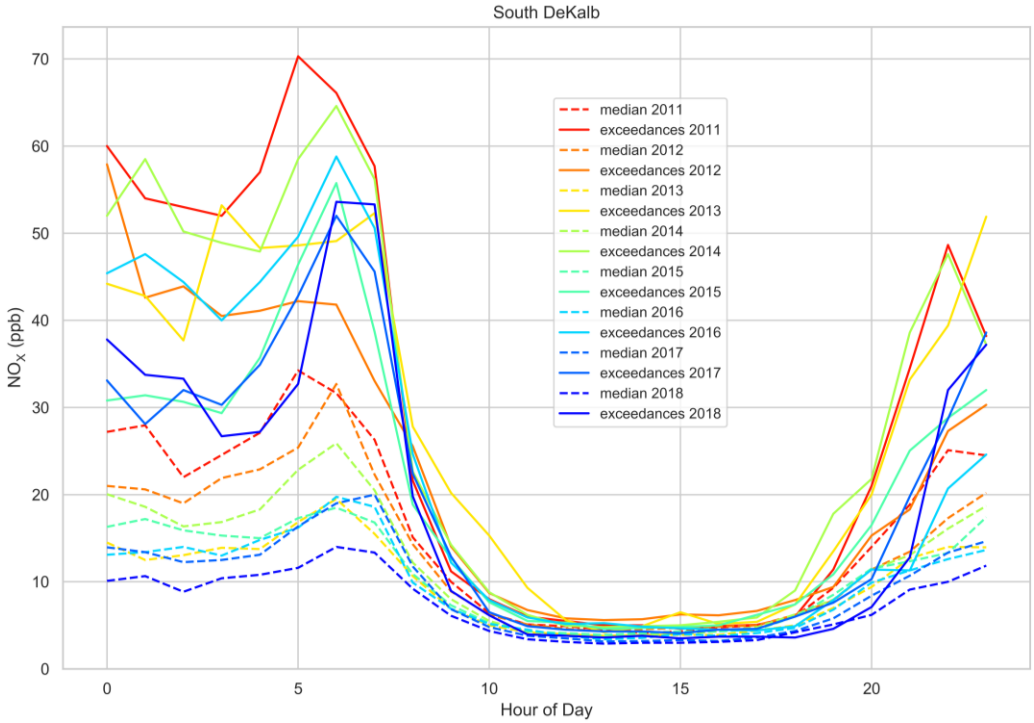

Figure 51. Diurnal profile of median NOx for each ozone season (dashes) and exceedance days (solid lines) during 2011-2018.

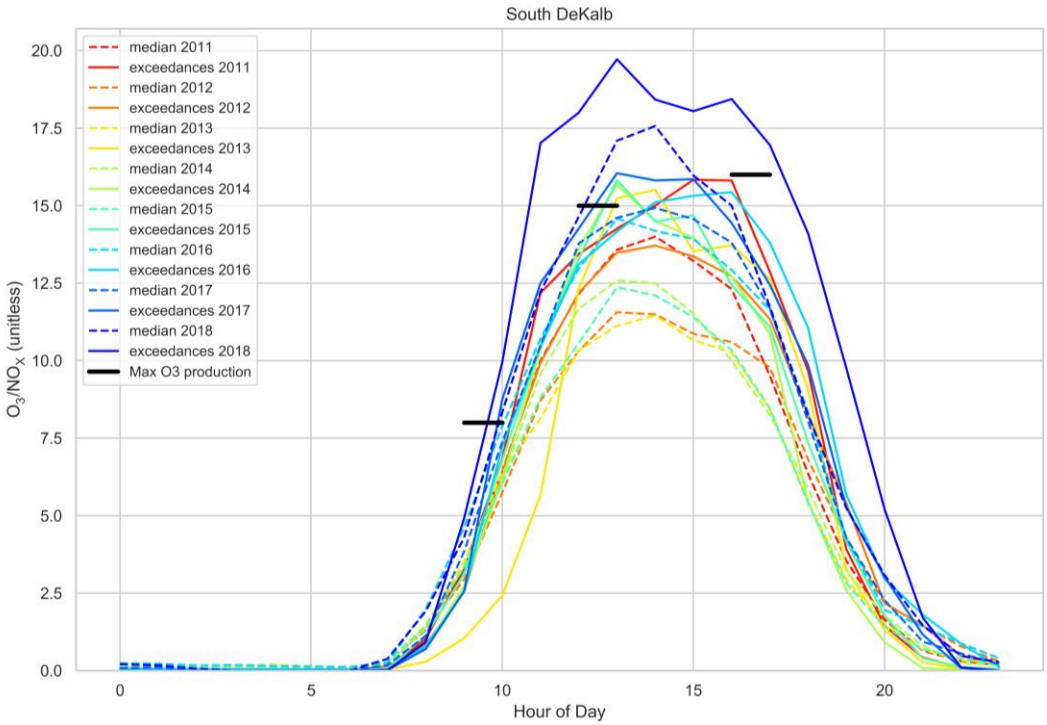

Figure 52. Diurnal profile of median ozone to NO_X ratio for each ozone season (dashes) and exceedance days (solid lines) during 2011-2018. The black bars at 9 AM to 10 AM, noon to 1 PM, and 4 PM to 5 PM represent the ratios where peak ozone production occurs according to Tonnesen's 2010 study.

6.5 NO_X Trends Based on OMI Satellite Data

NO_X trends in the Metro Atlanta area during 2005-2018 ozone seasons are evaluated using the daily tropospheric NO_2 columns by Ozone Monitoring Instrument (OMI) onboard NASA's Aura satellite. OMI provides NO_2 information at 1:45 PM (±15-minute) EST when local ozone production is near its daily peaks. Since there are large fractions of tropospheric NO_2 columns at the ground level as shown from in situ and aircraft measurements (e.g. Steinbacher et al., 2007; Heland et al., 2002; Martin et al., 2004), the tropospheric NO_2 columns can generally represent the surface NO_X conditions, especially at hot spots over urban areas. The standard tropospheric OMI NO_2 column product has a resolution of 13×24 km^2 (Bucsela et al., 2013), and was processed onto 0.1×0.1 $degree^2$ global grid (Lamsal et al., 2014). The Metro Atlanta area is defined in this study as 9×9 grids centering at Five Points and covering 4 grids (=0.4°) in all 4 directions. Spatial distribution of the 14-year average OMI NO_2 columns during 2005-2018 over the Metro Atlanta area (Figure 53) shows higher NO_2 concentrations in the urban core extending slightly to the suburban areas in the southeast. The hot spot of NO_2 columns clearly shows strong local NO_X emissions in the Metro Atlanta area.

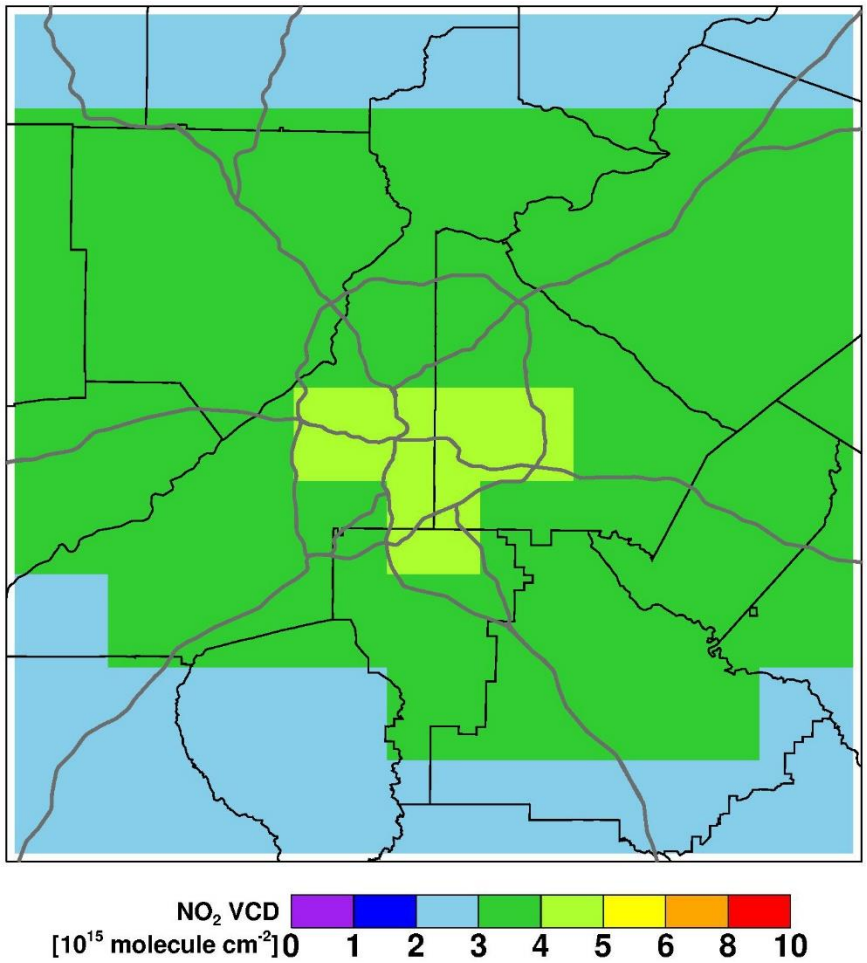

Figure 53. Mean OMI Tropospheric NO_2 columns over the Metro Atlanta area during 2005-2018.

The interannual comparison of NO_2 columns in ozone season shows significant decrease in NO_2 concentrations from 2005 to 2018 (Figure 54 and Figure 55). NO_2 columns in warm months are much lower than in cold months (Figure 56) due to additional photochemistry during the warmer months. Therefore, only OMI NO_2 columns during the ozone season (April to October) were used to develop the interannual trend (Figure 55). The interannual NO_2 variation based on OMI data matches well with the large ozone decreasing trends in recent years. Day-of-week patterns of OMI NO_2 columns (Figure 57) show higher values during weekdays than weekends, consistent with findings based on NO_2 ground-based observations and temporal patterns of onroad mobile sources. In summary, OMI NO_2 columns and ground-based NO_X observations show similar monthly and day-of-week patterns, which is consistent with the ozone concentration pattern. This indicates that NO_X plays an important role in tropospheric ozone formation in the Metro Atlanta area.

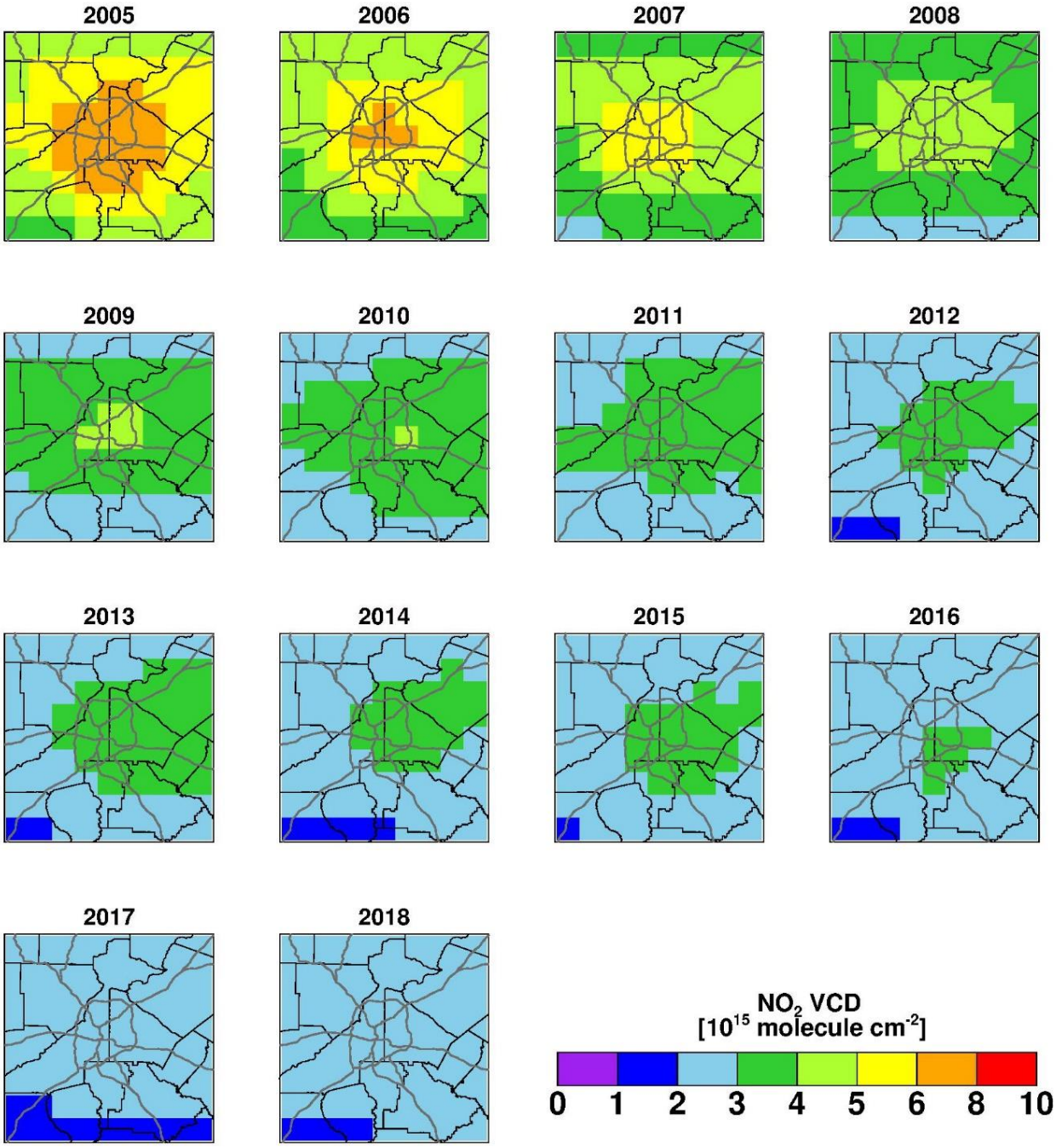

Figure 54. Annual mean OMI NO_2 tropospheric columns over the Metro Atlanta area during 2005-2018.

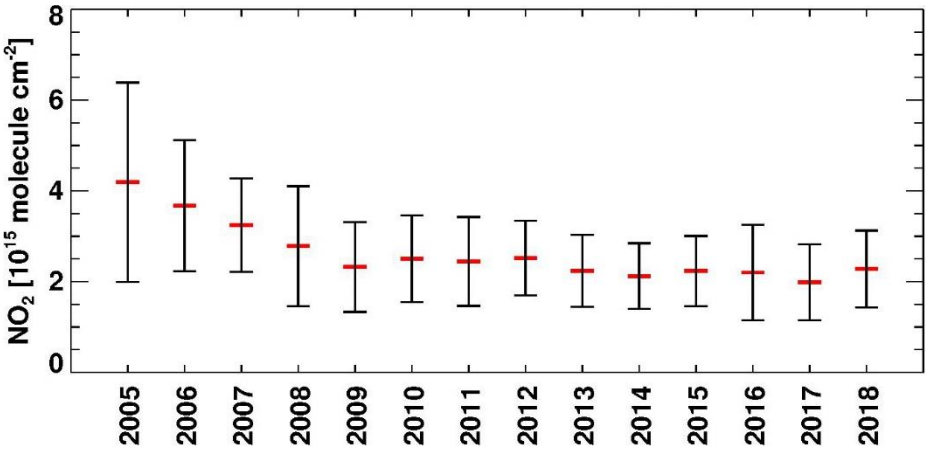

Figure 55. Annual spatial mean OMI NO_2 tropospheric columns over the Metro Atlanta area in April-October of 2005-2018. The means (red bar) and its standard deviations (black bars) are shown.

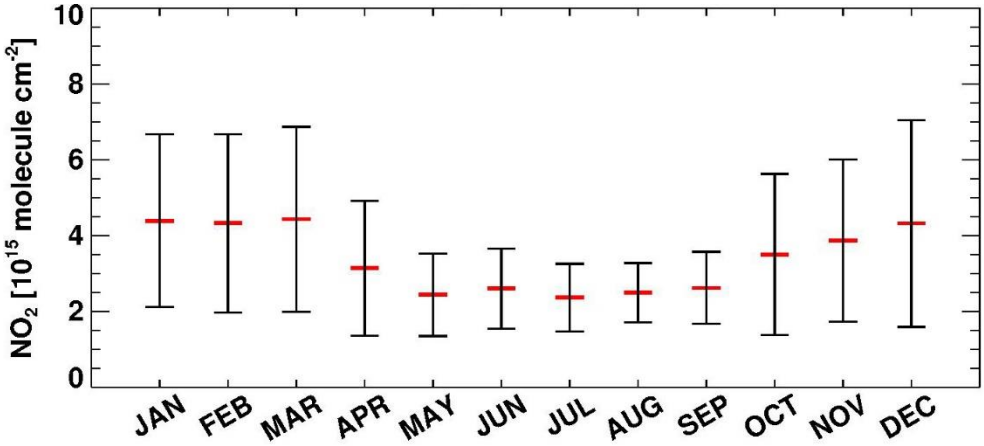

Figure 56. Monthly OMI NO_2 tropospheric columns in 2005-2018 over the Metro Atlanta area. The means (red bar) and its standard deviations (black bars) are shown.

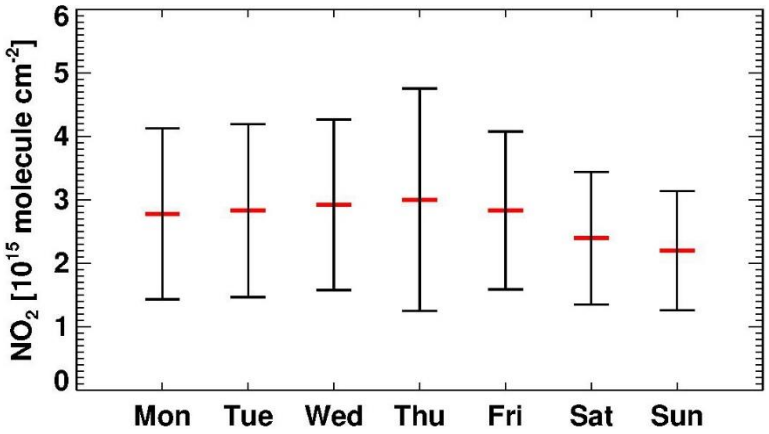

Figure 57. Mean OMI NO_2 tropospheric columns on each day of week over the Metro Atlanta area in April-October of 2005-2018. The mean (red bar) and its standard deviations (black bars) are shown.

6.6 NO_X Trends Based on TROPOMI Satellite Data

Spatial NO_X distributions in the Metro Atlanta area are further evaluated using the latest remote-sensing NO_2 products by TROPOspheric Monitoring Instrument (TROPOMI) on board the European Copernicus Sentienl-5P satellite (https://sentinels.copernicus.eu/web/sentinel/user-guides/sentinel-5p-tropomi). The TROPOMI tropospheric NO_2 columns were available after July 2018. TROPOMI provides NO_2 information around 1:30 PM when local ozone production is near its daily peaks. The standard tropospheric TROPOMI NO_2 column product has a resolution of 7×3.5 km^2. TROPOMI has much higher spatial resolution than NASA OMI NO_2 product and provides better daily representations of the surface NO_X conditions. It can be used to identify NO_2 hot spots over the Metro Atlanta area.

EPD processed the 7×3.5 km^2 data onto a 1.3×1.3 km^2 WRF grid over Georgia. Daily TROPOMI NO_2 columns were processed into the monthly maximum and monthly average NO_2 columns in July, August, September, and the 3-month period (July-September) in 2018 over the Metro Atlanta area (Figure 58 and Figure 59). Local high NO_2 concentrations are found in the southern portion of the Atlanta urban core and near Plant Bowen in the northwest. The hot spots are indicative of high local NO_X emissions.

The comparisons of daily NO_2 columns for 3-day periods around 3 exceedance days show significant increases of NO_2 concentrations on the ozone exceedance days: July 9 (Figure 60), July 26 (Figure 61), and August 15 (Figure 62). The correlation of high ozone and NO_X indicate that NO_X played an important role in the ozone formation on those days. The NO_2 hot spots on ozone exceedance days were located near HJAIA. Two potentially significant NO_X emissions sources near this area are the commercial aircrafts at the world's busiest airport and on-road mobile emissions from heavy-duty diesel vehicles that are transporting freight to and from warehouses along I-285, I-85, I-75, and I-675. More work will be needed to confirm and quantify their contributions.

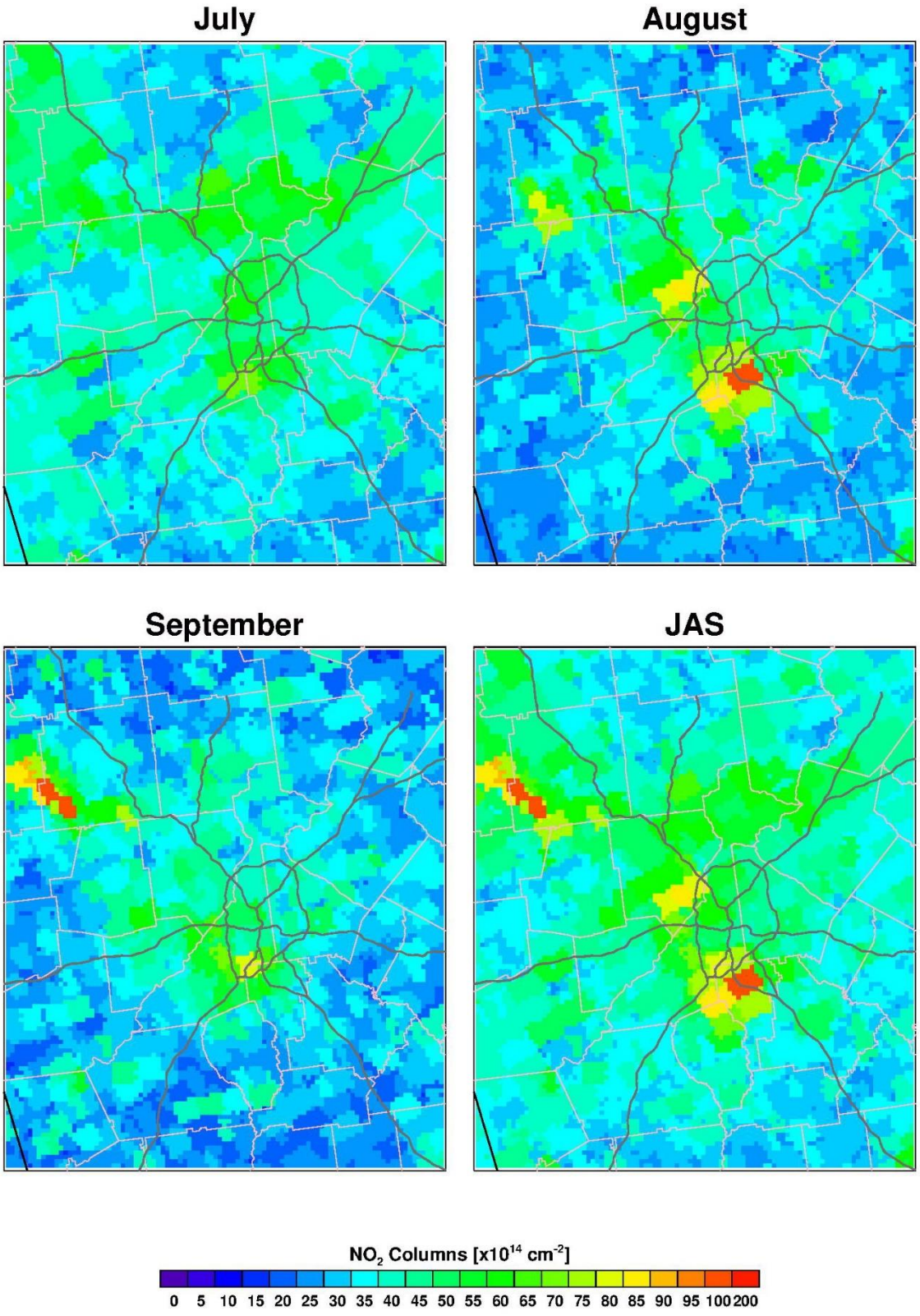

Figure 58. Maximum TROPOMI Tropospheric NO_2 columns over the Metro Atlanta area in July, August, September, and July-September 2018.

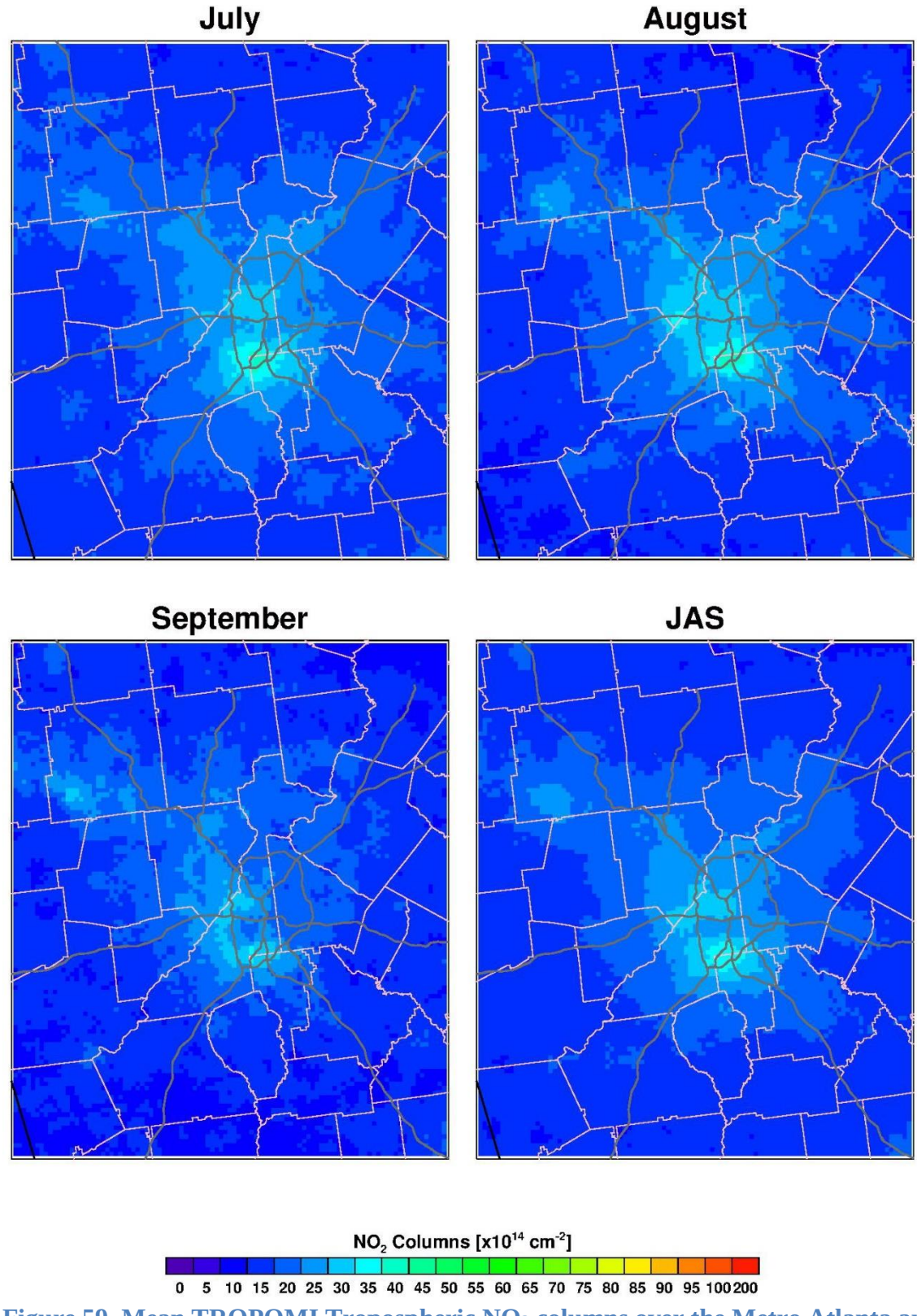

Figure 59. Mean TROPOMI Tropospheric NO_2 columns over the Metro Atlanta area in July, August, September, and July-September 2018.

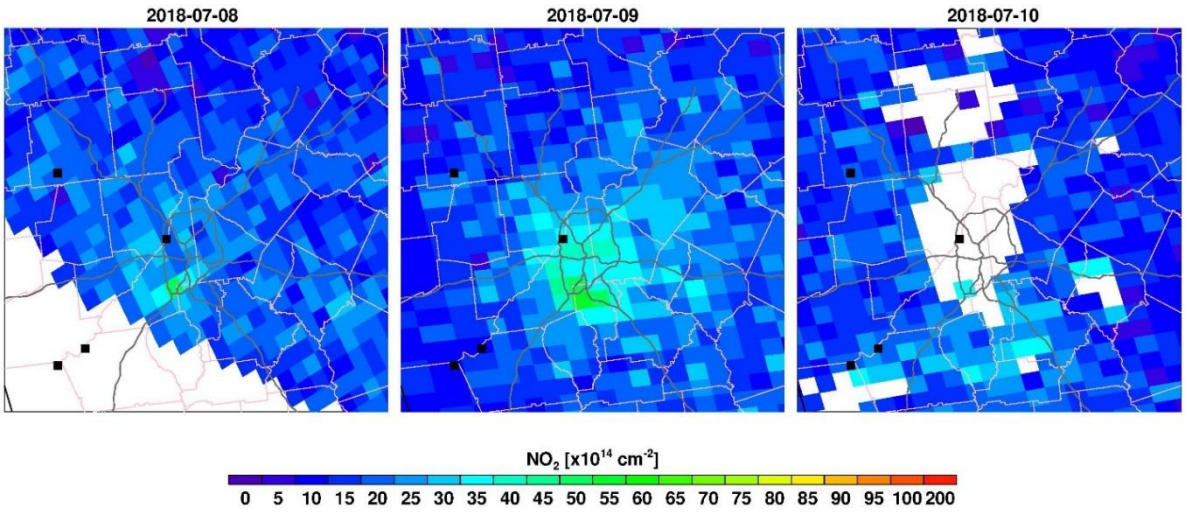

Figure 60. Daily TROPOMI NO_2 tropospheric columns over the Metro Atlanta area on July 8-10, 2018. Power plants are in black squares.

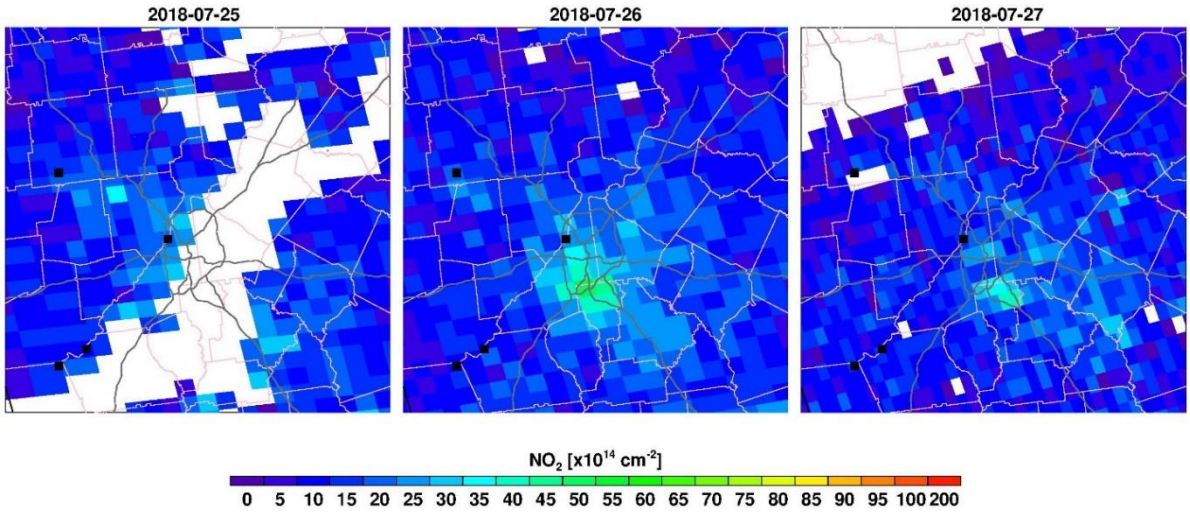

Figure 61. Daily TROPOMI NO_2 tropospheric columns over the Metro Atlanta area on July 25-27, 2018. Power plants are in black squares.

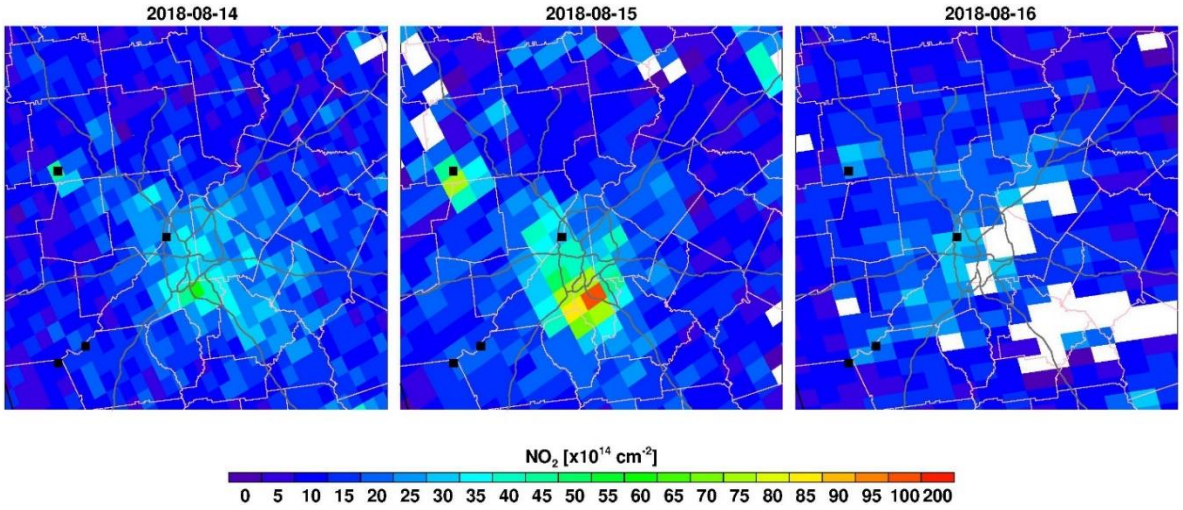

Figure 62. Daily TROPOMI NO_2 tropospheric columns over the Metro Atlanta area on August 14-16, 2018. Power plants are in black squares.

6.7 Ozone and Traffic Conditions

Past studies indicated that NO_X and VOCs emission rates tend to be higher in congested traffic conditions (Anderson, et al., 1996; De Vlieger, et al., 2000; Zhang et al., 2011). In the Metro Atlanta area, NO_X emissions are mainly from mobile sources (Figure 41). Thus, the impact of traffic congestion in the Metro Atlanta area on ozone exceedances was further investigated by analyzing hourly Google traffic maps. Traffic conditions in Google traffic maps are displayed in four colors (green, orange, red, and dark red) as pixels (hereafter, "traffic pixels"). Each traffic pixel represents a different traffic condition: green for free flow, orange for light congestion, red for heavy congestion, and dark red for severe congestion. Since detailed historical traffic data were not publicly available, screenshots of Google traffic maps over the Metro Atlanta area were captured every 10 minutes from April 1, 2018 to October 31, 2018. Higher numbers of red and dark red traffic pixels indicate more serious congestions than those of green and orange. Figure 63 is an example screenshot for June 1, 2018 at 15:10 EST which showed the heaviest traffic (i.e., the highest number of red and dark red pixels) in 2018.

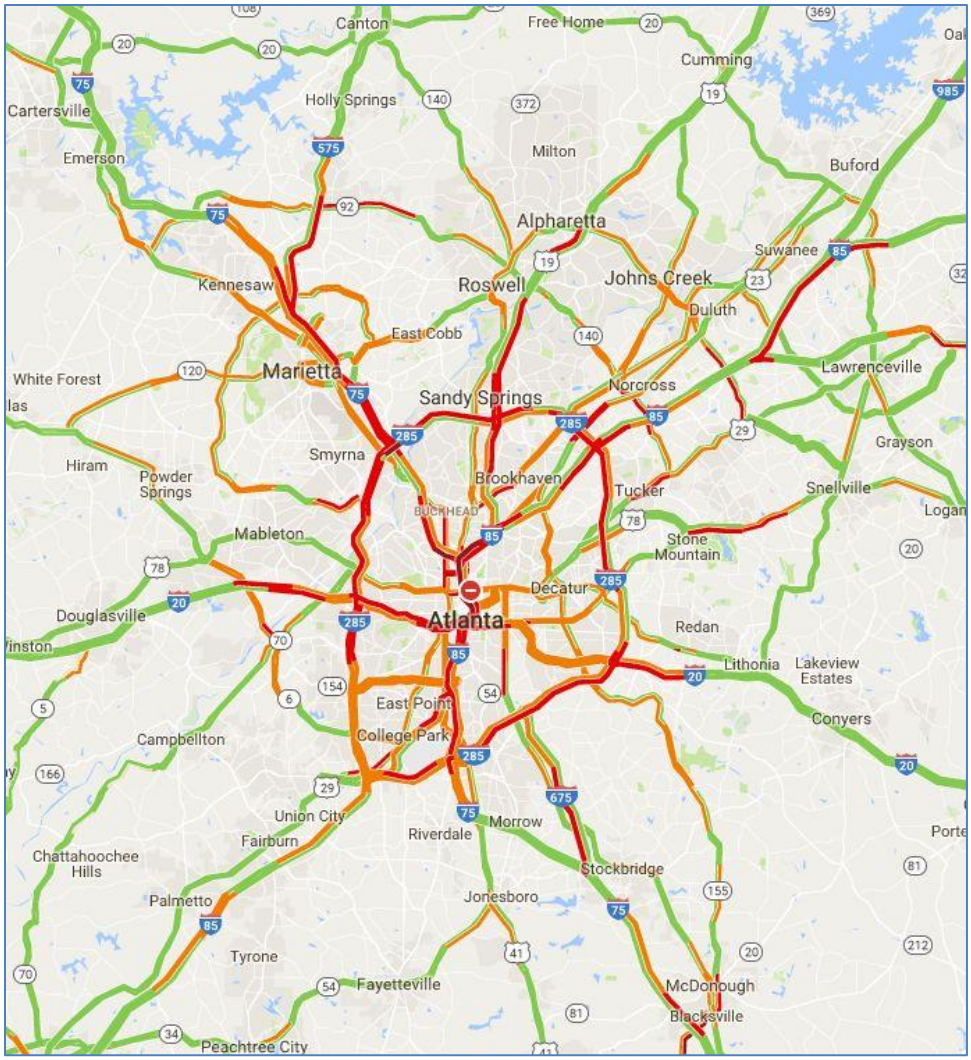

Figure 63. Google traffic map for the Metro Atlanta area for the hour with the heaviest traffic in 2018 (June 1 at 15:10 EST).

For each hour, the average number of traffic pixels for each color was calculated from screenshots that were captured every 10 minutes. In this analysis, only days with valid 24-hour data were used. A total of 5,136 hours of data were collected in the 2018 ozone season. Traffic data analysis is presented in Eastern Standard Time (EST) to be consistent with other analyses. Statistics show that the numbers of hourly traffic pixels in Google traffic maps range from 34,598 to 48,483, with a mean of 45,044 (Table 10). There are some days with missing data in May 2018 (Figure 64), including the two weekend ozone exceedances on May 12 and13, 2018. Therefore, no analysis is included for the weekend traffic pattern on ozone exceedance days. The hourly average number of traffic pixels in each month are very similar during the analysis period (Figure 64).

Table 10. Statistics of the number of pixels by colors in the hourly google traffic map over the Metro Atlanta area.

Color	Max	Min	Median	Mean	Standard Deviation
Dark Red	2,046	2	101	185	214
Red	5,756	1	248	666	941
Orange	10,640	111	1,411	1,880	1,609
Green	48,019	23,121	43,256	42,358	4,098
Total	**48,483**	**34,598**	**45,829**	**45,044**	**2,559**

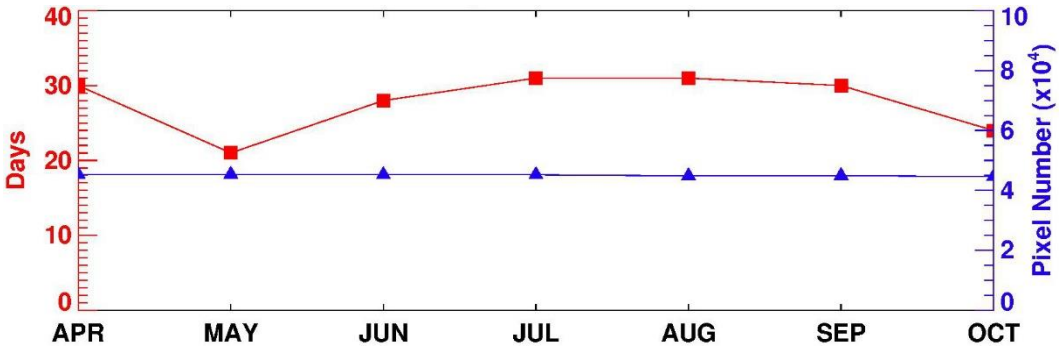

Figure 64. The number of valid days (red squares) and hourly average number of traffic pixels (blue triangles) for the Google traffic maps over the Metro Atlanta area from April to October 2018.

Traffic conditions varied greatly with the hour of the day (Figure 65). Most traffic pixels are in green while a lot of dark red, red, and orange pixels appeared in the Atlanta urban core. There are two peaks for the number of pixels in dark red, red, and orange: one peak during the morning rush hours of 6-8 AM EST (7-9 AM EDT) and the other in the evening rush hours of 3-5 PM EST (4-6 PM EDT). In addition to these two peaks, there is another sharp increase of the number of pixels in orange around 11 AM EST (12 PM EDT) which is likely due to the lunch-hour activity.

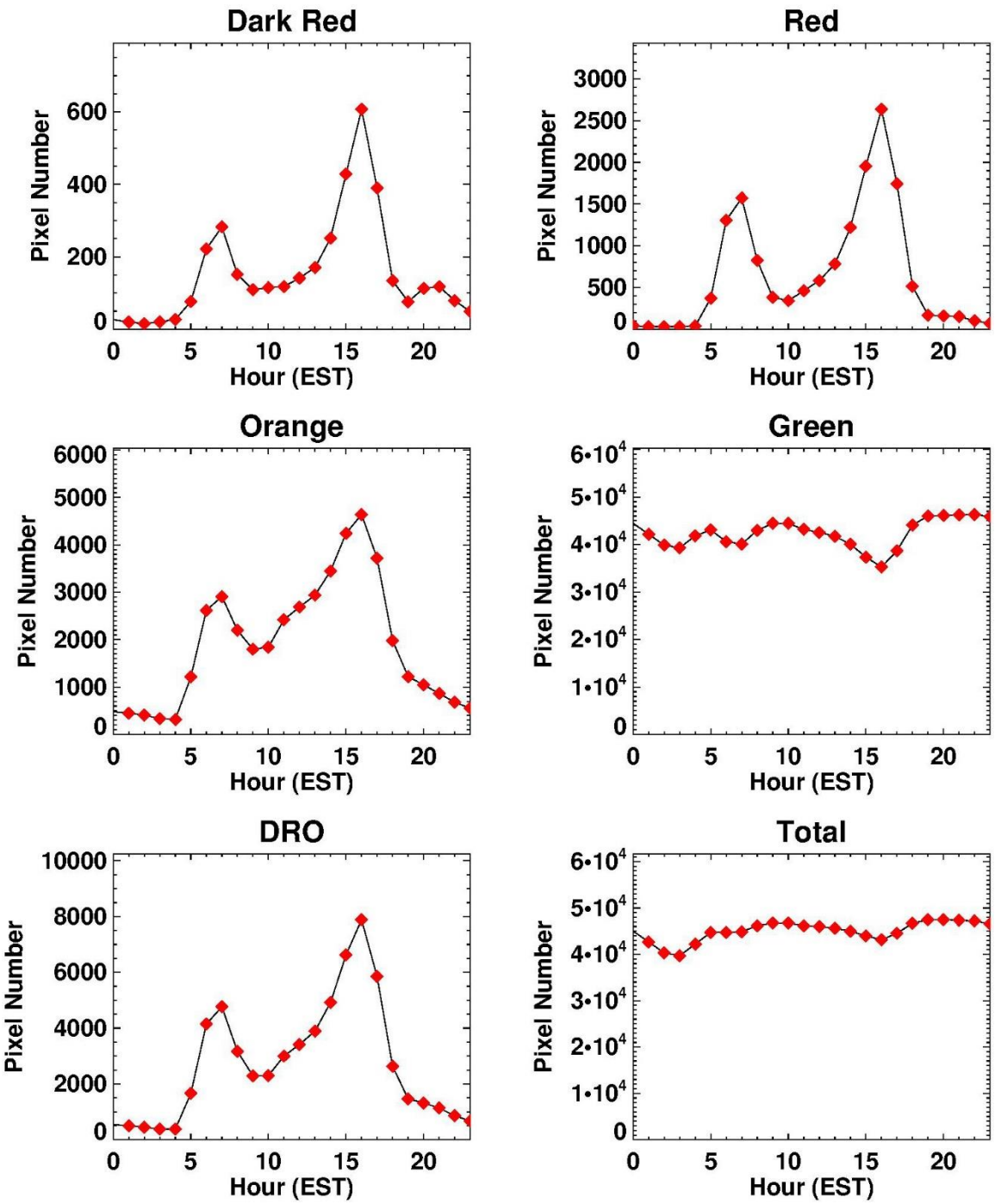

Figure 65. The average number of hourly traffic pixels over the Metro Atlanta area. DRO is the sum of dark red, red, and orange pixels.

In this study, the numbers of pixels for dark red, red, and orange were added together and referred to as DRO pixels to represent the overall congestion levels. A mean percentage of the total number of DRO pixels to the total number of all traffic pixels is 6%. The percentage of the total number of DRO pixels to the total number of all traffic pixels during morning and evening rush hours can reach 11% and 18%, respectively (Figure 66).

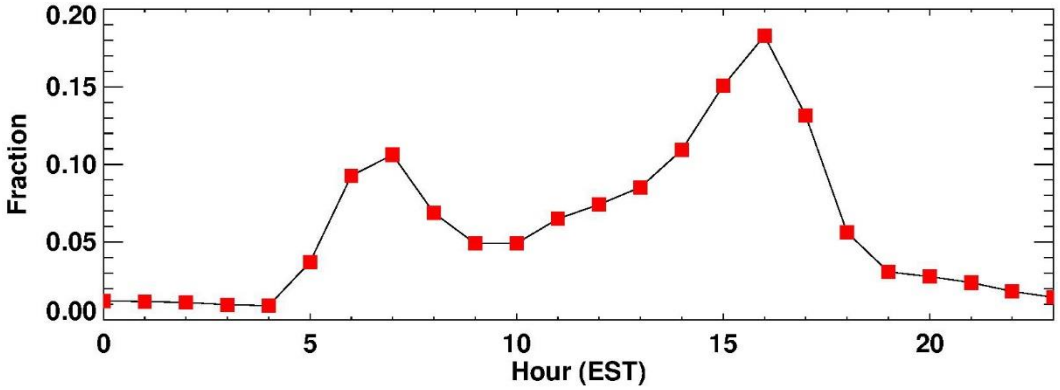

Figure 66. The average fractions of the number of DRO pixels to the total pixels in the hourly Google traffic pixel counts over the Metro Atlanta area.

The hourly traffic conditions varied greatly with the day of week. The number of DRO pixels was much lower on weekends than weekdays. Peak traffic patterns were different; two peaks for the weekdays and one longer plateau for the weekend (Figure 67). During the weekdays, the number of DRO pixels increases gradually from Monday to Friday, except that the number of DRO pixels for the morning period on Friday is less than other weekdays. For weekends, the number of DRO pixels on Saturday is higher than Sunday. The number of DRO pixels during the daytime were further summarized by three 4-hour windows (6 AM – 10 AM, 10 AM – 2 PM, and 2 PM – 6 PM EST) corresponding to morning hours, mid-day hours, and evening hours, respectively (Figure 68). The DRO numbers for the evening hours are higher than those for the morning hours and mid-day hours. The DRO numbers during the mid-day hours and evening hours increase from Monday to Friday and decrease on weekends. The DRO numbers during morning hours are similar from Monday to Thursday, less on Friday, even less on Saturday, and the least on Sunday.

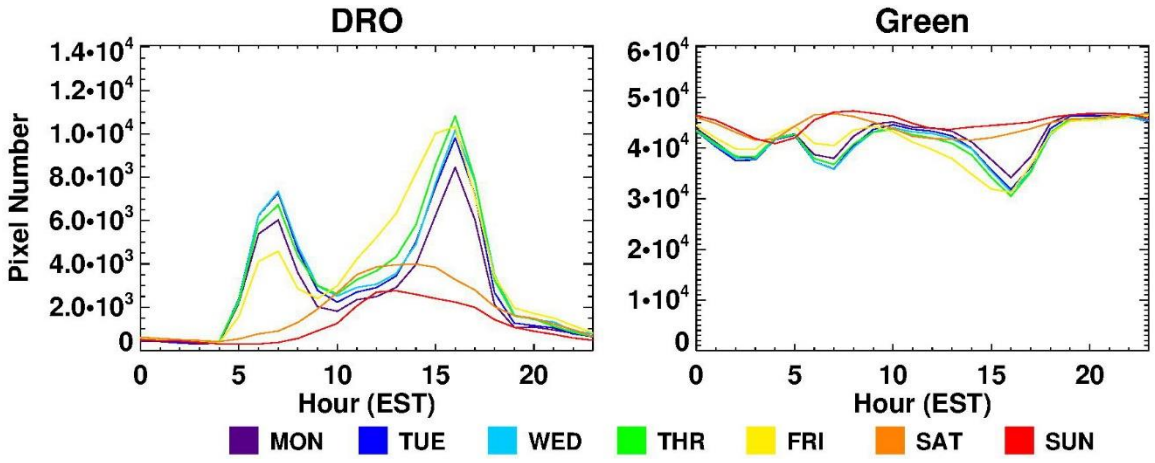

Figure 67. The number of DRO and Green pixels on each day of week over the Metro Atlanta area.

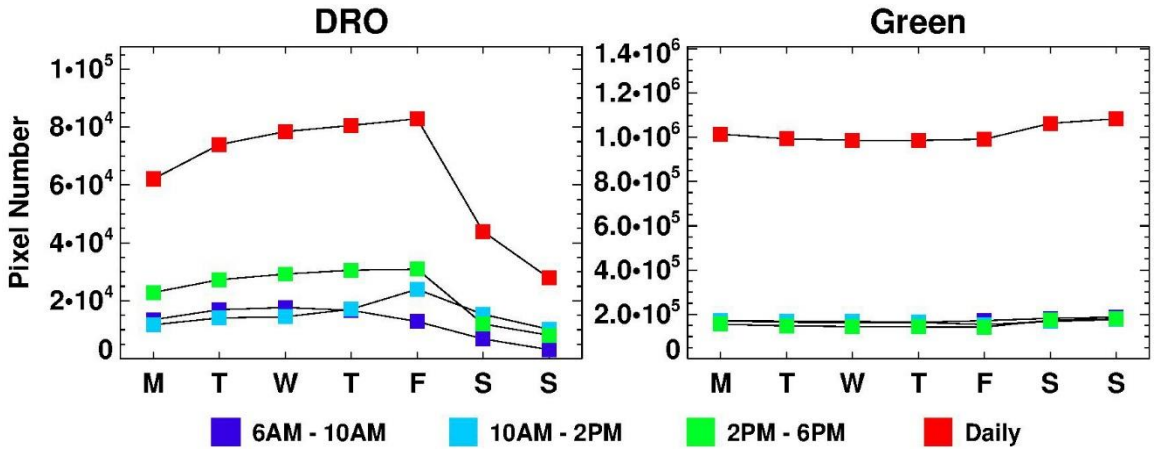

Figure 68. The number of DRO and green pixels during three 4-hour periods (6 AM – 10 AM, 10 AM – 2 PM, and 2 PM – 6PM EST) on each day of week over the Metro Atlanta area.

The number of DRO pixels on the eight ozone exceedance days were compared with those on the two days before and two days after the ozone exceedance days in 2018 (Figure 69). The DRO numbers do not have a clear spike pattern on the weekday exceedance days. Rather, they follow the weekday increasing pattern from Monday to Friday found previously (Figure 68).

The hourly number of DRO pixels on each ozone exceedance day was compared with the hourly averages on all days, all weekdays/weekends, and the corresponding day of week (Figure 70-Figure 77). On some ozone exceedance days (e.g., May 1, May 2, and August 15, 2018), the numbers of DRO pixels are generally higher than the average weekday and the corresponding weekday conditions during the morning and afternoon hours. On other ozone exceedance days (e.g., June 4, June 6, June 7, July 9, and July 26, 2018), the numbers of DRO pixels are generally close or lower than the average weekday and the corresponding average weekday conditions.

Ozone exceedances in June and July 2018 corresponded to lower or close to average traffic conditions, while ozone exceedances in other months corresponded to more congested traffic conditions. This pattern is much clearer for the morning (AM) peaks. This is consistent with the significantly higher NO_X concentrations in the morning rush hours on ozone exceedance days (Figure 51). The traffic conditions on the exceedance days in 2017 follow a similar pattern (Table 11).

The traffic patterns work closely with the meteorological conditions to impact local ozone production. July has the highest monthly temperature and June has the highest solar elevation angle. These two factors can lead to higher chemical reaction rates and thus more ozone production (Coates et al., 2016). We speculate that the buildup of NO_X emissions from mobile sources is less critical for ozone exceedances in June and July. Under favorable ambient conditions (e.g., hot and dry days), ozone exceedances can take place with typical traffic congestions. In contrast, the buildup of NO_X emissions due to high traffic congestion may be more essential for ozone exceedances in other months that have relatively lower temperature and less sunlight (i.e., less active ozone production) than June and July.

Table 11. The comparison of hourly DRO numbers on weekday ozone exceedance days with the average weekday and the corresponding average day of week conditions over the Metro Atlanta area in 2017 and 2018.

Date	Average weekday		Average day of week	
	AM peak	PM peak	AM peak	PM peak
7/19/2017	Close	Close	Low	Close
7/21/2017	Low	Close	Low	Low
7/26/2017	Close	Low	Close	Close
8/1/2017	**High**	**High**	**High**	**High**
8/24/2017	**High**	Close	**High**	Low
9/28/2017	**High**	Close	**High**	Low
5/1/2018	**High**	**High**	**High**	**High**
5/2/2018	**High**	**High**	**High**	**High**
6/4/2018	Close	Low	Close	Close
6/6/2018	Close	Close	Close	Close
6/7/2018	Close	Close	Close	Low
7/9/2018	Low	Low	Low	Close
7/26/2018	Low	**High**	Low	Close
8/15/2018	**High**	Close	**High**	Close

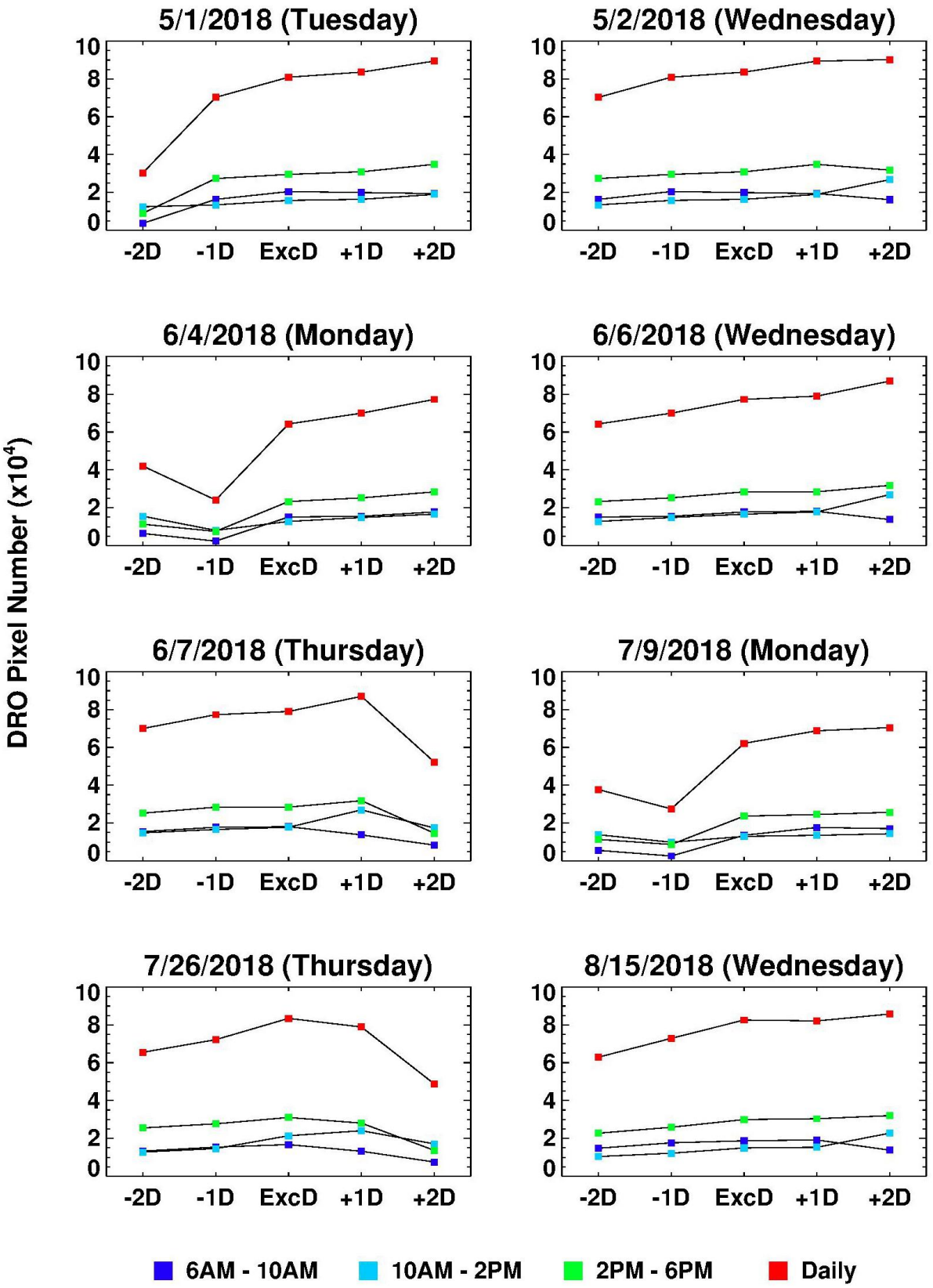

Figure 69. The number of DRO pixels by three 4-hour periods on eight ozone exceedance days and 2 days before and after ozone exceedance days in 2018.

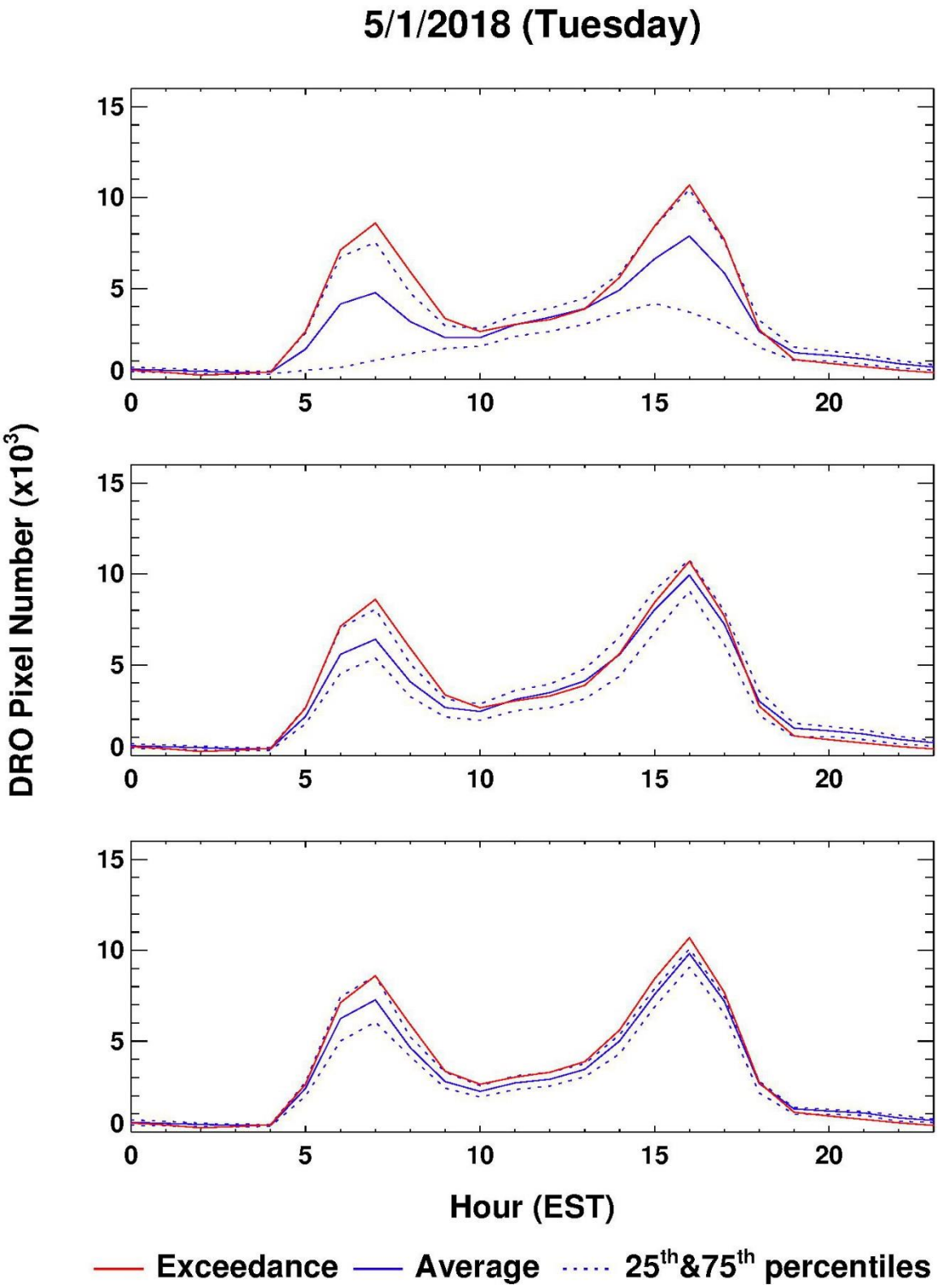

Figure 70. The hourly DRO pixel numbers on May 1, 2018, an ozone exceedance day (red line), and the hourly averages (blue solid line), 25th and 75th percentiles (blue dash lines) of DRO numbers on all days (top), weekdays (middle), and Tuesday (bottom).

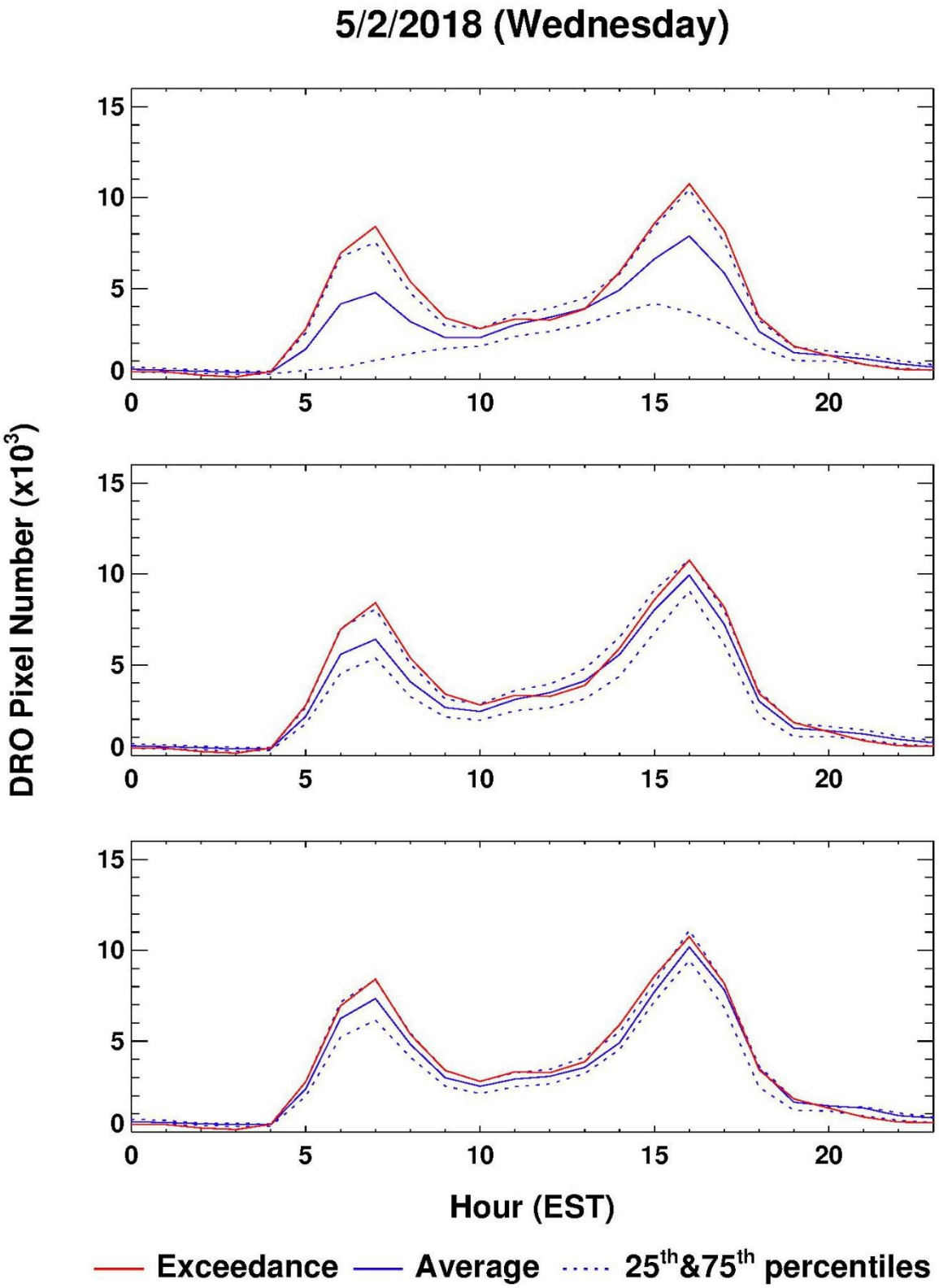

Figure 71. The hourly DRO pixel numbers on May 2, 2018, an ozone exceedance day (red line), and the hourly averages (blue solid line), 25th and 75th percentiles (blue dash lines) of DRO numbers on all days (top), weekdays (middle), and Wednesday (bottom).

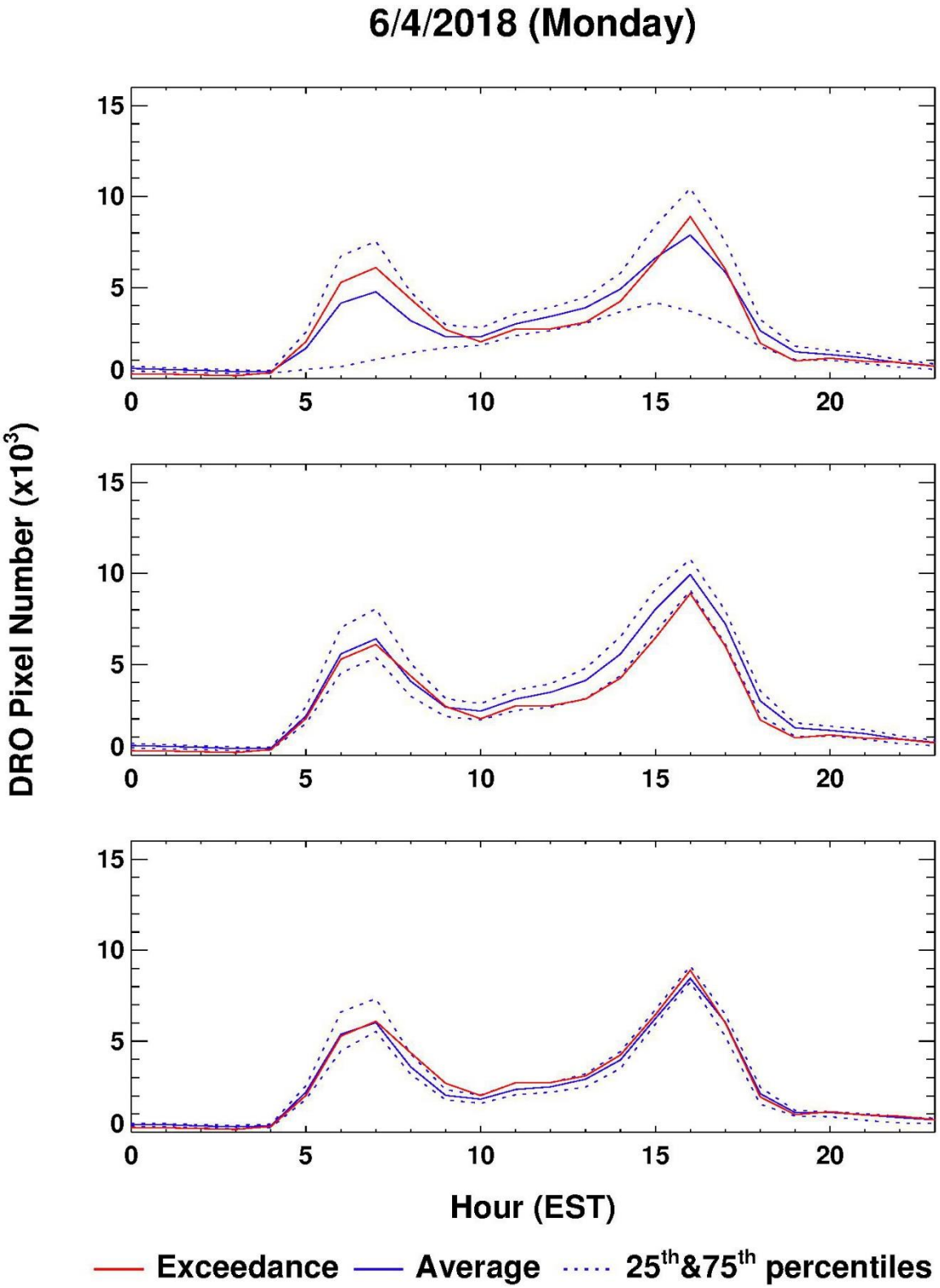

Figure 72. The hourly DRO pixel numbers on June 4, 2018, an ozone exceedance day (red line), and the hourly averages (blue solid line), 25th and 75th percentiles (blue dash lines) of DRO numbers on all days (top), weekdays (middle), and Monday (bottom).

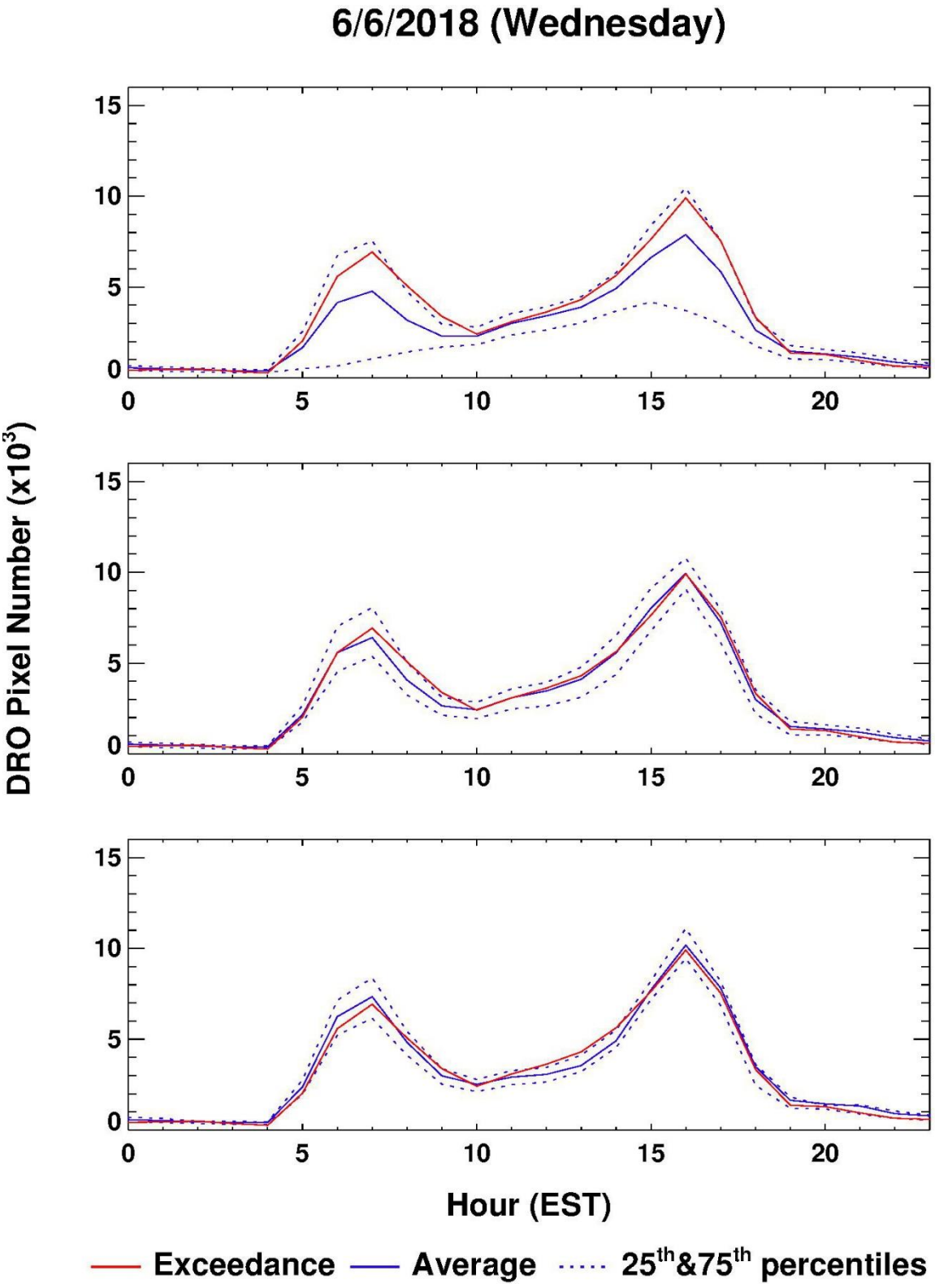

Figure 73. The hourly DRO pixel numbers on June 6, 2018, an ozone exceedance day (red line), and the hourly averages (blue solid line), 25th and 75th percentiles (blue dash lines) of DRO numbers on all days (top), weekdays (middle), and Wednesday (bottom).

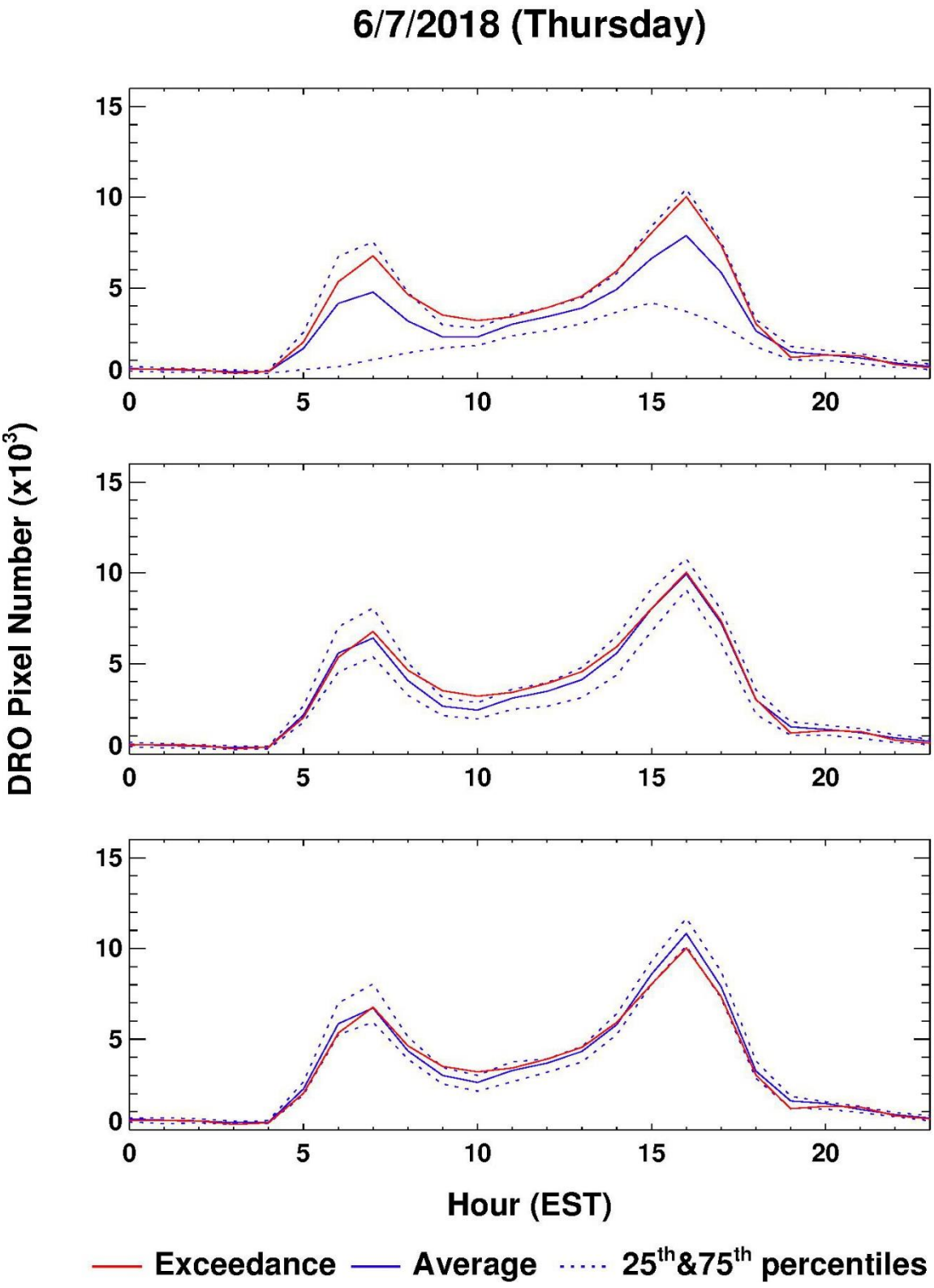

Figure 74. The hourly DRO pixel numbers on June 7, 2018, an ozone exceedance day (red line), and the hourly averages (blue solid line), 25th and 75th percentiles (blue dash lines) of DRO numbers on all days (top), weekdays (middle), and Thursday (bottom).

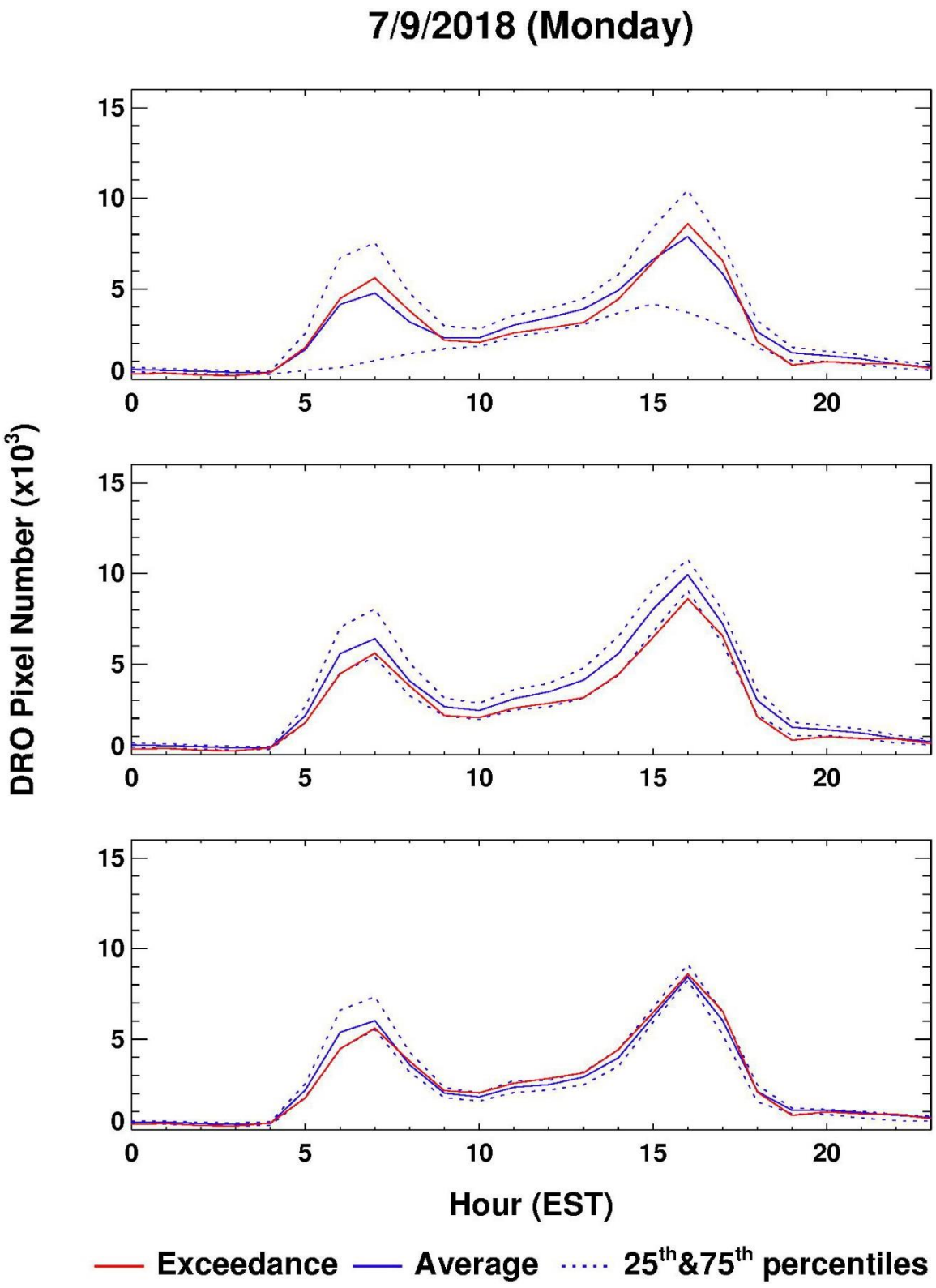

Figure 75. The hourly DRO pixel numbers on July 9, 2018, an ozone exceedance day (red line), and the hourly averages (blue solid line), 25th and 75th percentiles (blue dash lines) of DRO numbers on all days (top), weekdays (middle), and Monday (bottom).

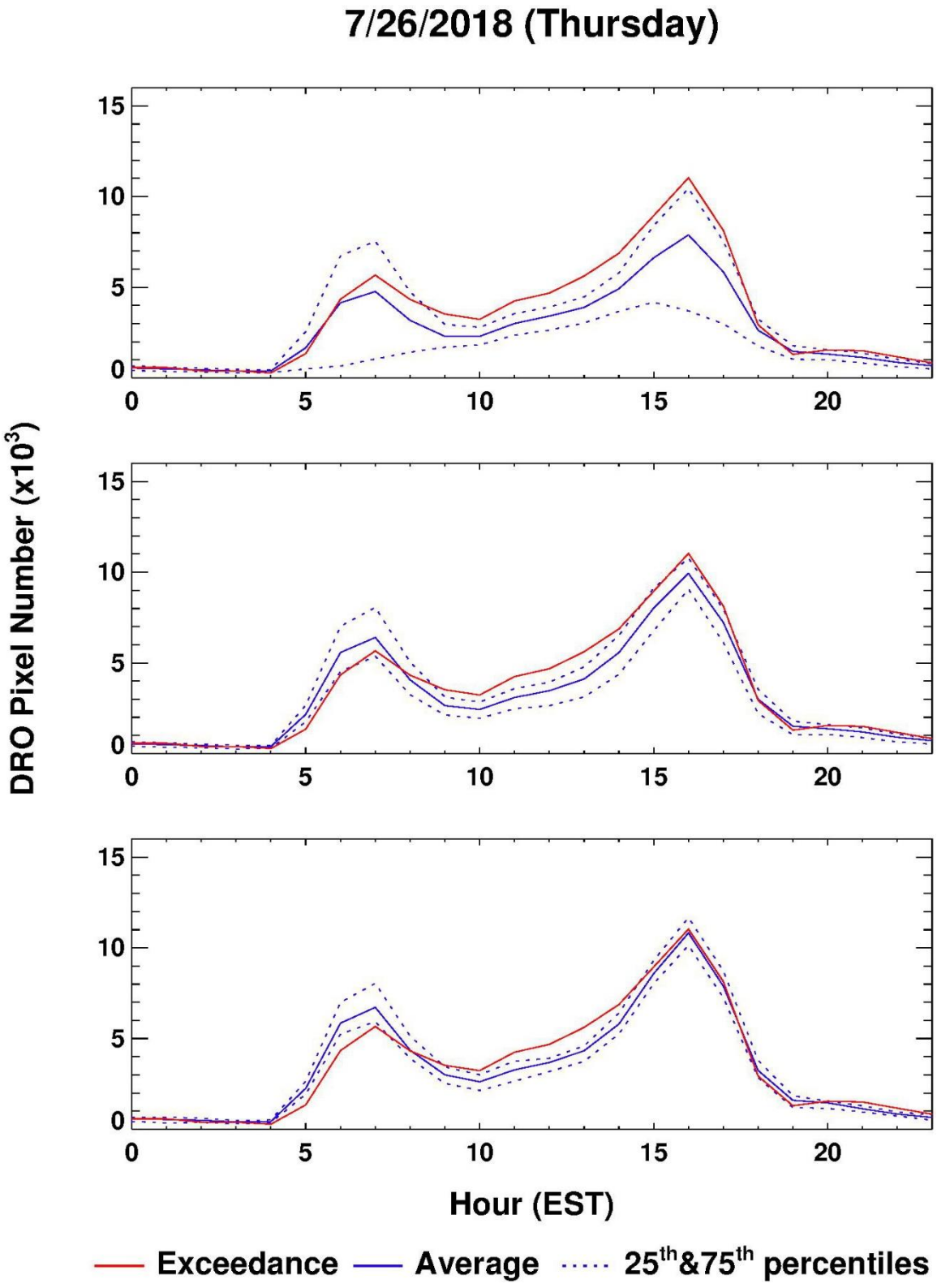

Figure 76. The hourly DRO pixel numbers on July 26, 2018, an ozone exceedance day (red line), and the hourly averages (blue solid line), 25th and 75th percentiles (blue dash lines) of DRO numbers on all days (top), weekdays (middle), and Thursday (bottom).

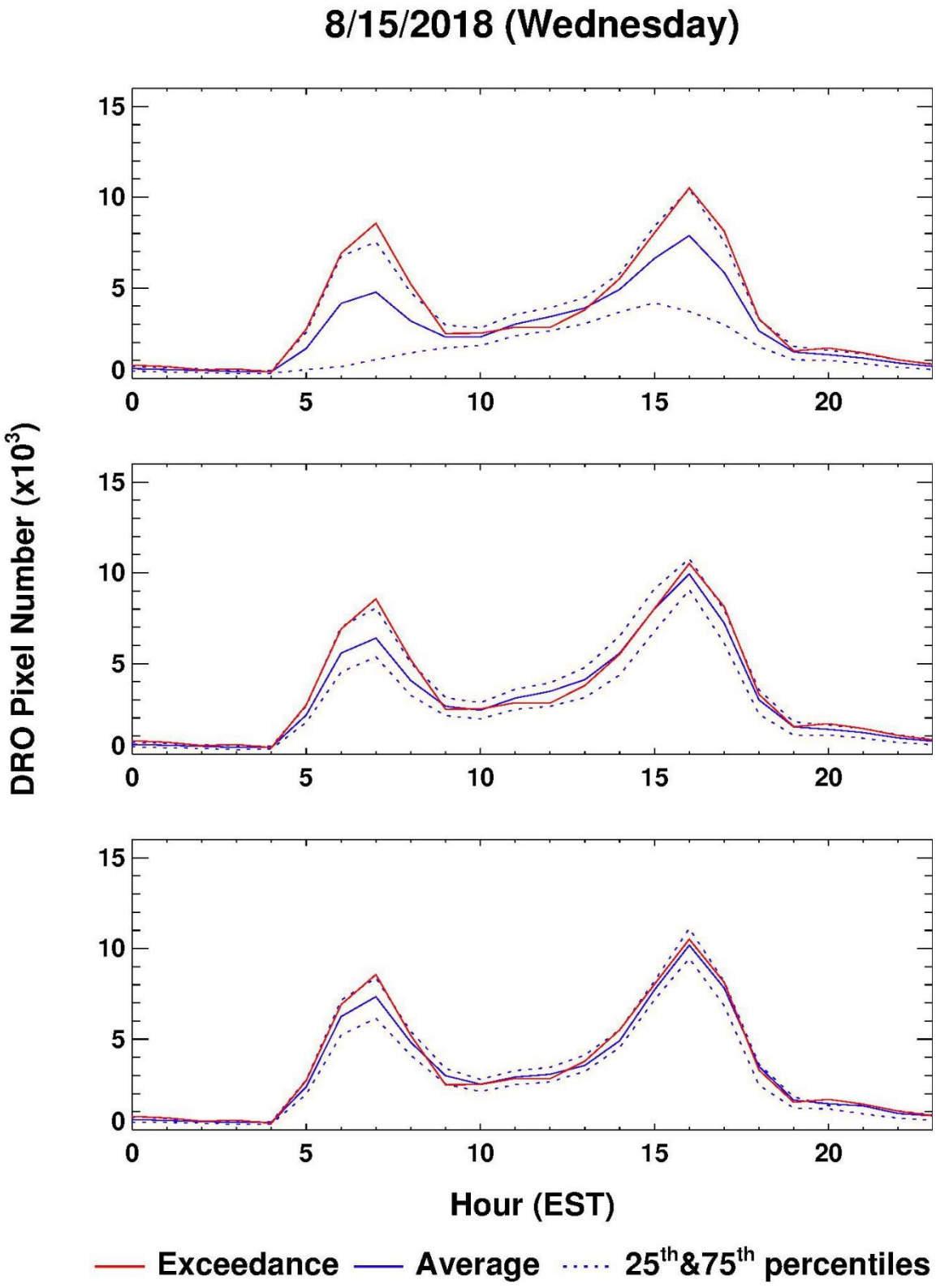

Figure 77. The hourly DRO pixel numbers on August 15, 2018, an ozone exceedance day (red line), and the hourly averages (blue solid line), 25th and 75th percentiles (blue dash lines) of DRO numbers on all days (top), weekdays (middle), and Wednesday (bottom).

7. Ozone and VOCs Precursors

7.1 HCHO Trends Based on OMI Satellite Data

Formaldehyde (HCHO) has been widely used as a proxy of VOCs emissions. It is formed through the oxidation of VOCs to produce ozone in the atmosphere. Biogenic VOCs (mainly isoprene) is believed to be the main source of HCHO in the Southeastern U.S. due to the large amounts of forest coverage (Bauwens et al., 2016), although HCHO can be emitted from anthropogenic sources (e.g., mobile sources).

Tropospheric HCHO monthly columns from the OMI observations were used to examine HCHO trends. Level 3 monthly gridded vertical columns derived at Belgian Institute for Space Aeronomy (BIRA) from 2005 to 2016 were downloaded from the European TEMIS project website (http://h2co.aeronomie.be/). Level 2 daily gridded vertical columns data from 2017 and 2018 were downloaded from NASA's Goddard Earth Sciences Data and Information Services Center (GES DISC) (https://disc.gsfc.nasa.gov/datasets/OMHCHOG_003/summary). The daily gridded data in 2017-2018 were converted into monthly averages using IDL scripts. The monthly OMI HCHO has a global coverage with a spatial resolution of 0.25 degree.

The interannual variation of tropospheric HCHO columns is relatively small (Figure 78), ranging from 10.2×10^{15} molecules/cm^2 in 2006 to 7.8 in 2015. This is likely due to the dominance of biogenic sources whose emissions haven't changed much over the years. Tropospheric HCHO columns vary greatly by months following the growing season cycle for biogenic sources in the Southeast (Figure 79), peaking in June (15.1×10^{15} molecules/cm^2) which is almost 3 times the concentration in January (5.7×10^{15} molecules/cm^2). The spatial difference of tropospheric HCHO columns is small over metro Atlanta (Figure 80) due to widespread biogenic emissions in the Southeast U.S.

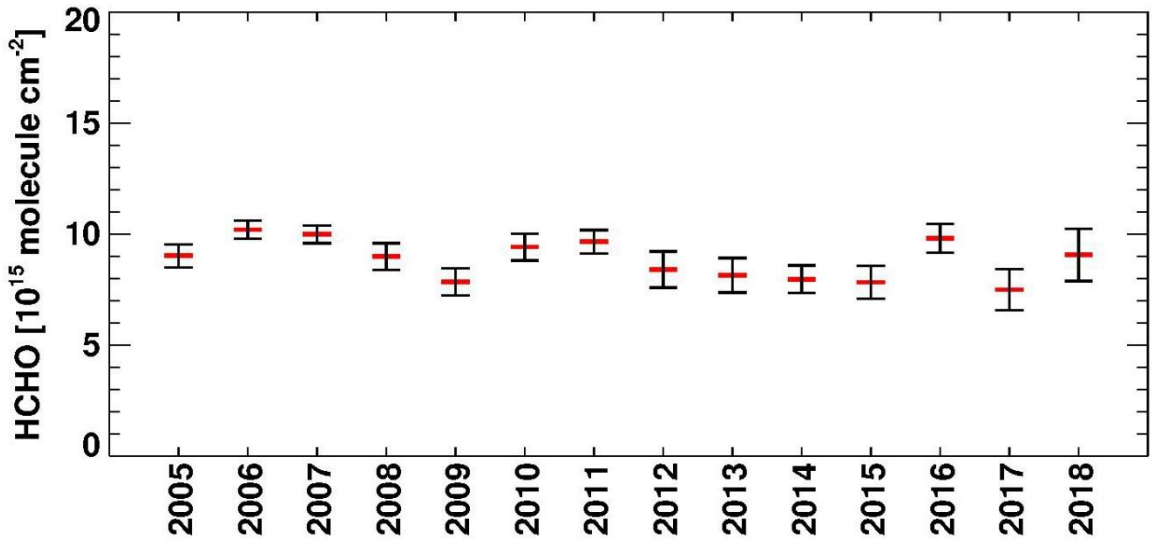

Figure 78. Annual mean OMI HCHO tropospheric columns over the Metro Atlanta area in 2005-2018. The means (red bar) and its standard deviations (black bars) are shown.

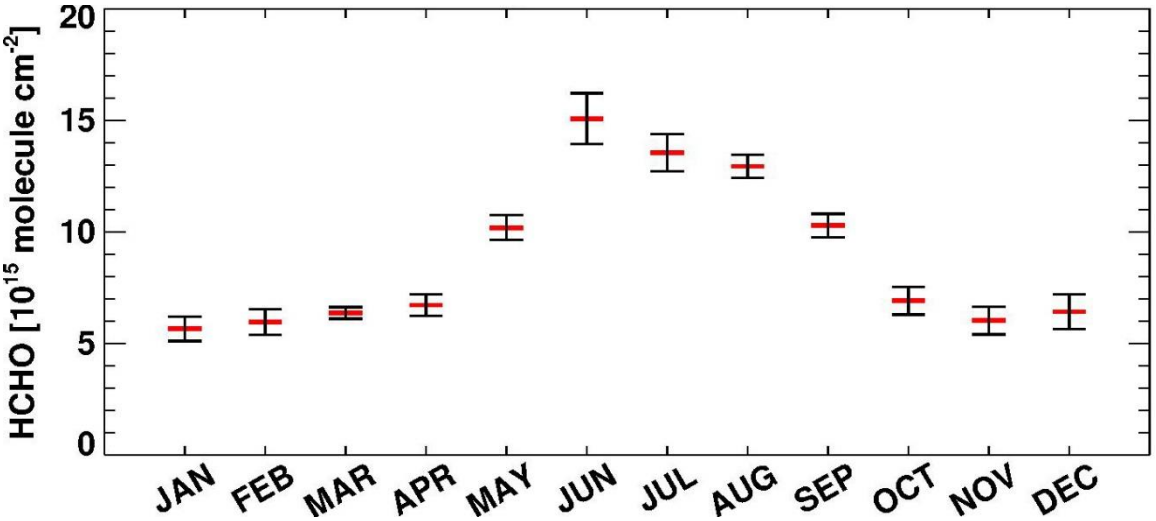

Figure 79. Monthly HCHO tropospheric columns in 2005-2018 over the Metro Atlanta area. The means (red bar) and its standard deviations (black bars) are shown.

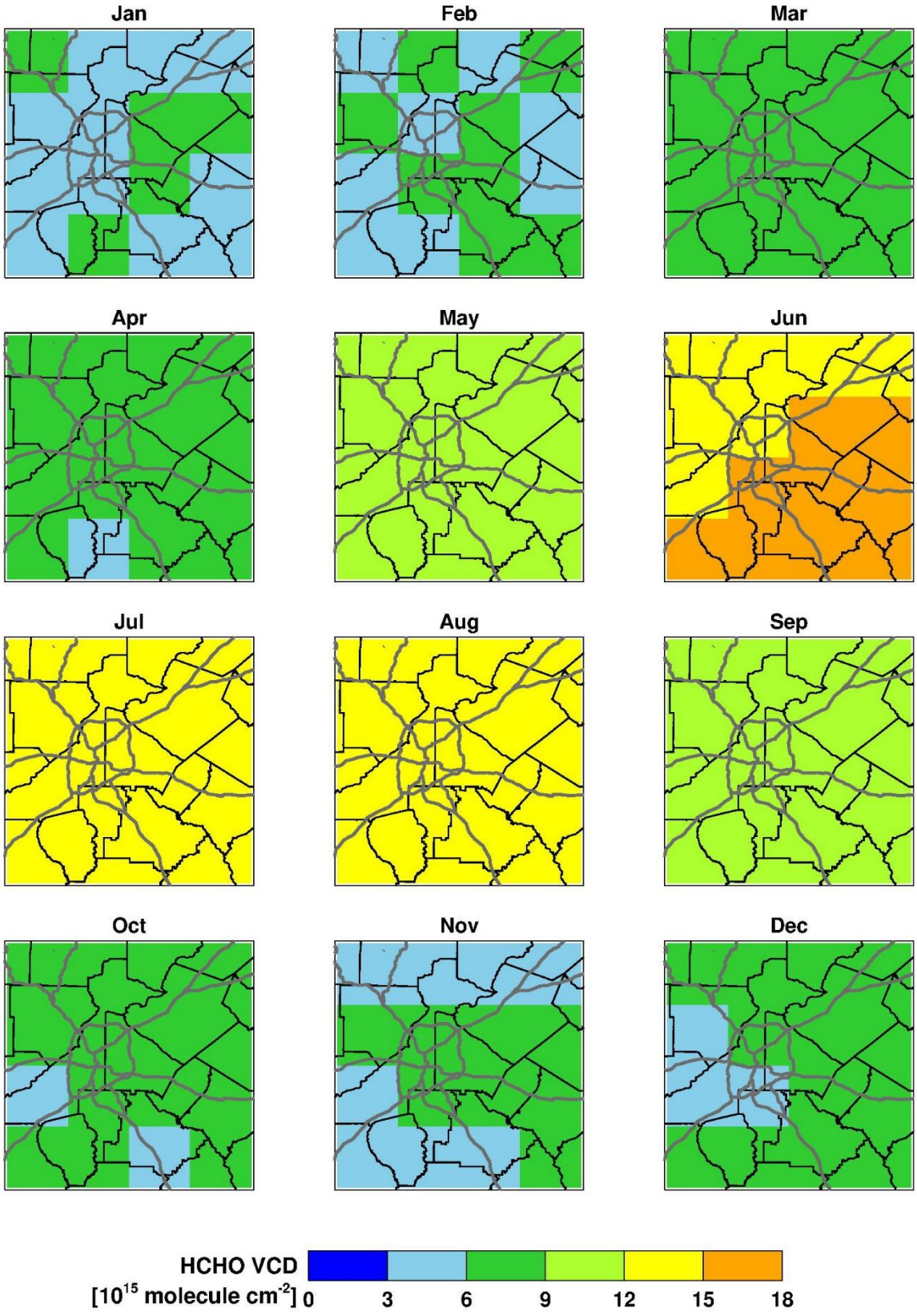

Figure 80. Monthly mean HCHO tropospheric columns over the Metro Atlanta area during 2005-2018.

The satellite derived formaldehyde (HCHO) to NO_2 ratios (FNR) were used to investigate the ozone production regime in the Metro Atlanta area (Martin et al., 2004 and Jin et al., 2017). High HCHO and NO_2 were generally observed near their source regions due to their short lifetime in the ambient air. FNR represents the OH radical competition between VOCs and NO_2. Figure 81 compares the monthly means of OMI NO_2 and HCHO tropospheric columns over the urban core of the Metro Atlanta area. GEOS-Chem model derived ozone precursor results were applied to determine the threshold of NO_X-limited and NO_X-saturated regimes in each month (Jin et al., 2017). The OMI satellite data shows that ozone formation in the Metro Atlanta area was mostly in the NO_X-limited regime on average except in some winter months when biogenic VOCs emission was very low.

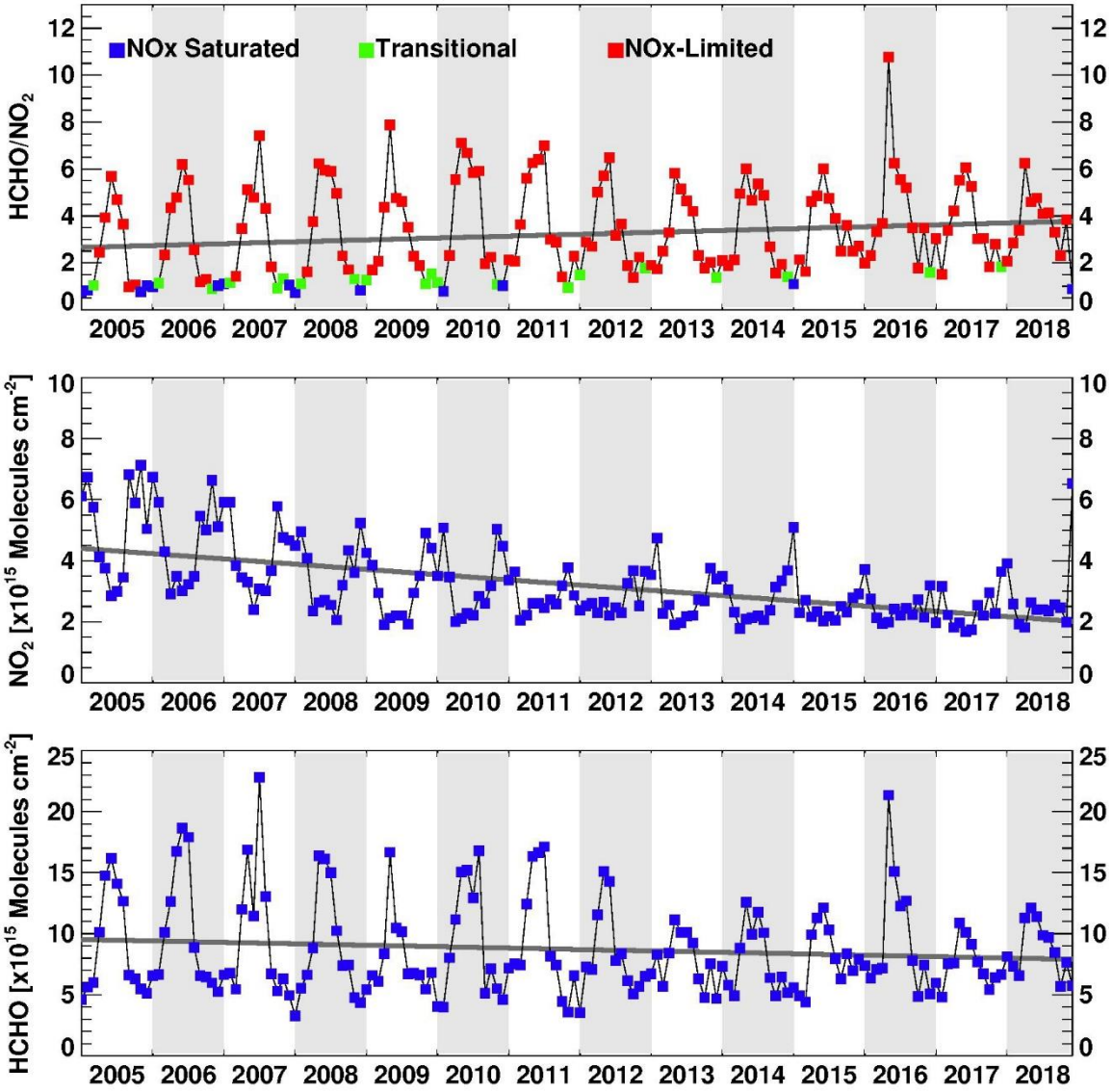

Figure 81. Monthly mean HCHO/NO_2 ratios (top), NO_2 (middle), and HCHO (bottom) over the Metro Atlanta area during 2005-2018. The linear trends are shown in dark grey.

8. Summary

Various in-depth analyses have been conducted to understand the causes of ozone exceedances in the Metro Atlanta area during 2018. These analyses include: trend analysis of ozone exceedance and meteorological conditions in Atlanta during 1990-2018; multiple linear regression (MLR) analysis to understand the relationship of Atlanta ozone and environmental variables; HYSPLIT back trajectory analysis to determine the origin of air masses and establish source-receptor relationships on ozone exceedance days; animation of ozone and wind conditions to illustrate ozone formation and transport; and analysis of VOCs and NO_X measurements including satellite products to understand the impacts of precursors on ozone exceedances. Also, a preliminary investigation of traffic congestion impacts on ozone exceedances was performed.

The MLR analysis has shown that ozone exceedances are likely to occur when relative humidity in the afternoon is low and daily maximum air temperature is high. These summertime meteorological conditions can occur in the Metro Atlanta area under stable and stagnant conditions due to the presence of Bermuda and subtropical high-pressure systems. The ozone exceedances are also associated with high ozone concentrations on previous days, low wind speed, and other meteorological variables with decreased correlation. HYSPLIT back trajectory analysis and combined analysis of ozone and wind conditions found that most 2018 ozone exceedances were linked to local air parcels. Also, the emissions from the Atlanta urban core area have been demonstrated to impact local downwind monitors.

Analysis of NO_X measurements in the Atlanta urban core area along with ozone measurements found that ozone exceedance occurred more often on weekdays than weekends when the NO_X emissions from the dominant NO_X source (on-road mobile) in the Metro Atlanta area are higher. The morning time NO_X measurements on ozone exceedance days also tend to be higher due to commuter traffic. The ratio of ozone and NO_X, an indicator of local ozone production efficiency, indicate a strong impact of NO_X on ozone formation and higher than usual ozone production efficiency in 2018 compared to past years. Satellite data have similarly shown high NO_2 concentrations on weekdays and a downward trend consistent with the trend in ozone concentrations. In addition, the NO_2 hot spots on ozone exceedance days near HJAIA were observed with satellite data. The OMI HCHO data showed small interannual variations and large monthly variations in tropospheric HCHO likely due to biogenic emission sources.

In summary, the following factors likely contributed to 2018 ozone exceedances in Atlanta:

1) Low relative humidity in the afternoon;
2) High daily maximum air temperature;
3) Low cloud coverage;
4) High ozone on previous days;
5) Low wind speed;
6) NO_X emissions, mainly from local on-road mobile sources;
7) High traffic congestion (especially in the morning hours) during May, August, and September;
8) VOC emissions, mainly from biogenic sources in the summer months; and
9) Local transport of emissions from the Atlanta urban core to monitors outside the urban core.

The following studies and measurements are recommended to further understand the causes of future ozone exceedances in the Metro Atlanta area:

- Co-located measurements of NO_X and VOC species at United Ave.;
- Co-located measurements of NO_X and VOC species near Hartsfield-Jackson Atlanta International Airport;
- Aircraft measurements (ozone, NO_X, and CO) on elevated ozone days;
- Personal air sensors to understand spatial gradients;
- Ozone and NO_2 balloon soundings to understand vertical profiles;
- Ozone profiles from LIDAR;
- Geostationary satellite data from TEMPO (Tropospheric Emissions: Monitoring of Pollution) to be launched in 2020-2021;
- Additional traffic studies using vehicle count and speed data (Google maps and/or TOMTOM) or GDOT "Navigator" speed and traffic data; and/or
- High resolution photochemical modeling (e.g., 1-km grid cells) to examine the impact of various emission control strategies on ozone concentrations.

This additional information may help us explore new options to prevent future ozone exceedances in the Atlanta area.

9. References

Bucsela, E. J., Krotkov, N. A., Celarier, et al. (2013). A new stratospheric and tropospheric NO2 retrieval algorithm for nadir-viewing satellite instruments: applications to OMI, Atmos. Meas. Tech., 6, 2607–2626, doi:10.5194/amt-6-2607-2013.

Cardelino, C., M. Chang, J. St. John, et al. (2011). Ozone Predictions in Atlanta, Georgia: Analysis of the 1999 Ozone Season, J. Air & Waste Manage. Assoc. 51:1227-1236.

Coates, J., K. A. Mar, N. Ojha, and T. M. Butler, The influence of temperature on ozone production under varying NOx conditions – a modelling study, Atmos. Chem. Phys., 16, 11601–11615, 2016.

Heland, J., H. Schlager, A. Richter, and J. P. Burrows (2002). First comparison of tropospheric NO2 column densities retrieved from GOME measurements and in situ aircraft profile measurements, Geophys. Res. Lett., 29, 1983, doi:10.1029/2002GL015528, 2002.

Jin, X. Fiore, A. M., Murray, L.T., et al. (2017). Evaluating space-based indicator of surface ozone-NO_X-VOC sensitivity over mid-latitude source regions and applications to decadal trends. J. Geophys. Res. Atmos, 122. https://doi.org/10.1002/2017JD026720

Lamsal, L. N., N. A. Krotkov, E. A. Celarier, et al. (2014). Evaluation of OMI operational standard NO2 column retrievals using in situ and surface-based NO2 observations, Atmos. Chem. Phys., 14, 11587–11609.

Laughner, J. L., A. Zare, and R. C. Cohen (2016). Effects of daily meteorology on the interpretation of space-based remote sensing of NO_2, Atmos. Chem. Phys., 16, 15247–15264.

Martin, R. V., D. D. Parrish, T. B. Ryerson, et al. (2004). Evaluation of GOME Satellite Measurements of Tropospheric NO_2 and HCHO Using Regional Data from Aircraft Campaigns in the Southeastern United States. J. Geophysical Research 109 (D24): D24307. doi:10.1029/2004jd004869.

Martin, R. V., Fiore, A. M., & Van Donkelaar, A. (2004). Space-based diagnosis of surface ozone sensitivity to anthropogenic emissions. Geophys. Res. Lett., 31, L06120. https://doi.org/10.1029/2004GL019416

Tonnesen, Gail S., and Robin L. Dennis. 2000. "Analysis of Radical Propagation Efficiency to Assess Ozone Sensitivity to Hydrocarbons and NO_X : 1. Local Indicators of Instantaneous Odd Oxygen Production Sensitivity." Journal of Geophysical Research 105(D7): 9213.

Seinfeld, J. H., S. N. Pandis (1998). Atmospheric chemistry and physics: from air pollution to climate change, Wiley.

Steinbacher, M., C. Zellweger, B. Schwarzenbach, et al. (2007). Nitrogen oxides measurements at rural sites in Switzerland: Bias of conventional measurement techniques, J. Geophys. Res., 112, D11307, doi:10.1029/2006JD007971.